DETERMINATION OF THE DYNAMIC CHARACTERISTICS AND LOCAL SITE CONDITIONS OF THE PLIO-QUARTERNARY SEDIMENTS SITUATED TOWARDS THE NORTH OF ANKARA THROUGH SURFACE WAVE TESTING METHODS

A THESIS SUBMITTED TO
THE GRADUATE SCHOOL OF NATURAL AND APPLIED SCIENCES
OF
MIDDLE EAST TECHNICAL UNIVERSITY

BY

ARİF MERT EKER

IN PARTIAL FULFILLMENT OF THE REQUIREMENTS
FOR
THE DEGREE OF MASTER OF SCIENCE
IN
GEOLOGICAL ENGINEERING

JULY 2009

Approval of the thesis:

DETERMINATION OF THE DYNAMIC CHARACTERISTICS AND LOCAL SITE CONDITIONS OF THE PLIO-QUARTERNARY SEDIMENTS SITUATED TOWARDS THE NORTH OF ANKARA THROUGH SURFACE WAVE TESTING METHODS

submitted by **ARİF MERT EKER** in partial fulfillment of the requirements for the degree of **Master of Science in Geological Engineering Department, Middle East Technical University** by,

Prof. Dr. Canan Özgen _____
Dean, Graduate School of **Natural and Applied Sciences**

Prof. Dr. Zeki Çamur _____
Head of Department, **Geological Engineering**

Prof. Dr. Haluk Akgün _____
Supervisor, **Geological Engineering Dept., METU**

Dr. Mustafa Kerem Koçkar _____
Co-Supervisor, **Earthquake Research and Implementation Center (DEPAR), Gazi University**

Examining Committee Members:

Prof. Dr. Asuman G. Türkmenoğlu _____
Geological Engineering Dept., METU

Prof. Dr. Haluk Akgün _____
Geological Engineering Dept., METU

Dr. Mustafa Kerem Koçkar _____
DEPAR, Gazi University

Prof. Dr. Erdal Çokça _____
Civil Engineering Dept., METU

Assist. Prof. Dr. Ünal Dikmen _____
Geophysical Engineering Dept., Ankara University

Date: 20.07.2009

I hereby declare that all information in this document has been obtained and presented in accordance with academic rules and ethical conduct. I also declare that, as required by these rules and conduct, I have fully cited and referenced all material and results that are not original to this work.

Name, Last name : Arif Mert EKER

Signature :

ABSTRACT

DETERMINATION OF THE DYNAMIC CHARACTERISTICS AND LOCAL SITE CONDITIONS OF THE PLIO-QUARTERNARY SEDIMENTS SITUATED TOWARDS THE NORTH OF ANKARA THROUGH SURFACE WAVE TESTING METHODS

Arif Mert Eker

M. Sc., Department of Geological Engineering

Supervisor : Prof. Dr. Haluk Akgün

Co-Supervisor: Dr. Mustafa Kerem Koçkar

July 2009, 145 pages

The purpose of this study is to assess the engineering geological and geotechnical characteristics and to perform seismic hazard studies of the Upper Pliocene to Quaternary (Plio-Quaternary) deposits located towards the north of Ankara through surface wave testing methods. Based on a general engineering geological and seismic site characterization studies, site classification systems are assigned in seismic hazard assessments. The objective of the research is to determine the regional and local seismic soil conditions (i.e., shear wave velocities, soil predominant periods and soil amplification factors) and to characterize the soil profile of the sites in this region by the help of surface geophysical methods. These studies have been supported by engineering geological and geotechnical field studies carried out prior to and during this study. By integrating these studies, local soil conditions and dynamic soil characteristics for the study area have been assessed by detailed soil characterization in the region. As a result, seismic hazard assessments have been performed for Çubuk and its close vicinity with the aid of Geographical Information Systems (GIS) through establishing seismic characterization and local soil conditions of the area.

Keywords: Surface Geophysical Methods, Local Soil Conditions, Seismic Hazard Assessments, Plio-Quaternary Sediments, Çubuk, Ankara

ÖZ

ANKARA'NIN KUZEYİNDEKİ PLİYO-KUVATERNER ZEMİNLERİN DİNAMİK KARAKTERLERİNİN VE YEREL ZEMİN KOŞULLARININ YÜZEY DALGASI YÖNTEMLERİ İLE BELİRLENMESİ

Arif Mert Eker

Yüksek Lisans., Jeoloji Mühendisliği Bölümü

Tez Yöneticisi : Prof. Dr. Haluk Akgün

Ortak Tez Yöneticisi: Dr. Mustafa Kerem Koçkar

Temmuz 2009, 145 sayfa

Bu çalışmanın amacı Ankara'nın kuzeyindeki Üst Pliyosen'den Kuvaterner'e (Pliyo-Kuvaterner) kadar olan zeminlerin dinamik karakterlerinin mühendislik jeolojisi, jeofizik ve jeoteknik arazi çalışmalarıyla ve yerel zemin koşullarının yüzey dalgası yöntemleri ile belirlenmesini kapsamaktadır. Mühendislik jeolojisi ve jeoteknik zemin karakterizasyonu çalışmalarına bağlı olarak proje alanındaki zemin sınıflandırma sistemleri, sismik tehlike değerlendirmeleri için belirlenmiştir. Bu amaç doğrultusunda proje alanındaki bölgesel ve yerel sismik zemin özellikleri, kayma dalgası hızları, yer salınım periyotları ve zemin büyütme oranları ile karakteristik zemin profilleri yüzey jeofiziği yöntemleri yardımıyla belirlenmiştir. Bu çalışmalar, daha önceden yapılmış ve bu çalışma ile yapılan mühendislik jeolojisi ve jeoteknik arazi çalışmalarıyla desteklenerek bir bütünsellik sağlanmıştır. Daha sonra, bölge için detaylı zemin karakterizasyonlarının yapılması sonrası çalışma alanının yerel zemin koşulları ve dinamik zemin karakterleri belirlenmiştir. Sonuç olarak, zeminlerin sismik karakterizasyonları yapılarak ve yerel zemin koşulları belirlenerek Coğrafi Bilgi Sistemleri (CBS) yardımıyla Çubuk ilçesi ve çevresi için sismik tehlike değerlendirmeleri gerçekleştirilmiştir.

Anahtar Kelimeler: Yüzey Jeofiziği Yöntemleri, Yerel Zemin Koşulları, Sismik Tehlike Değerlendirmeleri, Pliyo-Kuvaterner Sedimanlar, Çubuk, Ankara

To my love and happiness, Fatma Eker

and

To my family, Menşure, İlker and Berk Eker

ACKNOWLEDGMENTS

I must acknowledge and express my deepest gratitude to my supervisor Prof. Dr. Haluk Akgün for his understanding, guidance, patience and continuous support during my Master Program and this thesis. I am indebted to him for giving me the chance to study on this project and for his trust in my work.

I would like to express my respectful gratitude to my co-supervisor Dr. Mustafa Kerem Koçkar for his invaluable guidance, comments, motivation and support at every stage throughout this study.

I would like to acknowledge the financial support provided by the Middle East Technical University Research Fund Project (BAP-2007-03-09-05). I am very grateful for this support.

Additionally, I would like to thank The Scientific and Technological Research Council of Turkey (TUBİTAK) for financial support throughout my master program. I am very thankful for this support.

I would like to especially thank Kaya Engineering, Consulting, Commitment and Trading Inc. for who provided the assistance and conducted the all field tests implemented in this study.

I would like also to thank several governmental organizations including, General Directorate of State Hydraulic Works (DSİ), especially General Directorate of Mineral Research and Exploration (MTA), General Directorate of Highways (TCK), Çubuk Municipality, Earthquake Research Institute (AFET), General Directorate of Provincial Bank and General Directorate of Railways, Harbors and Airports Construction Railroad (DLH) for their documentation supports.

I would like to thank Mr. Mete Mirzaoğlu (AFET), Mr. Aydın Durukan (TCK), Mr. Güven Karaçuha (DSİ), Mr. Yusuf Ziya Coşar (MTA), Mr. Adem Tuğluca (The Mayor of Çubuk), Mr. Kıvanç Okalp, Mr. Evrim Sopacı, Mr. Aydın Çiçek (METU) and Özgür Erecekler for their contributions and assistances during the study. I am very grateful for their contributions.

I would like to especially thank Mr. Selim Cambazoğlu and Mrs. Fatma Eker for their infinite support and great contribution through out my thesis study.

Finally, I would like to express my deep thanks to my wife Fatma Eker and my family for their patience, endless moral support and encouragement during my master program.

TABLE OF CONTENTS

LIST OF TABLES

TABLES

LIST OF FIGURES

FIGURES

CHAPTER 1

INTRODUCTION

1.1. Purpose and Scope

The purpose of the study is to determine the local site effects, to characterize the dynamic soil properties and to develop a seismic hazard map of the Upper Pliocene to Pleistocene fluvial sediments and especially Quaternary alluvial deposits of the Çubuk district and its close vicinity. By this study, sediment conditions were determined and soil profiles were characterized by non-invasive seismic methods such as the Microtremor Array Method (MAM) and the Multi-Spectral Analysis of Surface Wave (MASW) Method at different locations. To meet the requirements of preserving high resolution at shallow depths while also extending the Vs measurement to greater depths, a combined usage of the active and passive surface wave methods was adopted. Additionally, soil predominant periods and soil amplification factors of the weak soils in the region have been determined by the microtremor method through measuring natural seismic noise of the soil in a short period. All of these studies have been supported by geological, hydrogeological, engineering geological/geotechnical field studies and geotechnical boreholes carried out prior to and during this investigation.

1.2. Location of the study area

The study area covers the Çubuk district and its close vicinity, mainly the north part of the Çubuk Plain which is situated approximately 38 km north of Ankara. The location of the study area is given by Figure 1.1.

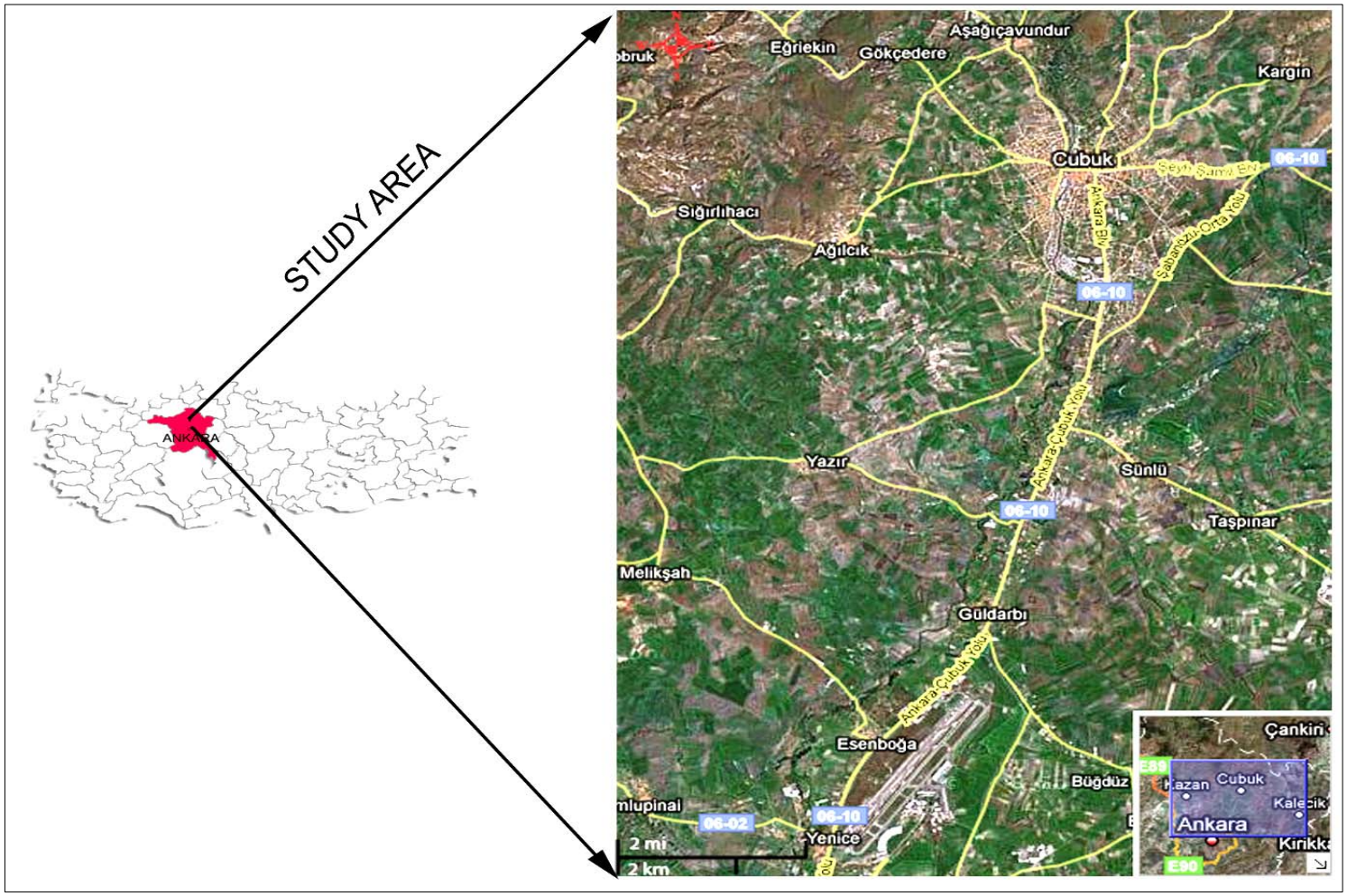

Figure1.1. Location map of the study area.

The study area is 120 km^2 in size and covers a number of villages such as Güldarpı, Yazır and Ağılcık at the west; Sünlü and west of Taşpınar at the east; north of Esenboğa at the south and south of Aşağı Çavındır at the north in addition to the Çubuk district. The area is included in 1/25.000-scaled topographic quadrangles of H30-d1, H29-c2, H30-a4 and H29-b3; and, 1/100.000 scaled geological maps of Ankara H29 and Çankırı E16. The investigation was conducted at a moderately populated area with mostly residential settling and a lesser amount of small to large industrial buildings which has a major potential for increased urbanization in the near future. The area is developing towards the western and eastern parts of the district with a bus terminal at the planning stage, relatively small industrial estate and building complex, villa, and apartment blocks as residences and vacation homes, etc. The investigated part of the Çubuk plain covers mostly Plio-Quaternary and especially late alluvium soils and these mentioned structures are also present at these deposits.

The Çubuk plain is surrounded by the Idris Mountain (1992 m) in the east; Aydos (1896 m) in the north; Mire (l635 m), Çicekdağ (1388 m), and Sedlik Hill (1535 m) in the west ; Aşar (1409 m), Meşelik (1350 m) and Hüseyin Gazi Ridges in the south. The elevation of the plain varies from 910 to 1030 m as can be seen in Figure 1.2. Additionally, the area has a potential of being seriously affected by a possible earthquake occurring along the Çubuk Fault Zone that is thought to be a continuation of the Dodurga Fault Zone a sub-fault belt of the North Anatolian Fault System which is one of the most prominent active fault systems in Turkey with a significant earthquake potential. Seismic activities that have occurred in this region recently, especially the Orta earthquake (M_W=5.9) in June 6th, 2000 and the Çubuk earthquakes (M=4.0) in June 6th, 2000; (M_l = 4.6) in December 29th, 2004 and in January 31st, 2008 (M_l = 4.9) are the most important indicators of this phenomenon. Because of this reason, sediment conditions and soil profiles were characterized in regards to seismic hazard assessment.

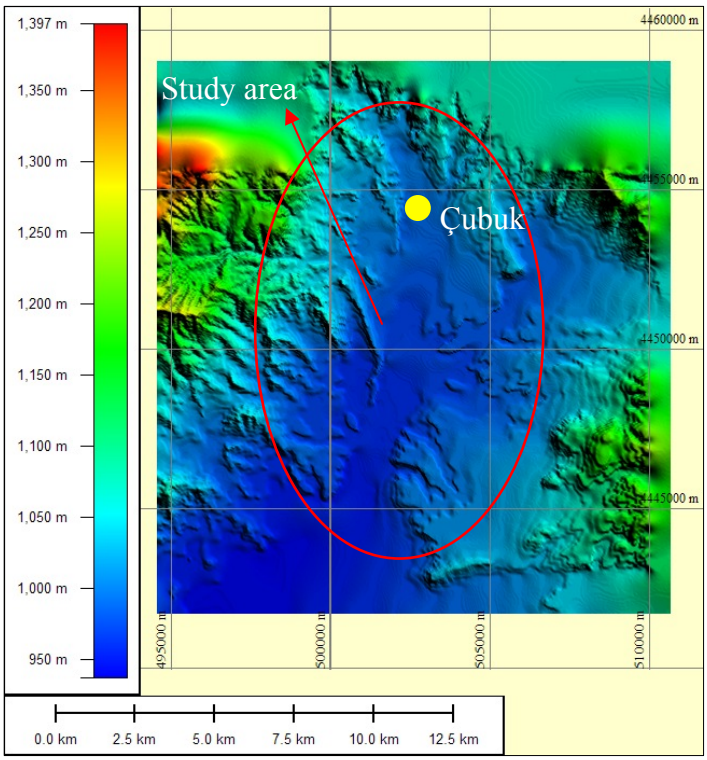

Figure 1.2. Digital elevation map of the study area generated from topographic maps of General Command of Mapping in Global Mapper Software.

1.3. Methods of the study

In the content of this study, sediment conditions were determined and soil profiles were characterized by surface geophysical methods at different locations. Non-invasive seismic methods were used to obtain a 1-D shear wave velocity profile of the subsurface at 51 sites. Two measurements were taken at each of the 41 sites for passive and active surface wave methods. 10 of the sites were characterized by the passive method only. The Multichannel Analysis of Surface Wave Method (MASW) and the Microtremor Array Method (MAM) were used as active and passive surface wave methods, respectively.

Soil predominant periods and soil amplification factors of the weak soils in this region have also been determined by microtremor measurements recorded at the 106 sites. The microtremor results were obtained by using the Nakamura technique

(1989) and all of the studies have been supported by geological, engineering geological, hydrogeological, geotechnical studies and by the information supplied by geotechnical boreholes carried out prior to and during this investigation. By integrating all of the studies carried out, local site conditions and dynamic soil characteristics of the study area have been assessed by detailed geotechnical seismic site characterization in the region. Based on the results, site classification systems were utilized for seismic hazard assessment studies followed by a preparation of a seismic zonation map of the site utilizing GIS software.

CHAPTER 2

REGIONAL GEOLOGY

2.1 Introduction

The purpose of this chapter is to provide an overview of the regional geologic and tectonic setting of the study area and to indicate the general character and distribution of the major geologic and structural units. Rather than carrying out a detailed geologic survey and examining the geological problems of the study area, relevant information was obtained through a detailed literature review.

The geologic, tectonic and geomorphologic characteristics of Çubuk and its surrounding regions have been studied by various researchers since the twentieth century. Particularly, geological characteristics of this region have been studied by Chaput (1931), Salamon-Calvi (1940), Salamon-Calvi and Kleinsorge (1940), Chaput (1947), Lahn (1949), Bailey and McCallien (1950), Erol (1954, 1955 and 1956), Erentöz (1975), Kasapoğlu (1980), Akyürek et al. (1984, 1996), Tokay et al. (1988), Koçyiğit and Türkmenoğlu (1991); geomorphological characteristics of Ankara region has been studied by Salamon-Calvi (1936), İlyüz (1940), Pfannenstiel (1941), Chaput (1947), Erol (1964, 1973, 1980 and 1993) and Erol et al. (1980); tectonical characteristics of this region have been studied by Bailey and McCallien (1953), Erol (1961), Ketin (1959) and Koçyiğit (1987, 1989, 1991 and 2003).

The scope of this study is to mainly investigate the engineering geological, seismic and geotechnical site characteristics, and to perform site classification of the Upper Pliocene to Pleistocene fluvial red clastics and Quaternary alluvial and terrace

deposits located at the Çubuk district and its close vicinity which is situated towards the north of Ankara. In this respect, based on the tectonic regime and style of deformation, the units exposed in and nearby the study area are classified into two categories, namely, paleotectonic units or basement rocks, and neotectonic units. The paleotectonic units are outside the scope of this study and hence, only brief information regarding their lithostratigraphical characteristics will be given in Paleotectonic units section. However, the neotectonic units, Upper Pliocene to Pleistocene fluvial red clastics and Quaternary alluvial and terrace deposits, are described in more detail in regards to their geologic, geomorphologic, paleogeographic and neotectonic characteristics.

2.2. Paleotectonic units

Basement rocks of the area are the Triassic schists and greywackes with carbonate blocks present in the northwest, west and east of the Çubuk Plain. Upper Miocene-Lower Pliocene volcanics and Pre-Miocene rocks are exposed in the north, northeast and northwest, and east and northwest, respectively, which delineate the boundaries of the study area (Figure 2.1).

Çubuk depression is occupied by both lacustrine and fluvial clastics and contains volcanic intercalations (Koçyiğit and Türkmenoğlu, 1991). This depression area is indicated as a tectonic basin by Tabban (1976). Basement rocks of the area are green schists and detrital rocks such as greywacke and Permian crystalline limestone (Kupan, 1977). This unit is classified as the Elmadağ formation belonging to the Ankara group of Middle-Upper Triassic age at the base of the stratigraphic sequence in the region (Akyürek et. al, 1984). It is a metamorphic unit in the green schist facies composed of metadetritic rocks that are highly deformed, and have undergone low-grade metamorphism, and contains intercalation of meta-sandstone, shale, mudstone, meta-conglomerate, tuff and agglomerate with Permo-Carboniferous limestone blocks and recrystallized limestone (Erol, 1961; Akyürek et al., 1984 and Duru and Aksay, 2002). Elmadağ formation grades upwards into Middle-Upper Triassic Keçikaya Formation consisting of generally grey and white colored, crystallized and medium to thick bedded limestone (Akyürek et al., 1984).

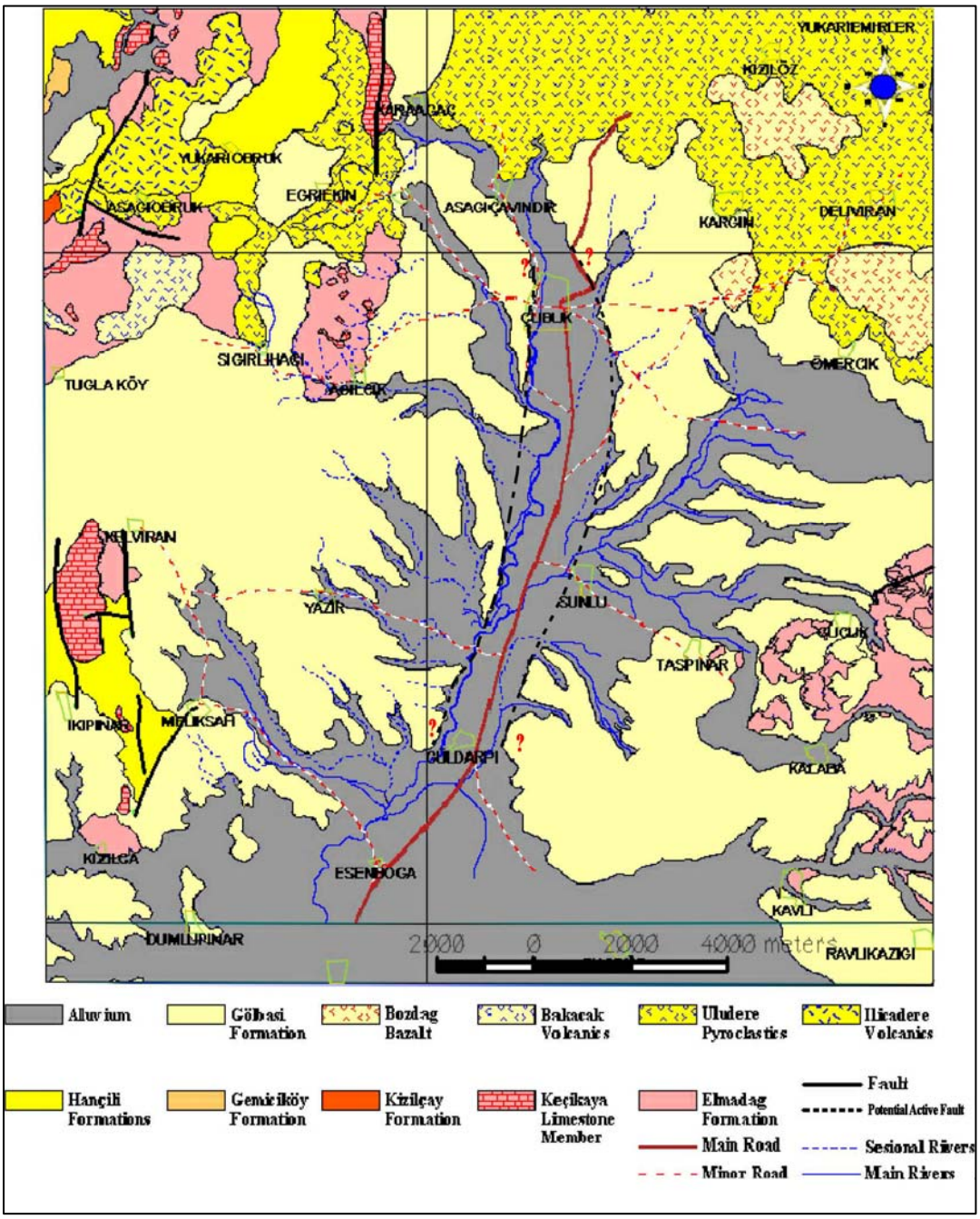

Figure 2.1. Geological map of the study area (modified from MTA, 2008 digital database based on the results of the field studies).

The limestones which are preserved as cap-rocks on the hills are folded, and faulted. The thickness varies between 50 and 300 m in the investigation area (Kupan, 1977). Also, according to DSI (1979), the bedrock depth is greater than 300 m at center of the basin.

The volcanics of Early-Middle Miocene age are described considering their compositions and times of eruptions. They are known as the Galatia massive and are interfingering with each other, and are identified from bottom to top as: the Karasivri, Kirazdağı, Ilıcadere, Deveören and Bakacaktepe volcanics. Except the Ilıcadere volcanics, the other volcanics of the Galatia massive are present throughout the study area. The Uludere pyroclastics (Mamak formation) form the pyroclastic products of these volcanics (Duru and Aksay, 2002). Uludere pyroclastics are classified as the Mamak formation by Akyürek et al (1984), which is the classification that is preferred in this study. As can be seen in Figure 2.1, at the northern part of the study area, Miocene Tekke volcanics (are present throughout the periphery of the area) and the mostly Mamak formation composed of andesite, trachyandesite, basalt, agglomerate, tuff and agglomerate, tuff, andesite are exposed, respectively. Mamak formation is formed by deposition of volcanic material of varying particle size which was transported to the lakes while at the same time Tekke Volcanics was being formed (Akyürek et al., 1984).

The lacustrine environmental products, which are interfingering with the volcanics and pyroclastics, on the other hand are distinguished as the Hançili formation. This unit is composed of clayey limestone, marl, claystone, sandstone, conglomerate, shale and tuff (Akyürek et al., 1984). Lignite levels are present between the upper series of the Miocene green colored marl and clay layers (DSI, 1979). These lacustrine sediments can be distinguished from the other Miocene sedimentation by the gypsiferous marl and limestones (Kupan, 1977).

The Bozdağ basalt is composed of the basaltic volcanics, which have started the activity in the region during Late Miocene; and cut the underlying volcanics. It is the last product of the volcanic activity in the region spread over the Upper Miocene and

Pliocene deposits (Akyürek et al., 1984). At the uppermost part of the sequence, terrestrial-lacustrine deposits of Pliocene age cover unconformably all of the older units (Figure 2.1).

2.3. Neotectonic units

The Çubuk depression area or tectonic basin is occupied by both lacustrine and fluvial clastics and contains volcanic intercalations (Salomon-Calvi and Kleinsorge, 1940; Tabban, 1976; Koçyiğit and Türkmenoğlu, 1991). They are folded or steeply tilted in places and they are overlain unconformably by the horizontal or gently dipping Plio-Quaternary sediments of neotectonic units (Koçyiğit and Türkmenoğlu, 1991).

After the regression of the Miocene lake, mostly continental deposition of Pliocene was formed at the Çubuk basin. The Gölbaşı formation consisting of terrestrial – lacustrine deposits of Pliocene age is composed of unconsolidated to poorly consolidated clastics which are grey, grizzle and red colored, unsorted, polygenetic in composition that incorporates conglomerate, sandstone and siltstone (Duru and Aksay, 2002). Generally, deposits are unsorted but horizontally bedded at some places. Conglomerate is widespreadly present as a result of debris flow between sandstone and siltstone deposits (Akyürek et al., 1980). Kupan (1977) divided the Pliocene units into two groups because of differences in their color, texture and lithology. These groups are Early Pliocene units containing sand, gravel and gypsum sediments and Late Pliocene units with river deposits of clay, sand and gravel.

2.3.1. Upper Pliocene to Pleistocene sedimentary deposits

As a result of regression of the Miocene lake in the Çubuk Plain, mostly continental deposition of Pliocene age was formed at the Çubuk basin. Lacustrine origin Pliocene deposits which constitute the lower levels settled down during the short lacustrine period of Pliocene (DSI, 1979). Generally, pink colored Lower Pliocene deposits are mainly composed of lava origin transported gravels and tuffs mixed with marl and clay and a little amount of nodular limestone (Kupan, 1977). These

lithologies are present as a thin band around Mire Mountain and extend towards the north of the Çubuk plain. Although Lower Pliocene units show variations in facies, the overlying deposits show fully fluvial environment characteristics all over. The unit includes light tile red and red colored clay, sand and gravel. White colored limestone nodules characterize the unit. Upper Pliocene fluvial sediments generally fill the depression area of the river basin (Kupan, 1977).

Stratigraphic characteristics of the Upper Pliocene fluvial sedimentary units (Yalıncak Formation) consists mainly of unsorted loose debris flow conglomerate, braid plain conglomerate to sandstone and clay-bearing finer clastics of flood plain origin from bottom to top (Koçyiğit and Türkmenoğlu, 1991). Briefly, as can be seen in Figure 2.2, the lower parts of the Yalıncak Formation is composed of debris flow conglomerate with rare carbonate concretion, and wedge to trough cross-bedded conglomerate to sandstone. The lithofacies and the sedimentary structures of these two units show that they were deposited in a alluvial fan and braidplain type of depositional setting. On the other hand, the thicker half of the Yalıncak Formation contains clay bearing finer red clastics with abundant carbonate concretions, and displays well-developed synsedimentary features, such as channel and growth faults. The Yalıncak formation continued in a flood plain under the tectonically unstable condition (Koçyiğit and Türkmenoğlu, 1991).

In general, the grain size distribution of the basin fill becomes finer towards the center of deposition. These sedimentary units lie uncomfortably on the irregular erosional surface of the highly deformed older basement rocks, and are overlain by Quaternary alluvial and terrace deposits or, are rarely thrusted over by older rocks (Koçyiğit, 1991).

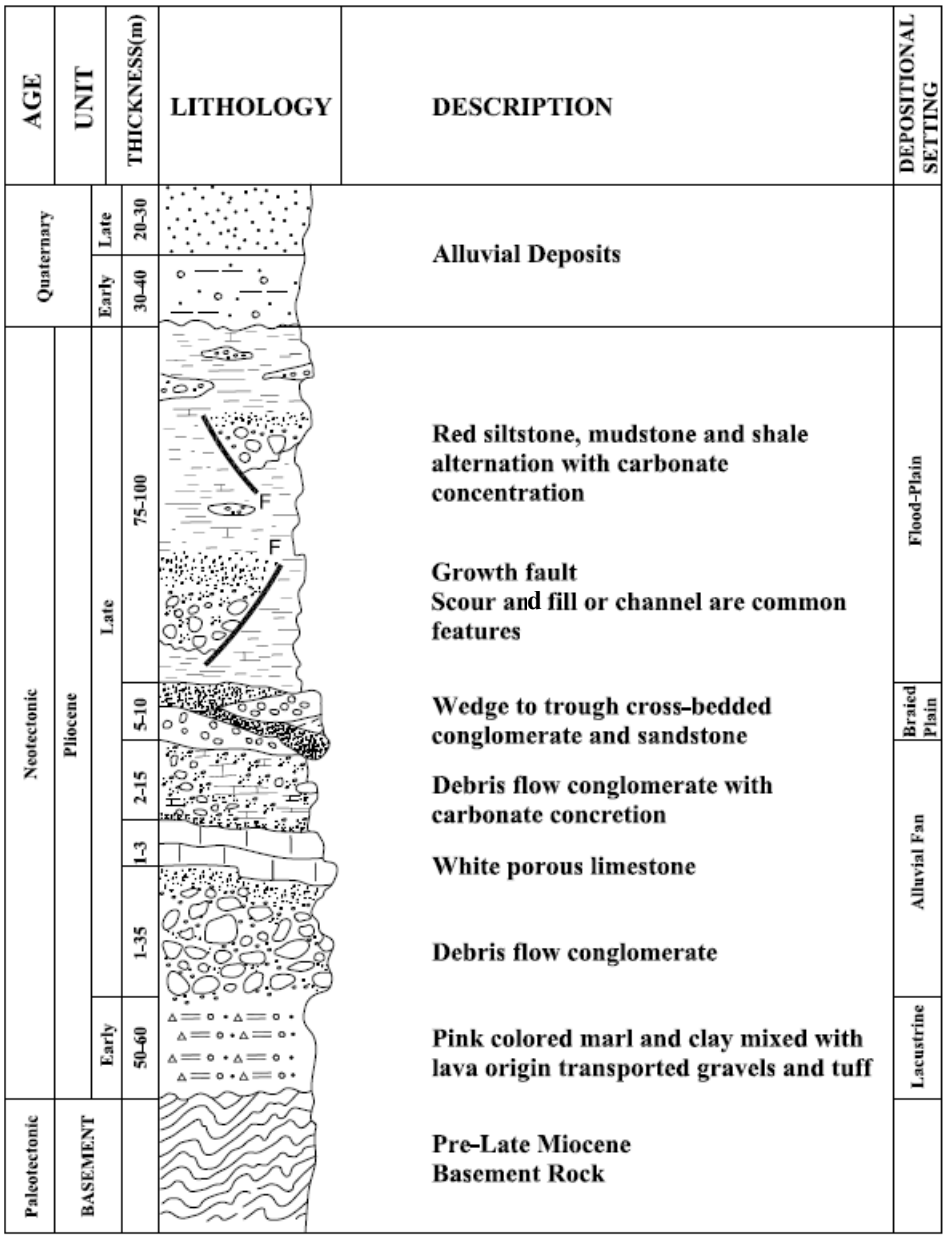

Figure 2.2. Generalized stratigraphic columnar section of the Çubuk Basin (compiled from Kupan, 1977; Koçyiğit and Türkmenoğlu, 1991 and Kasapoğlu, 2000).

The source of the continental Pliocene material (Upper Pliocene) is weathering. As a result of this, these Pliocene materials are closely related with the parent rock both in material type and in color. The Upper Pliocene fluvial deposits near the Paleozoic greywacke is red and brown colored in the Çubuk Plain, but the deposits near Lias rocks are red colored around Körselik village. That is; the Upper Pliocene fluvial deposits possess the same material as the near basement rocks (DSİ, 1979). The thickness of Pliocene sedimentary deposits varies between 50 and 100 m in the Çubuk Plain. The horizontal or gently dipping Upper Pliocene fluvial deposits rest unconformably over Bozdağ basalt and the older units, and show a considerable lateral extension.

2.3.2 Quaternary sedimentary deposits

The Çubuk basin extends nearly 20 km from northwest to southeast. The study area covers approximately 14 km of this length. Approximately 60 km^2 of the study area includes the Quaternary deposits (Figure 2.1). The width of the plain increases towards the south and reaches the maximum width, 7 km, at Esenboğa village in the study area. The regions containing recent gravel, sand and clay deposited by fluvial activity are classified as Quaternary deposits. The terraces consisting of gravels and the materials forming alluvial cones can be classified as Lower Quaternary deposits, noting that the Upper Quaternary deposits contain sand, clay, silt and gravel that are present at the stream beds of the Çubuk Plain. The Quaternary alluvial fill is widely exposed at the central parts of the fault bounded depression drained by the Çubuk River. The Quaternary alluvial fill forms a relatively thick layer that disconformably covers the older units. The alluvial fill contains both coarse grained marginal and fine grained axial depositional system. The coarse grained depositional system is composed of terrace and alluvial fan conglomerates deposited by debris flow and braided rivers. The axial depositional system consists of fine grained alluvial plain sediments such as sand, silt and clay. Terrace deposits are exposed at different elevations at the margins of the fault bounded depression. These mark an active tectonic uplift in the region (Koçyiğit, 1991).

2.3.2.1. Quaternary terrace deposit

In the study area, Quaternary alluvial fill and terrace sediments were deposited by the flood waters in the fault-bounded Çubuk Basin throughout the flood plains in a nearly northeast-southwest direction of the Çubuk River and its tributaries namely Koyunözü, Ravlı and Kızılhisar Creeks at the east, and Azman and Karapınar Creeks at the west. The terrace sand alluvial cones are characteristic of Quaternary deposits which are defined by clay, sand and gravel deposited by the rivers. The coarse elements forming the alluvial cones have been introduced to the old alluvium with a thickness varying from 30 to 40 m (Kupan, 1977).

Quaternary alluvial fills are considered as recent and terraces as considered as older sediments on the basis of their morphology, even though they might be confused with Upper Pliocene sediments. The study region contains the early alluvium terraces at the plains of the area. Generally, the terrace deposits which are mostly formed by erosional setting are separated with a thin gravelly layer overlying older basement units. Terrace deposits containing grey colored conglomerate without limestone nodules are present (DSİ, 1979). The differentiation between this unit and the Upper Pliocene red colored conglomerate can be made by means of the existence of this limestone nodule (Kupan, 1977; Koçkar, 2006). Furthermore, regarding the depositional setting of the fluvial clastics, even though larger sediment particles have naturally deposited near the edges of the basin, some thin sand and gravel layers and lenses are encountered in the clay deposits in the middle of the flood plain due to sediments which have been disorderly and irregularly deposited by flood waters. Due to these reasons, since the stratigraphic characters of the Quaternary sediments and the Upper Pliocene sediments could not be completely differentiated to date, they have been defined as a single geologic unit on the geological map of the Çubuk region (Figure 2.1.).

2.3.2.2 Quaternary alluvium deposit

Çubuk River is the main river of the basin and traverses the basin. Main tributaries joining the Çubuk River in the north-south direction from the east are Koyunözü,

Ravlı and Tilkiinleri Creeks, and from west Alaçoral, Bostanlık, Yaylaca, Azman, Karapınar and Ulu Creeks. The Çubuk Rivers, Sirkeli Creek and other creeks flow throughout the plain with meanders. Upper Quaternary deposits composed of gravel, sand, clay and silt have been deposited by flood waters along and both sides of the recent river beds and disconformably overly the Pre-Quaternary units. These sediments have not been settled long enough to show any appreciable signs of soil forming.

The alluvium of the Çubuk River is about 1 km wide at the basin. Around the Esenboğa village, this unit extends more than 1 km. Groundwater level in the inner basin is close to the surface in general, though it varies within the alluvium, depending upon the soil characteristics of the depositional environment and proximity of the major course of the recent stream beds. It is gradually deeper beneath the terrace and older deposits bordering the basin. It ranges between 0.75-5.22 m (DSİ, 1979) and it is 4.67 m on the average (this study). Also, thickness of the recent alluvial deposits observed along the Çubuk River and their major tributaries approximately range between 16 – 30m (Tabban, 1976; DSİ, 1979; Erol, 1980 and this study).

2.4. Paleogeography of the region

Conglomerate, sandstone, siltstone and sandy limestone deposition took place at the shelf margin of the sea at Late Triassic. This formation settled down at the continental site of the deep marine environment. Pelagic sediment, turbidity currents and partly debris flow have affected the formation. Effect of the turbidity flows increased at the region from time to time. By these flows, the sediments were carried towards to the deep sea. The tectonic movements, caused by tensile forces, led to volcanic products which flew over the detritic materials and intercalated with the sediments at different times. The same forces caused tectonic activities such as vertical movements at the basin. These movements resulted in sliding, collapsing and rolling of the rocks at the basin, so Permian Limestone was transported into the basin as blocks from the continental slope. At Late Triassic, the basin was mostly filled by sedimentation and shallow marine carbonates of the Keçikaya Formation deposited

at the environment. At the end of the Triassic, as a result of the compression forces, sedimentary rocks, volcanics and blocks which form the Ankara Group gained a complex structure and partly rised above the sea level (Üzüm, 1984 and Akyürek et. al., 1984).

In the Miocene, the depressions, which were formed due to the weathering, were filled with Miocene lakes. The sediments which were deposited were mixed with lava and tuff. Volcanic activities also took place in Late Miocene and volcanic products interstratified with the lacustrine units. The sequences contain poorly consolidated pebbles, different rock groups and horizontally bedded sedimentary deposits (Akyürek et al., 1984 and Üzüm, 1984). It also appears that the lacustrine environments gradually disappeared by Pliocene. Meanwhile, the volcanic activities frequently continued in the surrounding regions, therefore the sedimentary sequences intricated with the products of these activities (Hatipoğlu, 1996).

At the end of the Miocene, folding and faulting caused the uplifting of the lands and the lakes have been filled by fluvial sediments. The rivers formed under the moist and rainy climatic conditions in the Pliocene. Deposition of the fluvial sediments has started at the piedmonts of the Mire, Aydos and İdris Mountains and the fluvial sediments filled these depression areas (Erol, 1980). At that time, Upper Miocene or Post-Miocene normal faults occurred at both sides of the basin. The center of the plain was affected excessively as a result of tectonic movements and subsided along the NE-SW trending faults. The faults present at the west and east of the basin caused to form a graben structure at today's plain. This led to thick sedimentary deposits at the basin along the faults (Kupan, 1977; DSI, 1979; Erol, 1980, and Koçyiğit and Türkmenoğlu, 1991). The exact location of the normal faults can not be defined due to the excess cover materials. Therefore, these faults are shown by dash lines on the geological map of the study area (Figure 2.1). Also, they are illustrated on the seismotectonic map of the area given in Figure 2.4. The last volcanic product of the region is the basalt which spread over the deposits in Late Miocene and Pliocene age. At the end of the Pliocene, the volcanic activity ceased and the alluvial fan and fluvial sediments were deposited in the basin (Akyürek, 1984).

In Miocene and Pliocene times, as mentioned above, the basin has been filled with material brought by streams. As the streams that formed subsequently over these deposits have been connected to the outer drainage, they started to cut through their beds and thus the basin has started to be discharged while static terraces have started to form on the riverbanks. The Çubuk River which forms the main river network of the basin has connected to the outer drainage by cutting the elevated andesitic area as a strait where Çubuk Dam I is located today (Erol, 1973; Kupan, 1977).

Presence of filling materials at the valley base is the evidence of the discontinuous behavior of the basin depletion and vertical river excavation (Erol, 1980). The Çubuk valley was excavated nearly 20 meter below the recent topography at that time and then depositional settings took over the erosional activity. At Çubuk river valley, this process has occurred a few times (Pfannensriel, 1941). These support that Pleistocene terraces are the result of a cut and fill sequence and as such their present surfaces are depositional. This means that these deposits are normally consolidated deposits (Sürgel, 1976). Therefore; these sediments have not been settled long enough to show any appreciable effect of soil forming processes (Koçkar, 2006). This is also confirmed by the result of this study.

2.5. Structural geology of the Çubuk Region

The study area is situated within the Çubuk plain located towards the north of Ankara. It has a north-south trend. The Çubuk plain is a depression in between rises of the Paleozoic Elma - İdris - Tekebeli Massifs and Paleozoic-Mesozoic series of Kuşçu - Karyağdı - Mire - Aydos Mountains, and this geologic depression continues towards the Tezme Stream – Şabanözü basins at the northeast. The plain is cut across by the Çubuk River in the northeast-southwest direction and also the nearly east-west oriented several sub-branches are joining to this major river of the area. The Çubuk plain is developed within this depression (Erol, 1956). The area mostly constitutes fluvial and alluvial deposits that are formed in and near the fault bounded depression as a result of fault controlled continental sedimentation.

At a regional scale, the area is located within the boundaries of Central Anatolia Province which is the broad and structurally triangular shaped area outlined by the Kesikköprü and the Seyfe Fault Zone in the east, the Salt Lake Fault Zone in the southeast, the İnönü-Eskişehir Fault Zone in the west-south-west, and the North Anatolian Fault System in the north (Figure 2.3). The central part of Anatolia includes folds, normal faults, low to high angle thrust faults, strike slip faults and fault parallel depressions like Çubuk Plain covered by widespread Quaternary alluvial deposits (Koçyiğit, 1991). "Based on the nature of the tectonic regime, these geological structures can be classified into two major groups which are pre-Late Pliocene and Late Pliocene-Quaternary structures. The former group is dominated by north trending southeast-vergent, thrust faulted monoclines, northeast (NE) trending strike-slip fault with thrust component, approximately east-west (E-W) trending strike-slip faults, and northeast (NE) trending folds. Despite of the fact that the first group of structures was inherited from the last phase of the former collisional tectonic regime, these structures were reactivated during the neotectonic regime that has operated since the Late Miocene. Consequently, the first group of structures indicates that a northwest-southeast (NW-SE) directed contraction prevailed before Upper Pliocene in the Çubuk region. The second group of structures comprises the NNE trending normal faults, NE and NW trending sinistral and dextral strike-slip faults, oblique-slip fault, ENE trending thrust faults and folds. These Upper Pliocene-Quaternary structures collectively form a well-developed strike-slip fault system that suggests an approximately N-S directed contraction continuing since Upper Pliocene in the Ankara Region. Thus, these two groups of structures reveal that the contractional stress orientation in the progressive intercontinental deformation in the Ankara region has changed from NW-SE to NS direction during the neotectonic period since Pliocene" (Koçyiğit, 1991).

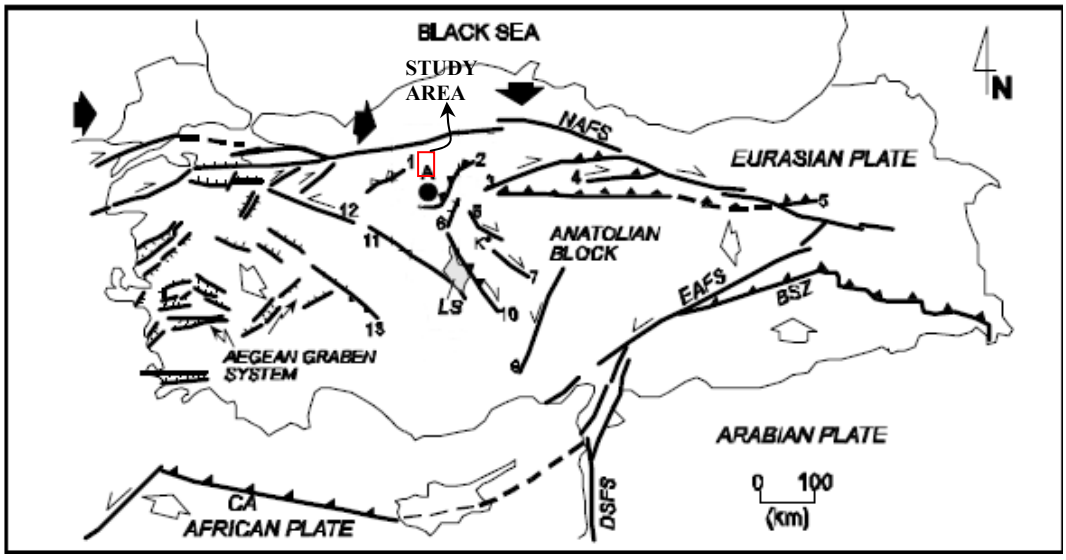

Figure 2.3. Simplified neotectonic map showing the general outline of the study area and some of the major neotectonic structures of Turkey. A-Ankara; LS-Salt Lake; BSZ-Bitlis Suture Zone; CA-Cyprian arc; DSFZ-Dead Sea Fault Zone; EAFZ-East Anatolian Fault Zone; NAFZ-North Anatolian Fault Zone; 1-Beypazarı-Çayırhan faulted monocline; 2-Elmadağ imbricate thrust zone; 3-Kırıkkale-Erbaa fault; 4-Almus Fault; 5-Ankara-Erzincan Suture; 6- Seyfe Fault Zone; 7-Salanda Fault Zone; 8- Kesikköprü Fault Zone; 9-Ecemiş Fault Zone; 10-Salt Lake Fault Zone; 11-Eskişehir Fault Zone; 12-İnegöl fault; 13- Akşehir-Simav Fault Zone. Note that the black arrows show the orientations of the maximum compressive stresses along the NAFZ; white arrows show the sense of the plate motions and half arrows show the relative sense of movements on the faults (Koçyiğit, 1991 as reported by Koçkar, 2006).

Based on the type and nature of active tectonic regimes and related structures such as faults and basins, an intracontinental tensional neotectonic regime and oblique slip normal faulting characterize the study area (Koçyiğit, 2003). There are many faults having capability to produce frequently small to moderate seismic events present in the Çubuk Region and the surrounding area. In the area, as can be seen in Figure 2.4, the main tectonic unit is the Çubuk Fault Zone which is a normal fault with an approximate trend of N20º - 30º (Kupan, 1977, Koçyiğit, 1991). It defines the margins of the NE-SW trending Çubuk basin. The tectonic movements are the first sign of the beginning of today's Çubuk Plain formation (Erol, 1980). The basin has taken the form of a graben due to normal faulting (State Hydraulic Works, DSİ, 1979).

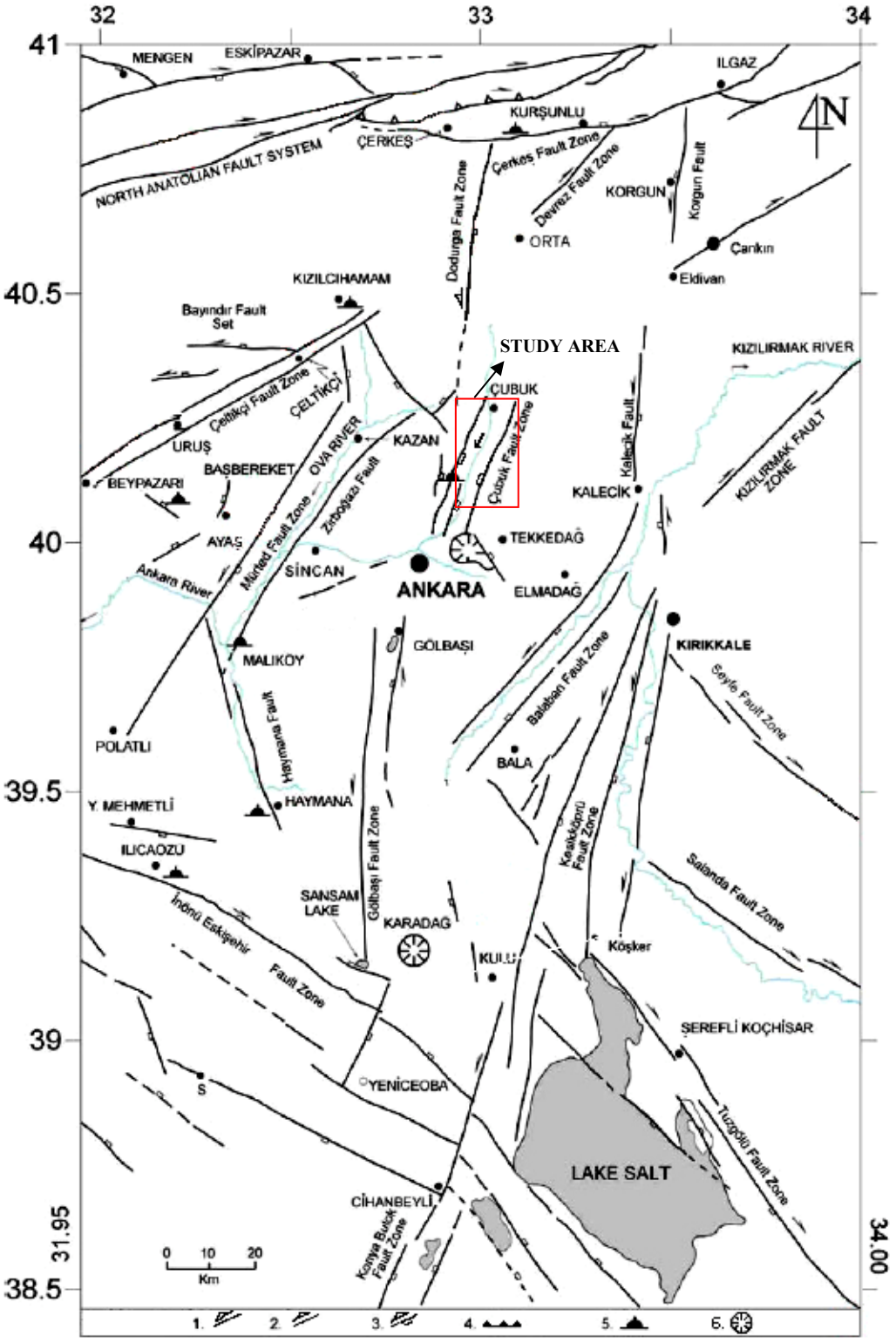

Figure 2.4. Simplified seismotectonic map of the Ankara region and its vicinity (Koçyiğit 2003, as reported by Kaplan, 2004). 1. sinistral strike-slip fault, 2. dextral strike-slip fault, 3. strike-slip fault with normal component, and oblique-slip normal fault with considerable strike-slip component, 4. thrust fault, 5. thermal spring and 6.volcanic center.

As a large scale around Ankara, other faults, which are incapable of producing large destructive seismic events, are the Çeltikçi Fault Zone, Mürted Fault Zone, Kalecik Fault Zone and Balaban Fault Zone from east to west. This means that the area is not threatened by the direct effects of the earthquakes. However, from the regional point of view, the area can be affected indirectly by the surrounding the large scale fault zones. Among the fault zones which are capable of producing destructive earthquakes with magnitudes greater than 6.0, the North Anatolian Fault Zone (NAFZ), the Çerkeş-Kurşunlu Fault Zone (ÇKFZ) and the Dodurga Fault Zone (DFZ) are the most prominent ones to consider as potential sources of earthquake hazard due to proximity to the area. The area has a significant potential to be affected by the DFZ and NAFZ located at nearly 30 km and 60 km away from the area, respectively. Also, the sources of the historical and the recent earthquakes indicate that Çubuk and its close vicinity have been affected seriously by the significant seismic events that had taken place along these fault zones.

The above mentioned ÇKFZ and DFZ, having a capability to produce destructive earthquakes have the anastomosing type geometry and the splay type geometry fault zones along the NAFZ and detailed information about these fault zones are as follows:

The North Anatolian Fault Zone (NAFZ) is an intercontinental transform fault boundary between the Eurasian plate in the north and the Anatolian Plate in the south (Şengör, 1979). NAFZ is the major tectonic feature of Turkey. It is a morphologically distinct and seismically active fault where countless damaging earthquakes have occurred throughout history. The NAFZ is an approximately 1500 km long, broad arc shaped, dextral strike-slip fault system running sub-parallel to the Black Sea coast from eastern Turkey (Karlıova) in the east to Greece in the west at North Anatolia (Bozkurt, 2001). The NAFZ has 4 –110 km wide dextral shear zone and it starts around Karlıova in the east shows firstly NW, and then E-W, and finally SW trends from the east to the west (Koçyiğit, 2009). The NAFZ bends towards the north and results in a northward convex arc at the North Anatolian Province that is

characterized by a number of strike-slip faults and faults with strong E–-W thrust component (Koçyiğit, 1991 and Bozkurt, 2001).

Generally, the North Anatolian transform fault forms a wide belt of numerous, sometimes parallel, sometimes anastomosing strike-slip faults (Şengör, 1979). Therefore, according to distribution patterns or geometries along its length, two common geometry types can be observed along the NAFZ: (1) splay-type geometry, and (2) anastomosing-type geometry. The splay type is well developed in both the Erzincan-Çerkeş and the Marmara sections of the NAFZ. In the area between Erzincan in the east and Çerkeş in the west, a number of fault zones, fault sets and isolated faults of varying sizes branch as splay structures from the master strand of the NAFZ. These structures first trend E-W for some distance, and then bend southward and trend in an approximately NE-NNE direction, running into the Anatolian Plate for several hundreds of kilometers, cutting across and deforming it (Koçyiğit et al., 2000). The E-W trending sections of the splay faults displays fairly strike-slip character with some reverse components, whereas the NE to NNE trending sections mainly have the normal oblique-slip character (Bozkurt, 2001). Some of the well defined splay faults are the Kırıkkale-Erbaa, the Devrez and the Dodurga Fault Zones. The Dodurga Fault Zone with a 4-7 km width, 36 km length and approximately N-S trending sinistral strike-slip fault zone is a potential seismic source for the study area located between the Çubuk district and the northern part of the Çubuk Plain (Koçyiğit et al., 2000).

In the second pattern or geometry of the NAFZ, the master strand first bifurcates into several subfault zones, fault sets and isolated faults of varying sizes, and then they rejoin and rebifurcate several times, leaving behind a series of lensoidal highlands (pressure ridges) and lowlands (basins) whose long axes parallel the general trend of the master strand of the NAFZ. This pattern is the most diagnostic characteristic of the Kargı- East Marmara section of the NAFZ. Examples of subfault zones, fault sets and isolated faults having anastomosing geometry along the NAFZ in its Kargı-East Marmara section are, from east to west, the Ulusu-Gerede-Abant, Tosya, Çerkeş-

Kurşunlu, Karadere-Kaynaşlı-Mengen-Eskipazar and the Hendek-Yığılca subfault zones (Koçyiğit, et al., 2000).

2.5.1 Seismicity of the Çubuk Region

As mentioned before, seismic sources with high magnitude earthquake generation potential exist at relatively far distances and sources with frequent low and moderate magnitude earthquake generation potential exist in close vicinities of the study area. The area lies on boundary of the second and third degree sub-zones of the seismic zonation map of Turkey. It includes numerous earthquake epicenters having small to moderate earthquakes with magnitudes smaller than 5.0. The distribution of the epicenters of major earthquakes that occurred in the Çubuk region and its surroundings since 1900 with magnitudes greater than 4.0 is shown in Figure 2.5. The aforementioned Çerkeş-Kurşunlu Fault Zone (ÇKFZ) and Dodurga Fault Zone (DFZ) are present at the İsmetpaşa-Kargı section of the NAFZ. This section is geologically one of the most complicated parts of the NAFZ. As mentioned before, the DFZ is a left lateral strike-slip fault zone, whereas the ÇKFZ is right lateral strike slip fault zone similar to the Eskipazar, Ulusu, Tosya and Devrez Fault Zones. Seismicity of the İsmetpaşa-Kargı section has been very high both in historical periods and in recent times (Koçyiğit et al., 2000).

The dates and magnitudes of some of recent (after 1900) seismic activities that took places mostly along the Ulusu, Çerkeş-Kurşunlu, Tosya and Dodurga fault zones in the İsmetpaşa-Kargı section are; 01.02.1944 Bolu-Çerkeş (M= 7.2); 13.08.1951 Kurşunlu (M= 6.9); 07.09.1953 Çerkeş-Kurşunlu (M= 6.4); and the 06.06.2000 Orta Earthquakes [M_w= 5.9 and two after shocks (M_w= 5.0 and M_w= 5.2)] (Koçyiğit et al., 2000). In addition to these, significant seismic events took place along the central part of the NAFZ at the western part of this section, namely the 26.11.1943 Bolu and 01.02.1944 Gerede earthquakes. Especially the Gerede earthquake led to the loss of life and property in the Çubuk region (Koçyiğit, 2009). Moreover, four historical earthquakes of which the epicenters are not known took place in the İsmetpaşa-Kargı section of the NAFZ. These are the 109, 1668, 1845 and 1881 events with intensities

are changing between V and IX. (Koçyiğit et al., 2000). The historical and recent earthquake data show that this section is seismically a very active area and has a potential seismic risk for the delineated area.

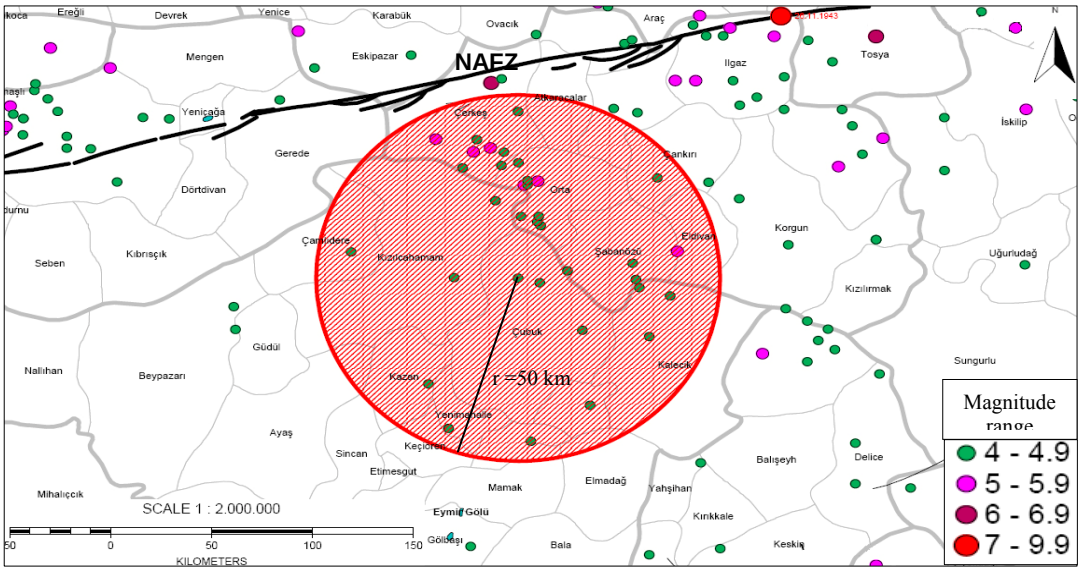

Figure 2.5 The distribution of epicenters for major earthquakes that occurred in the Çubuk region and its surroundings since 1900 with magnitudes greater than 4.0 (KOERI, Sayısalgrafik, 2009).

In addition to these, the region has many earthquake epicenters with magnitudes less than 5.0 namely, the 22.08.2000 Uruş (M_d= 4.3), 27.02.2003 Çamlıdere (M_d= 4.0), 09.06.2000 (M=4.0); 29.12.2004 (M_l= 4.6) and 31.01.2008 (M_l= 4.9) Çubuk earthquakes (obtained from Kandilli Observatory and Earthquake Research Institute, KOERI, 2009). This indicates that these fault zones (the Çeltikçi and Çubuk Fault Zones) have a potential to produce relatively higher (moderate) seismic events that might affect Çubuk and have to be taken into consideration in seismic hazard studies. In addition to these, the area is located at a region which has a potential of being seriously affected by a possible earthquake occurring along the Çubuk Fault Zone that is thought to be a continuation of the DFZ (Koçyiğit, 2008). The occurrence of the Çubuk earthquake in June 9th, 2000 after the Orta earthquake (M_W=5.9) in June 6th, 2000 along more or less the trend of the DFZ may be an indicator that Çubuk

Fault Zone is the continuation of the DFZ. Therefore, this increases the estimated seismic hazard potential for the area.

CHAPTER 3

MICROZONATION METHODOLOGIES

3.1. Introduction

The rapid growth of the world's population over the past few decades has led to over-population of people, buildings and infrastructure in urban areas. The tendency of urban areas to be developed in sedimentary valleys has increased their vulnerability to earthquakes, due to the presence of soft sediments. Nearly all recent destructive earthquakes, such as the 1985 Michoacan event, in Mexico; the 1988 Spitak event, in Armenia; the 1989 Loma Prieta and the 1994 Northridge events in USA; the 1995 Kobe event in Japan; and the 1999 Kocaeli event in Turkey have clearly showed that local soil conditions can have a significant influence on the ground motion and on the damage pattern. The importance of estimating the seismic ground motion in such areas for earthquake risk mitigation is world-wide accepted. The number of conducted studies in determining the effect of the local soil conditions on the ground motion and on the damage pattern have gradually increased (e.g., Fäh et al., 1997; Bour et al., 1998; Rodriguez-Marek et al., 2001; Tevez-Costa, 2001; Lebrun et al., 2004; Cara et al., 2008 and Koçkar and Akgün, 2008) and gained significant importance as the parameters should be considered and necessary precautions should be taken into consideration in order to protect from the effects of a potential destructive earthquake.

Damage patterns in past earthquakes show that local soil conditions at a site may have a significant effect on the ground motion intensity level. The earthquake damage is controlled by three interacting factor groups: Earthquake source and path

characteristics, local geological and geotechnical site conditions, and structural design and construction features. Mapping of seismic hazard at a local scale to incorporate the effects of local soil conditions is called microzonation for seismic hazard. Seismic microzonation is an interdisciplinary subject which considers the relationships among the earthquake source, path and site conditions in order to determine ground motion characteristics. Generally, it is the process for estimating the soil behavior under the earthquake excitation and thereby the variation of the earthquake characteristics on the ground surface (Kılıç et al., 2006). Earthquake recordings at soil surface include information that is related to these three site factors [i.e., the source activation (fault rupture), the propagation path of seismic energy and the effect of local geology on the wave-field at the recording site] that contribute to the overall site response either independently or in combination with the others (Pitilakis, 2004). In seismic microzonation studies, seismological, geological, hydrological, topographical and geotechnical data are necessary to implement the analysis. The key issue affecting the applicability and the feasibility of any microzonation study is the usability and reliability of the parameters selected for seismic zoning.

The microzonation methodology can be considered to be composed of three stages. In the first stage, regional seismic hazard analyses need to be conducted to estimate earthquake characteristics on rock outcrop for the area. In the second stage, the representative site profiles should be modeled based on the available in-situ tests. The third stage involves site response analyses for estimating the earthquake characteristics on the ground surface and the interpretation of the results for microzonation (Ansal et al., 2004). The microzonation shall be graded based on the scale of the investigation and details of the studies carried out. The Technical Committee on Earthquake Geotechnical Engineering (TC4) of the International Society of Soil Mechanics and Foundation Engineering (TC4-ISSMGE 1993) states that the first grade (Level I) map can be prepared with a scale of 1:1.000.000 – 1:50.000 and the ground motion can be assessed based on the historical earthquakes and existing information of geological and geomorphological maps. If the scale of the mapping is 1:100.000-1:10.000 and ground motion is assessed based on the

microtremor and simplified geotechnical studies then it is called a second grade (Level II) map. In the third grade (Level III) map ground motion can be assessed based on the complete geotechnical investigations and ground response analysis with a scale of 1:25.000-1:5.000.

Microzonation for seismic hazard has many uses. It can provide input for seismic design, land use management, and estimation of the potential for liquefaction and landslides. It also provides the basis for estimating and mapping the potential damage to buildings. The study presented herein is more related to producing zonation maps that may be used mainly for city and land-use planning. The results would be used for deciding where and how a building should be erected. The seismic zonation study is performed to determine the local geological, engineering geological, geotechnical and seismic site conditions of especially the Upper Pliocene to Pleistocene fluvial red clastics and Quaternary alluvial and terrace sediments that lie towards the northern part of the City of Ankara. Hence, the second grade of map of TC4, which is based on microtremor and simplified geotechnical studies was applied in this research for the zonation procedure.

3.2. Site effect

The term “site effect” introduces the effect of local geology in the modulation of the seismic wavefield at a recording site; where local geology consists of surface sedimentary sites and surface topography (Pitilakis, 2004). Seismic waves generated at the earthquake source propagate through different geological formations until they reach the surface of a specific site (Figure 3.1). The travel paths of these seismic waves in the uppermost geological layers strongly affect their characteristics, producing different effects on the earthquake motion at the ground surface (Oliveira, et al., 2004).

The bedrock can be divided into two types: seismic bedrock and engineering bedrock (Figure 3.1). In general the two conditions should be satisfied in order to call this interface seismic bedrock. These are that the interface has appreciable lateral extent

and the physical properties of the underlying layers do not vary along this interface and show a more homogeneous composition with respect to the overlying layers with the depths. Seismic bedrock is the rock having the shear wave velocity of more than 3000 m/s that is to be used for earthquake simulation and modeling. Seismic bedrock characteristics are included in the source and path effects of ground motions. Engineering bedrock is the rock having a shear wave velocity of 700-750 m/s and above, where engineers usually support their deep foundations and they generally accept as a bedrock in geotechnical site characterization studies(Nath, 2007 and Ansal and Tönük, 2007).

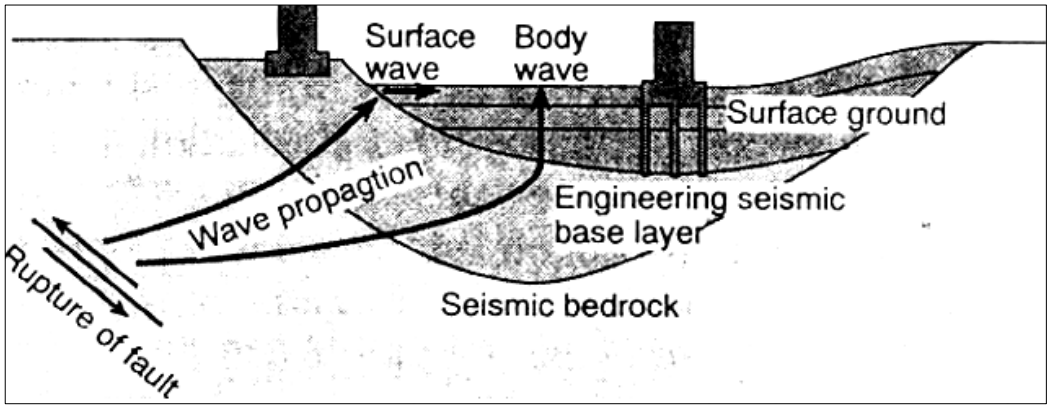

Figure 3.2. The propagation of a seismic wave from the fault rupture to the ground surface (Yoshida and Iai, 1998 as reported by Pitilakis, 2004).

It is well known that soft sediments yield larger earthquake damage than firm bedrock outcrops and as many settlements have been developed over these young river valley deposits, these sediments are of utmost importance. Soft and unconsolidated soil deposits tend to amplify selectively different wave frequencies due to the trapping of the seismic waves between the sediment layers and the underlying bedrock because of an impedance contrast between them. The effects of the soil deposits are observed at high or low frequencies for thin or relatively thick soft soil deposits, respectively (Lacave et al., 2002; Oliviera, 2004; Pitilakis, 2004 and Chavez-Garcia, 2007). The response of the soft soil under the earthquake excitation with different peak ground acceleration (PGA) can be seen in Figure 3.2. The figure shows that ground motions

amplified for PGA is less than 0.4g due to the soil effect (Idriss, 1991). It is a significant study showing the importance of the effect of soil on the local earthquake hazard.

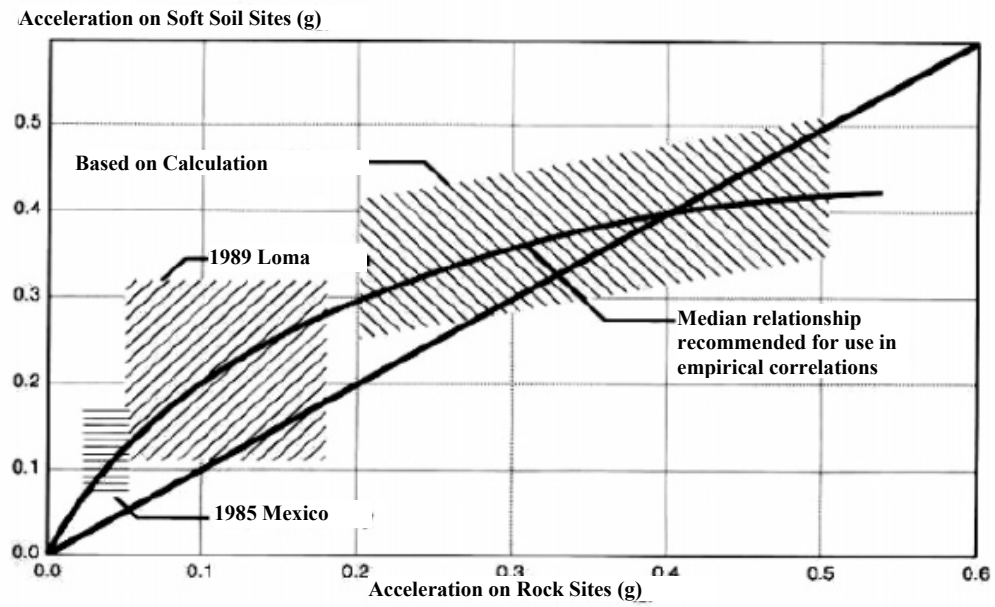

Figure 3.3. Variation of acceleration on soft soil versus rock sites (Idriss, 1991).

Damage pattern in past earthquakes show that soil conditions at a site may have a major effect on the level of ground shaking. However, the local topography can also modify the characteristics of the incoming waves, leading to the so-called topographic effects due to the concave (valley) and convex (hill tops, ridge) topographies. There are few but strong instrumental evidence that surface topography affects the amplitude and frequency content of ground motion (Jibson, 1987; Geli et al., 1988; Faccioli, 1991; Finn, 1991; Chavez-Garcia et al., 1996 and 1997; Lebrun et al., 1999). Theoretical models predict a systematic amplification of seismic motion at convex topographies such as hill tops and ridges while de-amplification phenomena are observed over concave geometries such as valleys (Pitilakis, 2004). As mentioned earlier, these two effects such as soil and topographic effects are considered under the general denomination of local site effects. Although, these two effects are important phenomena in understanding the effect of local soil condition

on ground motion, soil site effects are much more commonly investigated than the topographical effects. The main reason is that urbanization usually develops in soft soils deposits such as coastal plains and river basins.

When soil response studies are performed over some area rather than at a single point, the necessary microzonation methods should be carefully implemented in a gird system in order to characterize the local soils and to define the local seismic hazard distribution. Estimation of the local response of a site is a key component of any analysis of local seismic hazard. In practice, this requires numerical modeling of the dynamic behavior of the soil, which almost always implies good knowledge of the geometry and of the physical and mechanical characteristics of the formations underlying the site. The reliability of the modeling, therefore, depends on the number and quality of the investigations carried out, which are namely drilling, geophysical studies, geotechnical boreholes and related in-situ and laboratory tests and so on, to produce a representative model of the site. In practice, it is often difficult to have access to this type of data for a small area on a large scale (Bour et al, 1998).

Experimental methods in the evaluation of site effects have the advantage of avoiding the need for rigorous knowledge of the mechanical parameters of the soils and development of more-or-less reliable propagation models (Bour, et al., 1998). The next section contains briefly information about some of these methods that are used to estimate the site effect. Detailed information about the method used in this study is given in detail in Chapter 4.

3.3. Methods to estimate site effect

There are various methods which can be used for site effect estimation that can be classified under different titles. These methods are grouped under the experimental, empirical, semi empirical, numerical and hybrid categories. However, the method used in this study to evaluate the site effects is microtremor method (one of the experimental method) to record ambient noise in designating the fundamental periods and the amplification factors of sites.

3.3.1. Experimental methods

Experimental techniques are based on recordings of ground motion or ambient noise in order to estimate the basic characteristics of expected ground motion. These methods are usually used to analyze site effects in a frequency domain. In the next sections, the well established standard spectral ratio (SSR) and horizontal to vertical spectral ratio (Nakamura technique, or H/V noise ratio, or HVSR) techniques are described and compared.

3.3.1.1. Standard spectral ratio method (SSR)

The most popular and widely used technique to characterize site amplification has been the SSR (Borcherdt, 1970), which is based on the comparison of earthquake recordings obtained simultaneously on soil sites and on a reference rock site. The ratio of the Fourier amplitude spectra of a soil-site record to that of a nearby rock-site record gives only the effect of the local soil conditions at the specific site under the expected ground motion (Figure 3.3) since in this technique the processed recordings are taken at the nearby sites where the source and path effect of these are thought to be identical.

Although the SSR technique is a well established method in the estimation of local site effects (amplification and dominant period of the site), it has some restrictions and difficulties in the application stage. Firstly, this technique is applicable only to cases where the data are derived from dense local arrays with at least one station on outcropping conditions defined as the reference station and the simultaneous earthquake recordings should exist at a soil site and a reference site. Hence, the requirement of a dense array increases the instrumentation cost. Secondly, the reference site has to be free of any site effect in order to obtain more reliable records to use as a reference base (Pitilakis, 2004). For that, two requirements have to be satisfied. The first one is that the site should be in the close vicinity of a relevant station to guarantee that the differences between each site exist to only because of site conditions and these sites should have no relation with the differences in source radiation or travel path. The hypocentral distance is more than approximately ten

times the array aperture which is enough to eliminate the differences between sites in the travel path. The second one is that the reference site should not be affected by any kind of site effect. Therefore, the unweathered horizontal outcrop rock should be chosen as a reference site (Lacave et al, 2002). Otherwise, it could cause unsolvable problems and seismic stations at the bottom of the deep boreholes would be needed to avoid the site effects (Chavez-Garcia, 2007) which would also lead to increased costs regarding the method.

In summary, the SSR is the most reliable method to evaluate the site effects at specific sites. However, the one should note that the application of this method is not so easy especially in urban areas due to the high instrumentation costs, high level of noise, difficulties in finding an appropriate reference site, and the need for experiments of long duration to record earthquakes particularly in low or moderate seismic regions, the method has some shortcomings in terms of practicality.

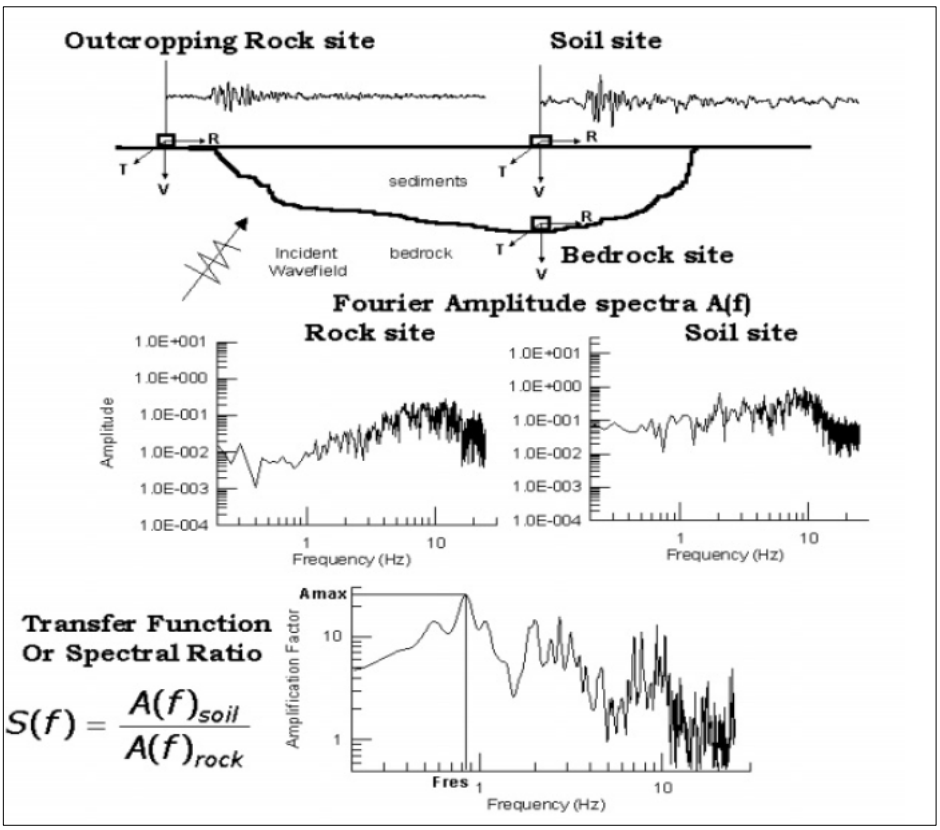

Figure 3.4. Schematic illustration of the SSR technique (Pitilakis, 2004).

3.3.1.2. H/V noise ratio

This empirical method is probably one of the most common methods utilized. The method, also called the Nakamura technique (Nakamura, 1989), was first introduced by Nogoshi and Igarashi (1971) based on the initial studies of Kanai and Tanaka (1961). The method consists of deriving the ratio between the Fourier amplitude spectra of the horizontal and the vertical components of the microtremor recorded at the surface (Figure 3.4). The signals used are simply recordings of ambient noise, so local or regional seismic activity, or adequate reference sites are not required in this technique. Therefore, the method is easily implemented with lower cost at every hour of the day (Nakamura, 1989). The Nakamura technique is based on the following assumptions:

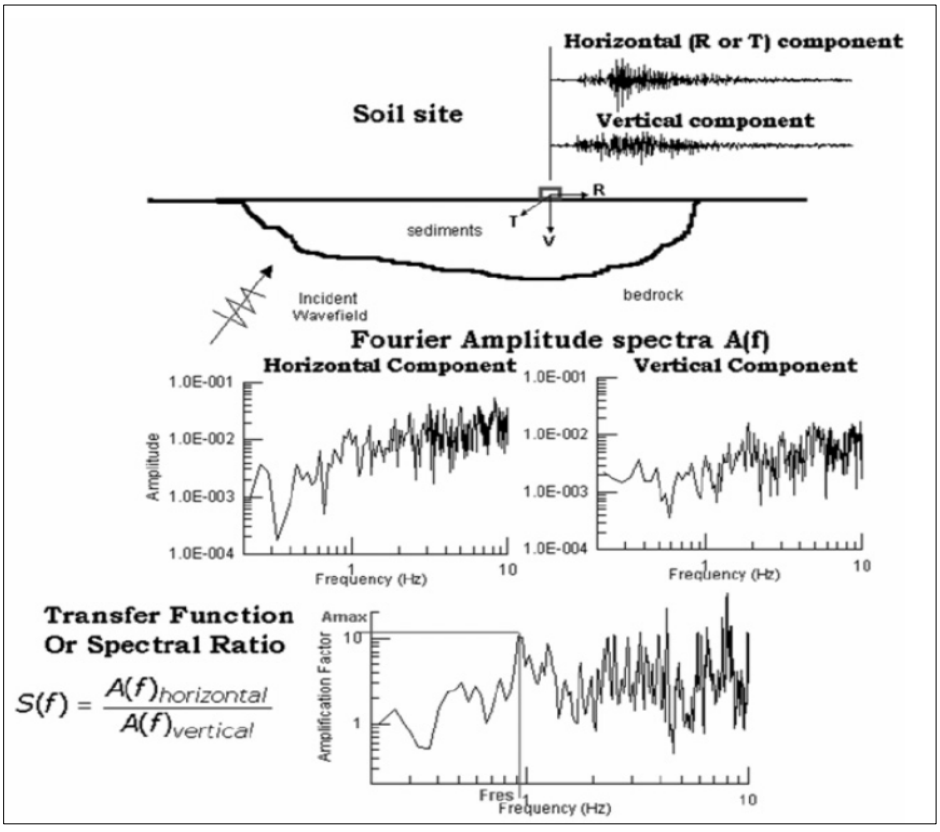

Figure 3.5. Schematic illustration of the H/V technique (Pitilakis, 2004).

1) Microtremors are composed of several waves, but essentially Rayleigh waves propagating in soft surface layers overlying a half space;
2) The effect of the Rayleigh waves on the noise motion is included in the vertical spectrum at the surface, but not at the base of the layer;
3) The effect of Rayleigh waves is equal for vertical and horizontal components;
4) Soft soil layers do not amplify the vertical component of ambient noise; and,
5) For a wide frequency range (0.2-20 Hz), the spectra of the vertical and horizontal components of ambient noise are equivalent at the bottom of the layer.

Due to the difficulties of the most reliable technique (i.e., SSR), the alternative way (H/V ratio method) has attracted the attention of a number of scientists to characterize seismic response by using ambient noise (microtremor) records. The details about the theory, literature review and debatable aspects are given in Chapter 4.

3.4. Methods for seismic site characterization studies

The sedimentary deposits that affect wave propagation should be identified by an efficient tool in order to characterize and classify the sites based on the effects of the soil types related with ground motion response. An important element in establishing seismic design criteria for an engineering site is the measurement of seismic shear wave velocity (V_s). The soil classification is performed according to seismic codes for the design of earthquake resistant structures based primarily on average shear-wave velocity in the upper 30 m of the soil profile (V_{S30}) (Pitilakis, 2004). If shear wave velocity information for the uppermost 30 m layer is not available, the other parameters (standard penetration resistance (N_{SPT}) or undrained shear strength (S_u)) are also used in soil classification of the system (ICC, 2003). These all are related to the soil stiffness which is one of the critical material parameters directly associated with V_s considered during an early stage of most of the geotechnical construction. It is related directly to the stability of structural load, especially as it relates to a possible earthquake hazard. Soil lacking sufficient stiffness for a given load can experience a significant reduction in strength under earthquake shaking resulting in

liquefaction, a condition responsible for tremendous amounts of damage from earthquakes around the world (Richart et al., 1970).

Besides these, shear wave velocity is used to compute the shear modulus or modulus of rigidity of the material at a small strain value, i.e. G_{max}. The shear modulus (G) is one of several quantities used for measuring the strength of materials defined as the ratio of the shear stress to the shear strain. Numerical soil models use the variation of shear modulus and damping with strain level, G-γ and D-γ curves, as fundamental input parameters for any numerical ground motion analysis. To compare measured shear moduli with standard degradation curves also requires a value for the small-strain shear modulus G_{max} against which the shear modulus is usually normalized (Brennan et al., 2005). Most of the seismic geophysical tests can be performed to obtain the shear wave velocity at shear strains lower than 3×10^{-4} %. The measured shear wave velocities can be used to compute G_{max} by using the equation below:

$$G_{\max} = \rho \times V_s^2 \qquad (3.1)$$

Where, ρ represents the density of material.

The use of measured shear wave velocities is generally the most reliable means for evaluating in situ value of G_{max} for a particular soil deposit, and the seismic geophysical tests are commonly used for this purpose (Kramer, 1996).

In addition to these, the shear wave velocity parameter is utilized to simply and quickly evaluate the ground motion characteristic parameters such as the fundamental frequency of the soil profile (Joyner et al., 1981) and the amplification ratio (Midorikwa, 1987). These methods are practically used to determine the site effects as a preliminary analysis or the obtained results can be evaluated according to seismic codes prescriptions in microzonation studies and/ or seismic design of the structures as mentioned before. The seismic prospecting to determine the structure and properties of the subsurface is one of the most reliable ways in the site effect studies. Instead of the parameters such as fundamental period and amplification ratio,

the average shear wave velocity (Borcherdt, 1994) is proposed to characterize the site. In this research, the multichannel analysis surface wave and microtremor array methods were used as the active and passive surface wave methods in order to characterize the Upper Pliocene to Pleistocene fluvial sediments and the Quaternary alluvial deposits.

3.4.1 General procedure code based site classification

The consideration of site conditions has become an important part for the assessment of seismic shaking hazard as explained before. In mapping geographic variations in shaking response and to predict the variations in ground motion due to differences in site geology, necessary parameters should be assigned to each key site. Recent studies show that the shear-wave velocity is a critical factor in determining the amplitude of ground motion (Joyner and Fumal, 1985; Boore et al., 1993; Borcherdt, 1994 and Anderson et al., 1996) and thus might be a useful parameter to characterize local geologic conditions for seismic zonation studies.

The amplification of ground motions at a site is significantly affected by the natural period of a site ($T_n = 4H/V_s$; where T_n = natural period, H = soil depth, and V_s = shear wave velocity) by considering both characteristic shear wave velocity and soil depth. Other important seismic site response factors are the impedance ratio between surficial and underlying deposits, the material damping of the surficial deposits, and the variation of these seismic site response characteristics as a function of the intensity of the ground motion, as well as other factors. To account partially for these factors, a site classification system should mainly include a measure of the dynamic stiffness of the site and a measure of the bedrock depth. The soil type and age should be used as secondary classification parameters to capture the expected different non-linear responses of the soil types deposited at different facies and times (Rodriguez-Marek, 2001).

In the code-based site characterization, the main improvement is that the amplification factors of spectral values are varying with the seismic intensity; lower

shaking intensity earthquakes introduce higher amplification factors due to the more linear elastic soil behavior, contrary to, the higher intensities where soils are generally exhibiting non-linear behavior resulting in a decrease of peak spectral values and a shift in period due to increasing of damping ratio and strain dependent modulus degradation properties of the soil. In IBC 2003, TSC 1998 and other codes of the same family, special attention is given to the near field conditions introducing higher amplification factors for the same earthquake magnitude. Also for soil layers of small thickness presenting high impedance contrast, the new version of codes attribute higher amplification factors which is compatible with observations and theory (Pitilakis, 2004).

Modern seismic codes (IBC 2000 and 2003, UBC97, NEHRP and TSC) which have all been introduced in the last decades, especially after the recent strong earthquakes in America, Europe, Japan produced numerous invaluable data. These codes have incorporated the most important experimental and theoretical results with the necessary adjustments and simplifications for purely practical reasons. "The Existing Model Code Groups" formed the International Code Council (ICC) with the express purpose of developing a single set of construction codes for the entire United States, leading to the combination of UBC (Uniform Building Code) and NEHRP (National Seismic Hazard Reduction Program) into the IBC 2000 and IBC 2003 (International Building Code International Code Council, ICC). The recent design code, IBC 2003 is a common code for all of the U.S. and is also acceptable internationally since it is indeed a significant forward step towards harmonization and is a major scientific breakthrough.

In the IBC 2003 site characterization, the site classification system is an attempt to capture the primary factors affecting seismic site response while minimizing the amount of data required for site characterization (Table 3.1 and 3.2). The main advantage of the system is that three parameters which are the standard penetration resistance, N, the undrained shear strength, S_u, and the shear wave velocity, V_s, are used for soil identification which easily enables site classification. Site categorization schemes have generally found distinct levels of amplification at sites with different

geologic and geotechnical characteristics that include surface geology, average shear wave velocity in the upper 30 m, geotechnical data including sediment stiffness, depth, and material type, and depth to basement rock. In case site-specific data are not available to a depth of 30 m, appropriate soil properties are permitted to be estimated by the registered design professional preparing the soils report based on known geologic conditions (ICC, 2003).

The site specified by IBC 2003 as defined in Table 3.1 practically distinguishes soil profiles in five main categories where the special conditions "E" and "F" that correspond to very loose or liquefiable material are also defined, respectively. When the soil properties are not known in sufficient detail to determine the site class, Site Class D shall be used unless the building official determines that Site Class-E or -F soil is likely to be present at the site. The site class shall be determined according to parameters described in Table 3.2 when the soil shear wave velocity, V_s, is not known (ICC, 2003).

The average of the V_s parameters are computed according to the following equation. Note that the notations presented below apply to the upper 30 m of the site profile. Profiles containing distinctly different soil layers shall be subdivided into those layers designed by a number that ranges from 1 to *n* at the bottom where there are a total of *n* distinct layers in the upper 30 m. The symbol, i, refers to any one of the layers between 1 and *n*.

$$\overline{V_s} = \frac{\sum_{i=1}^{n} d_i}{\sum_{i=1}^{n} \frac{d_i}{V_{si}}} \qquad (3.2)$$

Where:

V_s = the shear wave velocity in meter per second, or ft/s.

d_i = the thickness of any layer between 0 and 30 m and total thickness of the soil profile used in the formula corresponding to 30 m, or 100 ft.

Tabel 3.1. Soil classification according to IBC 2003 (ICC, 2003).

SITE CLASS	SOIL PROFILE NAME	AVERAGE PROPERTIES IN TOP 30 m (100 feet),		
		Soil shear wave velocity, V_s, (m/s)	Standard penetration resistance, N	Soil undrained shear strength, S_u (kPa)
A	Hard rock	$V_s > 1{,}500$	N/A	N/A
B	Rock	$7{,}600 < V_s \leq 1{,}500$	N/A	N/A
C	Very dense soil and soft rock	$360 < V_s \leq 760$	$N > 50$	$S_u \geq 100$
D	Stiff soil profile	$180 \leq V_s \leq 360$	$15 \leq N \leq 50$	$50 \leq S_u \leq 100$
E	Soft soil profile	$V_s < 180$	$N < 15$	$S_u < 50$.
E	—	Any profile with more than 10 feet of soil having the following characteristics: 1. Plasticity index $PI > 20$, 2. Moisture content $w > 40\%$, and 3. Undrained shear strength $S_u < 25$ kPa		
F	—	Any profile containing soils having one or more of the following characteristics: 1. Soils vulnerable to potential failure or collapse under seismic loading such as liquefiable soils, quick and highly sensitive clays, collapsible weakly cemented soils. 2. Peats and/or highly organic clays {H > 10 feet of peat and/or highly organic clay where H = thickness of soil) 3. Very high plasticity clays (H >25 feet with plasticity index PI >75) 4. Very thick soft/medium stiff clays (H > 120 feet)		

For SI: 1 foot = 304.8 mm, 1 square foot=0.0929 m^2, 1 pound per square foot = 0.0479 kPa. N/A = Not applicable

Tabel 3.2. Soil classification according to IBC 2003 (ICC, 2003).

SITE CLASS	$\overline{V_s}$	$\overline{N}$ or $\overline{N}_{ch}$	$\overline{S_u}$
E	< 180 m/s	< 15	< 50 kPa
D	180 to 360 m/s	15 to 50	50 to 100 kPa
C	360 to 760 ft/s	> 50	> 100 kPa

For SI: 1 foot per second = 304.8 mm per second, 1 pound per square foot = 0.0479 kN/m^2.
If the S_u method is used and the N_{ch} and S_u criteria differ, select the category with the softer soils (for example, use Site Class E instead of D).

However, it is questionable whether or not the Vs_{30} sufficiently characterizes the local amplification potential in some particular geological environments, such as deep sediment-filled basins. Recent studies show that the use of V_{S30} as a basis for site amplification is misleading in many cases. Hence it is necessary to use the actual engineering rock depth rather than V_{s30} for amplification study. In many cases it was shown that deeper layers may also significantly contribute to amplification effects

over a broad frequency range between 0.1 and 10 Hz. Therefore, shear wave velocity profiles need to be established down to the engineering bedrock with an estimated shear wave velocity of 700–750 m/s. (Pitilakis, 2004; Havenith et. al, 2007; Sitharam and Anbazhagan, 2008).

Although, IBC 2003 reflects the basic knowledge and technology of the present time, having an acceptable level of accuracy, and compatibility among others in terms of the tools used for the seismic design of structures, as being stated, site classification is performed based on only the average values of the necessary geotechnical and geophysical parameters for the uppermost 30 m of the soil profile. Therefore, alternatively, some other seismic codes (TSC), which use both shear wave velocity data and stratigraphy information in the local soil condition classification, should be utilized especially for the thick soft sediment deposits. Thus, the site classes were also assigned according to the Turkish Seismic Code (TSC) in addition to the IBC 2003 in this study (Ministry of Public Works and Settlement Government of Republic of Turkey, 1998).

TSC 1998 has similarities with the IBC 2003 for soil identification (Table 3.3). However, there is an additional classification criterion (relative density) to the parameters in the IBC 2003, namely, the standard penetration resistance, N, the undrained shear strength, S_u, and the shear wave velocity, V_s. Then, by using the variation of these values with the soil profile, local site classes are assigned to a site (Table 3.4). Table 3.3 categorizes the sites into the four main categories. Then, based on the soil column information, Table 3.4 distinguishes the soil profiles in four categories. The last step is the main difference between these two codes in the soil classification process. Due to the consideration of the stratigraphy information, D site class in the IBC code could be classified into three different soil classes (Z2, Z3 or Z4) in the TSC 1998.

Table 3.3. Soil groups according to TSC, 1998 (Ministry of Public Works and Settlement Government of Republic of Turkey, 1998).

Soil Group	*Description of Soil Group*	*Stand. Penetr.* (N/30)	*Relative Density* (%)	*Unconf. Compres. Strength* (kPa)	*Shear Wave Velocity* (m/s)
(A)	**1.** Massive volcanic rocks, unweathered sound metamorphic rocks, stiff cemented sedimentary rocks	—	—	> 1000	> 1000
	2. Very dense sand, gravel...	> 50	85–100	—	> 700
	3. Hard clay, silty lay……..	> 32	—	> 400	> 700
(B)	**1.** Soft volcanic rocks such as tuff and agglomerate, weathered cemented sedimentary rocks with planes of discontinuity……	—	—	500–1000	700–1000
	2. Dense sand, gravel.....	30–50	65–85	—	400–700
	3. Very stiff clay, silty clay..	16–32	—	200–400	300–700
(C)	**1.** Highly weathered soft metamorphic rocks and cemented sedimentary rocks with planes of discontinuity	—	—	< 500	400–700
	2. Medium dense sand and gravel.....…….	10–30	35–65	—	200–400
	3. Stiff clay, silty clay.....	8–16	—	100–200	200–300
(D)	**1.** Soft, deep alluvial layers with high water table.....……	—	—	—	< 200
	2. Loose sand.....…..	< 10	< 35	—	< 200
	3. Soft clay, silty clay.....…..	< 8	—	< 100	< 200

Table 3.4. Local site classes according to TSC, 1998 (Ministry of Public Works and Settlement Government of Republic of Turkey, 1998).

Local Site Class	*Soil Group according to Table 12.1 and Topmost Layer Thickness* (h_1)
Z1	Group **(A)** soils Group **(B)** soils with $h_1 \leq 15$ m
Z2	Group **(B)** soils with $h_1 > 15$ m Group **(C)** soils with $h_1 \leq 15$ m
Z3	Group **(C)** soils with $15 \text{ m} < h_1 \leq 50$ m Group **(D)** soils with $h_1 \leq 10$ m
Z4	Group **(C)** soils with $h_1 > 50$ m Group **(D)** soils with $h_1 > 10$ m

In the seismic zonation process performed herein, necessary parameters such as shear wave velocity, predominant site period and amplification ratio are attempted to be computed by using surface wave methods and microtremors, since these parameters are fundamental to understanding the dynamic response of a site, they can be used to produce seismic hazard maps with relative damage potential and provide guidance for decision making regarding land use. In the next chapter, the theories of the methods utilized in this study will be described and discussed in detail.

CHAPTER 4

METHODOLOGIES UTILIZED IN THE STUDY

4.1. Determination of the characteristic shear wave velocity

4.1.1. Introduction

An important element in establishing seismic design criteria for an engineering site is the measurement of the seismic shear wave velocity (V_s). The shear wave velocity, together with the other physical properties of earth materials, can be used to determine their elastic properties and hence the seismic response of the foundation to theoretical loads caused by local earthquakes (Schwarz and Musser, 1972) The related material properties in this manner are shear and compressional wave velocity, as well as density and non-linear properties of both soil and rock. Although the most common influence on the ground motions is the variations in the materials within tens to hundreds of meters of the surface, deeper variations can also be important (Boore, 2006). However, at present, site characterization is often reduced to the specification of a single number, i.e., Vs_{30}, shear-wave velocity over 30 m from the surface (Borcherdt, 1994). This number is used in some well-known building codes (IBC 2000-2003, UBC97, and NEHRP) to classify the site and to compute the expected site amplification characteristics and fundamental period of the soil profile. Also, Vs_{30} is used as a site classification parameter in the next generation attenuation model with the engineering rock depth (Abrahamson and Silva, 2008).

Rather than the determination of a ground type and estimation of the site amplification, the shear-wave velocity is a fundamental input parameter for dynamic analyses. Since it is directly related to the shear modulus, it is also very important in geotechnical and geo-environmental engineering. In order to determine the shear-wave velocity over 30 m from the surface, or its generalization to other depths, most in-situ seismic methods attempt to derive the shear-wave velocity as a function of depth.

4.1.2. Surface wave methods

Many in-situ geophysical techniques have been used to provide information about the subsurface characteristics to engineers and geologists who have evaluated the properties of soil deposits and rock formations since many decades. Several seismic survey techniques have been specially developed for the use of engineers to evaluate in-situ shear wave velocity (Vs) profiles for the last three decades (Lin, 2007). The recent geophysical methods have been developed by means of the theoretical studies and with the computer evolution. These geophysical methods are based on the physical theory, so the mathematical analysis is needed to implement these methods to obtain subsurface structure from measured data. The continuous development of computational ability has also triggered further development in the geophysical methods. Advanced geophysical methods will be able to provide accurate subsurface information much quickly and cheaply. Accurate subsurface information contributes to the construct on of a safe and sustainable society.

The conventional geophysical methods such as shear wave non-invasive seismic refraction method and invasive seismic methods have been used in shear wave velocity investigations for many decades. The classification of the methods as invasive or non-invasive is based on the need of a borehole or not during the shear wave velocity survey. The frequency of the wavelets form the seismic signals obtained during these surveys are higher than 30 Hz frequencies (Gosar et al., 2008).

When compared with non-destructive surface wave methods, seismic refraction method is also time consuming since it should be conducted separately to determine longitudinal- (P) and shear- (S) waves using vertical and horizontal sets of geophones, respectively and different ways of signal should be generated by a sledgehammer in order to obtain each waves individually. The P-waves and S-waves are needed to determine the depth structure and relevant velocities for seismological site characterization, respectively (Gosar et al., 2008).

Another disadvantage of the method is the character of the S-wave velocity in unconsolidated soil layers. In the unconsolidated soil ground, the S-wave velocity contrast is generally small and reversed layers or a higher velocity layer on the top of a lower velocity layer sometimes exists. In addition to this, a dipping layer can be present at the subsurface. These prevent the refractions returning from the interface. Also, in the S-wave refraction method, SH seismic motion must be used. However, P-waves and Love waves sometimes interfere and they complicate first arrival picking (Hayashi, 2008).

These all make the refraction analysis to be difficult. Another reason that makes the data acquisition difficult in conventional geophysical methods such as the EM method is that in a noisy urban environment, it is often difficult to generate strong enough signals to perform these methods effectively. These conditions have little or no impact on the generation or propagation and generally have no influence on the processing or interpretation of surface-wave data. “This flexibility in acquisition and insensitivity to environmental noise allow successful use of the shear-wave velocity profiling in areas where other geophysical methods are limited because of the relative high amplitude nature when compared to body waves” (Miller et al., 1999).

Moreover, destructive seismic techniques are more costly as compared to others in obtaining in-situ shear wave velocity profile. The necessity of a borehole is the major disadvantage of these seismic methods. For instance, down-hole and suspension logging invasive seismic methods are more costly than surface wave (non-invasive) methods, such as the Spectral Analysis of Surface Waves (SASW), Multichannel

analysis of Surface Wave (MASW), Microtremor Array Method (MAM), Refraction Microtremor (ReMi) methods and etc (Lin, 2007). A summary of the methods can be seen in Figure 4.1. Usually such studies should cover the investigated area and therefore require a pattern of measurements which should be dense enough to determine a given geological setting in terms of shear velocity classification. When compared with the conventional seismic methods (for example, S-wave refraction, reflection, down-hole, cross-hole surveys), the surface-wave method has several advantages:

- Field data acquisition is very simple and tolerant because surface waves always take the strongest energy;
- The data processing procedure is relatively simple and easy even for the non-experienced;
- A large area can be covered within a relatively short time period; and,
- Because of all above reasons, it is highly cost effective and time efficient. (Park Seismic, 2009).

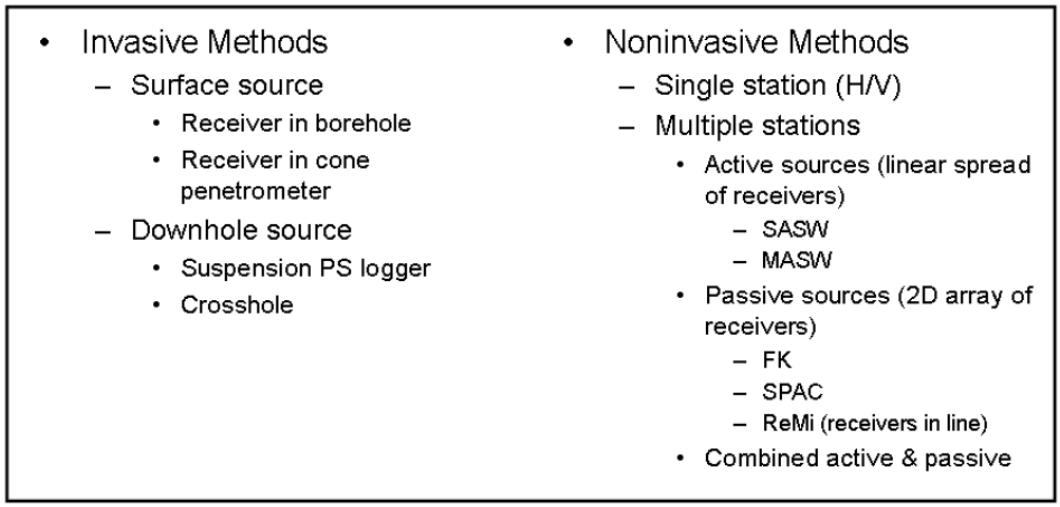

Figure 4.1. A summary of the seismic methods (Boore, 2006).

The use of V_{s30} as a basis for soil and site characterization is misleading in many cases. It should be used only when the actual site conditions are suitable to the relatively shallow "seismic bedrock" or very firm soil conditions, flat stratigraphy (Pitilakis, 2004). However, it is questionable if the Vs_{30} sufficiently characterizes the local amplification potential in some particular geological environments, such as deep sediment-filled basins. Also, recent studies on the deep basin show that more of the sediment column should be considered to obtain an appropriate ground motion projection (Bodin et al., 2001; Liu et al, 2004; Nguyen et al., 2004; Parolai et al., 2006). The recognized influence of the deeper geology on the seismic ground motion behavior at the surface implies a major challenge. Because of this reason, the need of developing geophysical techniques which are able to provide reliable information on the dynamic behavior over a large range of depths has came out.

4.1.3. Theory of the surface wave methods

Recently, the surface wave method has become the seismic technique most often used to estimate the V_S structure of soil because of its non-invasive nature and greater efficiency in data acquisition and processing (Miller et al., 1999; Stokoe et al., 1994). The surface wave methods are based on the dispersive nature of Rayleigh waves in a layered media to derive subsurface shear wave velocity profiles. The Rayleigh wave, which is the one of surface wave type, travels along a free surface such as the earth-air or the earth-water-interface. A relatively low velocity, low frequency and high amplitude are the characteristic properties of the Rayleigh wave. Rayleigh waves are the result of interfering P and SV waves which are the vertical and radial components of the surface waves, respectively. Particle motion of the fundamental mode Rayleigh waves in a homogeneous medium moving from left to right is elliptical in a counterclockwise (retrograde) direction along the free surface as illustrated by Figure 4.2. The amplitude of this wave motion decreases exponentially with depth. When reaching sufficient depth, surface waves become planar. The motion is constrained to a vertical plane consistent with the direction of wave propagation (Telford, et al., 1976 and Xia, et al., 2004). Also, the depth is the function of wavelength (Park et al., 1999).

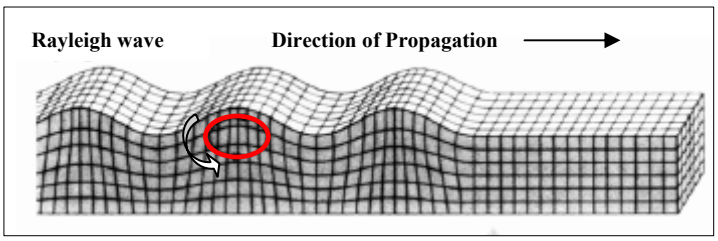

Figure 4.2. Motion during the passage of a Rayleigh wave (Hayashi, 2003).

Despite the different scales, these methods are based on the same principles. They are founded on the geometrical dispersion, which makes propagation of Rayleigh wave velocity frequency dependent in vertically heterogeneous media. As can be see in Figure 4.3, long wavelength (low frequency) Rayleigh waves penetrate deeper layers and their velocity is affected by the material properties at greater depth and they are informative about them. However, short wavelength (high frequency) Rayleigh waves propagate in shallow layers close to the surface and they contain the information about mechanical properties of shallow layers. Surface wave methods use this property to characterize materials in a very wide range of scales (Foti, 2005).

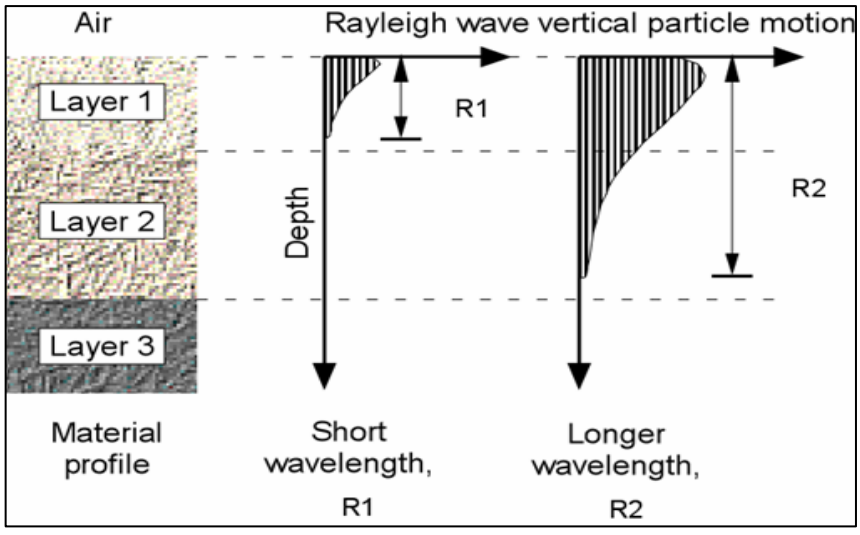

Figure 4.3. Principle of geometric dispersion (Geovision, 2009).

Propagation velocity (called phase velocity) of surface waves is frequency (or wavelength) dependent (this property is called dispersion). In other words; assuming vertical velocity variation, each frequency component of a surface wave has a different velocity propagation velocity at each unique frequency component. This unique characteristic results in a different wave length for each frequency propagated. This property is called dispersion (Park, et al., 1999). Shear wave velocities of the subsurface layers can be derived by backcalculation process using the constructed dispersive curve. Because of this property, unlike the conventional methods, surface-wave methods are based on elastic wave equation and these analyses are completely performed in frequency domain (Hayashi, 2008).

Although the frequency range of interest and the spatial sampling differences in the acquisition of experimental data are the main discrepancies between the methods, the entire procedure of the analysis of the surface wave methods are based on the same main three steps since these rely on the dispersive nature of Rayleigh waves in layer media (Foti, 2005). These steps are; 1) Acquisition of the experimental data, i.e., seismic waves are detected by mechanical sensors and recorded, 2) Signal processing to construct the experimental dispersion curve, and 3) Inversion of the calculated dispersion curve to obtain a 1D shear wave velocity profile (Foti, 2005, Jin et al., 2006). The procedure is given as a flow chart in Figure 4.4. Construction of dispersion relation is a very critical step to calculate the accurate shear wave velocity profile. Prutiy, specificity and accuracy of the dispersion relation are the significant properties affecting the accuracy of inverted shear wave velocity profile (Jin, et al., 2006).

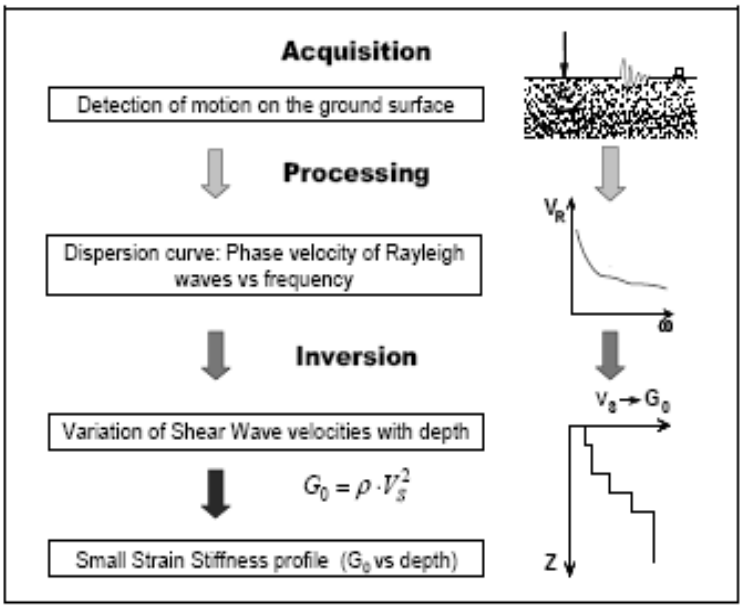

Figure 4.4. General procedure flows in surface wave methods (Foti, 2005).

4.1.3.1. Active and passive surface wave methods

Surface waves are generated by two ways which are active and passive sources. Active source means that seismic energy is intentionally generated at a specific location relative to the geophone spread and recording begins when the source energy is imparted into the ground. Multichannel Analysis of Surface Wave (MASW) (Park, 1999) and Spectral Analysis of Surface Wave (SASW) (Nazarian, 1984; Stokoe et al., 1994) methods are classified as active surface methods. This is in contrast to passive surface wave surveying, also called Microtremor Array Method (MAM) (Okada, 2003; Hayashi, 2008), or referred to as Refraction Microtremor (ReMi; Louie, 2001) methods, where there is no time break and motion from ambient energy generated by a range of natural phenomena (wind, wave motion) and artificial sources (cultural noise, i.e., traffic, machinery and so on) at various, and usually unknown locations relative to the geophone spread is recorded (SeisImagerSW Manual 2.2, 2006).

The choice of equipment (source type, geophone type and number) and testing configuration (geophone interval, spread length and offset distance) is closely linked

to the scope of the test and to the technique to be used in the field because of the interest in different frequency range as explained in Section 4.1.3. The principles and the interpretation steps are the same in other studies which are in need of obtaining information for much shallower or deeper layers. However, this study as described in the previous chapter is mainly interested in a depth of 30 m and more, so the related configuration and equipment was chosen for that purpose. In this study, Multichannel Analysis of Surface Wave and Microtremor Array Methods were preferred as the active and the passive surface wave methods, respectively, to obtain the shear velocity profile of the subsurface. The reasons and details related to the configuration and the equipment used in the surface wave methods are explained in next section.

4.1.3.1.1. Multichannel analysis of surface wave (MASW) method

Both body (P and S) and surface (e.g., Rayleigh, Love, etc.) waves are generated when seismic waves are generated at or near the surface of the earth. Body waves propagate through the whole body of the earth, whereas surface waves propagate along (or near) the surface of the earth. If vertical seismic sources (impulsive or swept) are used, the type of the generated surface waves is Rayleigh waves, more commonly called ground roll in the seismic surveys. In all kinds of surface seismic surveys using vertical sources, ground roll takes more than two thirds of the total generated seismic energy and usually appears to be most prominent on the multi-channel records (Park et al., 1997). It means that ground roll is Rayleigh-type surface waves generated most effectively in the surface seismic surveys. Generation and recording of ground roll is the easiest among all other types of seismic waves (Park et al., 1999). Therefore, most of the surface wave methods that use active sources attempt to measure Rayleigh wave phase velocities as a function of frequency (Boore, 2006). Multi-Channel Analysis of Surface Waves (MASW) measure the Rayleigh waves, which give information of the entire range of investigation depth, by one or a few generation of ground roll without changing receiver configuration. This leads to perform the method fast to evaluate the near surface V_s profile (Park et el., 1997).

The field configuration of the MASW method is to have multiple receivers (usually twelve or more) along a straight line with equal spacing and the seismic source acting on one end of the linear array. Then, the generated seismic waves propagate along the receiver line where they are recorded synchronously. The MASW survey can be conducted successfully by using the seismic waves generated by either impulsive source like sledge hammer or swept source like a vibrator. This approach allows recognition of the various propagation characteristics of the seismic wavefield.

In active surface wave methods, one challenging issue is to properly record and process the data. During the generation of planar, fundamental mode Rayleigh waves, a variety of wave types such as several types of body waves like direct, refracted, and reflected waves, backscattered waves, ambient noise, and higher-modes, reflected and non-planar surface waves are produced (Park et al., 1997 and Park et al., 1999) as can be seen in Figure 4.5. Relative amplitudes of each noise type generally change with frequency and distance from the source. These waves usually make the analysis of the fundamental mode for the dispersion curve difficult and also negatively affect the final shear wave velocity profile (Stokoe et al., 1994). To overcome inherent difficulties existing when evaluating and distinguishing signal from noise, multichannel recording allows to identify and to isolate effectively these noise types according to distinctive coherency pattern, arrival time, and amplitude of each (Park et al, 2000).

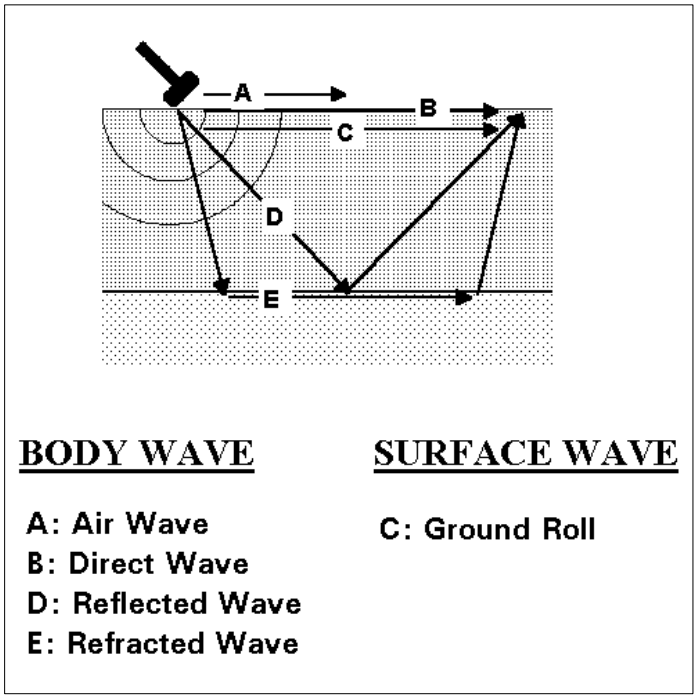

Figure 4.5. Major types of seismic waves based on propagation characteristics (Park et al., 1997).

The optimum recording, separation of broad bandwidth and high S/N ratio Rayleigh waves from other acoustic energy are provided by using the MASW method. The accuracy of the calculated dispersion curve is ensured by a high S/N ratio, while the broad bandwidth improves resolution and possible depth of investigation of the inverted V_S profile (Park et al., 1999). This basic field configuration and acquisition routine has similarities with conventional common midpoint (CMP) body-wave survey methods. Indeed, MASW method can be used as a by product of body wave surveying. However, there are some slightly different criteria on the optimum data acquisition configuration between them (Park et al., 1999).

The assumption in MASW method is that the nature of near-surface materials can be treated implicitly as a layered earth model with no lateral variation in elastic properties, so it gives information about the variations in elastic properties through the vertical direction. The detailed information about this concept is given in the inversion section.

When the MASW method is compared with the body-wave survey methods such as reflection or refraction, the MASW method usually has a far greater tolerance in the selection of optimum field parameters, since the surface waves have the strongest energy among all other types of seismic waves, ensuring the highest signal-to-noise ratio, as discussed above (Park et al., 2002). Nevertheless, recent studies have shown that the instrumental configuration used for field data acquisition can affect the dispersion results obtained in the MASW method (Nazarian and Stokoe, 1983; Park et al., 2001 and 2002, and Zhang et al., 2004).

Optimal recording of Rayleigh waves requires field configuration and acquisition parameters which provide effectively to record planar, fundamental mode Rayleigh waves. Although there is general agreement for the recording parameters which are record length and sampling interval, source and geophone type, there are debates about the other optimum field configuration components such as near offset (distance between the source and the first receiver), receiver spacing and offset range (distance between the first and the last receiver). These should be selected properly to prevent the record from spatial aliasing, near and far field (offset) effects (Stokoe et al., 1994; Park et al., 1997; 1999; 2001 and 2002; Lin et al., 2004 and Xia, et al., 2004). The field configuration of the MASW and the filed configuration components are illustrated in Figure 4.6.

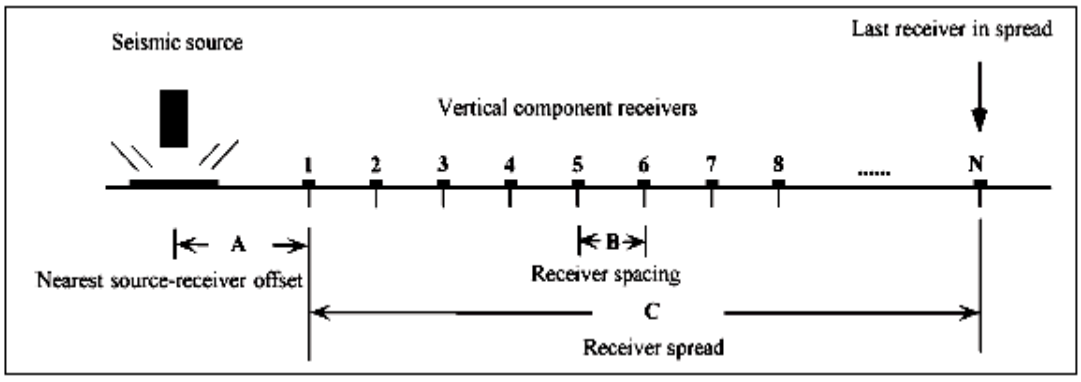

Figure 4.6 The basic field configuration of the MASW and the three important acquisition parameters (Xia et al., 2004).

4.1.3.1.1.1. Data acquisition and field configuration in the MASW method

As mentioned before, either sledge hammer or vibrator sources can be used to obtain an accurate shear wave velocity profile. When the effectiveness and economic advantage are considered, impulsive source choice is logical. However, there are two main drawbacks in this application. The frequency content of the signal is poorly controlled and the signal may not be repeatable (Rix, 2005). By considering the importance of the lower frequency components of the surface wave for deeper layers, stacking multiple shots, heavier sledge hammer and high-output low-frequency geophone with no recording filters should be used and so the influence of the source energy and receiver sensitivity can be reduced (Park et al., 1999; and Zhang et al., 2004).

The optimum values for the weight of the hammer and the natural frequency of the geophone depend on the investigated depth. It is certain that low frequency geophones such as 1 Hz and 2 Hz are the more convenient ones to get information for deeper layers. However, 4.5 Hz natural frequency geophones are more appropriate choice due to their relatively low cost and durability (Foti, 2005). As can be understood from this, the lower-frequency geophone has an advantage to record lower frequency components of the surface wave possessing the information of the deeper layers. Park et al. (2002) shows that, a 4.5 Hz geophone, outfitted with either flat base plates or short spikes, is enough to record the lowest frequency of 5 Hz which usually can be associated with the maximum investigation depths of about 30 m, the main target depth of this presented study. Also, the study (Park et al., 2002) states that, the weight of the hammer between 10 lb (4.5 kg) and 20 lb (9 kg) can produce sufficient seismic waves to acquire information for 50 m depth. In addition to these, stacking is a way to increase the signal-to-noise ratio by hitting the striker plate repeatedly at each shot point and it can be needed several times to improve the quality of data when the environment is very noisy.

Decision making regarding the relevant interested subsurface depth is the first step in choosing field parameters described above. Depending on the investigation depth,

Rayleigh waves of certain lengths need a specific amount of time to be developed into planar waves due to the nature of the wave (Xia et al., 2004). Indeed, it changes according to near surface properties, so the recording length should be adjusted with respect to this. For example, the more time is needed for softer layers in order to record the planar Rayleigh waves in the MASW survey. So it can get a value between 0.5 s and 4 s depending on the presence of hard or loose near surface material, respectively. The most recommended one is 2 s for the recording length with 1 ms sampling interval, since if the record length get longer, it can increase the chance of recording ambient noise (Park et al., 2006).

The source power is integrated with not only the near surface properties but also the near offset, another acquisition parameter. This means that if the source power is increased with respect to the investigated depth, the near offset should be lengthened to obtain information from deeper layers of the subsurface (Xu et al., 2006). Since surface wave needs to travel a certain distance from the source in order to become planar, this distance is known to be a function of the wavelength as explained in the previous section. This means that information on the deeper layers can be obtained accurately by the fully developed surface waves. Otherwise, the influence of near field effects is seen on the recording data. Due to this effect, the linear coherency at low frequencies can not be obtained in a multichannel survey and it leads to the underestimation of the shear wave velocity for deeper layers. Therefore, the near offset should be almost the same as the principle investigation depth in order to avoid the near filed effects. According to Stokoe et al. (1994), because of this reason, plane-wave propagation of surface waves does not occur in most cases until the near-offset is greater than half of the maximum desired wavelength. Therefore, the near offset should be greater than half of the maximum desired wavelength depending on the investigation depth accepted as two times of the maximum wavelength (Stokoe et al., 1994). However, this approach causes an increase in the far offset effects on the record so that the near offset should be smaller than suggested one by this rule (Park et al., 1999).

Besides these studies, many researches were carried out on the selection of the optimum of these acquisition parameters (Park et al., 2001 and 2002; Zhang et al., 2004 and Xu et al., 2006). In one of these studies (Park et al., 2001), different near offset locations (5 m, 25 m and 50 m distance form the first receiver) were tested without changing the other acquisition parameters with 1 m geophone interval and it is stated that changing near offset does not cause any significant effect in the resolution. However, another study on optimum field parameters of an MASW survey conducted by Park et al. (2002) shows that although the half-wavelength criterion has been adopted as a rule of thumb in the conventional surface wave method (Stokoe et al., 1994), this rule can be relaxed significantly and the actual distance is a function highly sensitive to the wavelength itself (Park et al., 2002). For example, in the mentioned study, two MASW records which were taken by using vibroseis and sledgehammer source indicate that a source-to-closest receiver distance of 10 m will be enough to assure the plane wave propagation for a wavelength as large as 60 m if the investigation depth is shallower than 30 m. Moreover, another study which was implemented by the Exploration Services Section at the Kansas Geological Survey (KGS) has suggested that properties of near-surface materials should be taken into consideration in selection of the optimum distance between the source and the first receiver like the record length as mentioned before. Because of that, an empirical chart was presented in a short course note on SurfSeis software and it was modified by Xu et al., (2006). According to this chart given in Table 4.1, the offset range gets longer if the stiffness of the near surface materials increases.

Table 4. 1 Suggested near offset corresponding to shallow shear-wave velocities (short course notes of SurfSeis by Exploration Services Section at KGS as reported by Xu et al., 2006).

Material type	**Very soft**	**Soft**	**Hard**	**Very Hard**
(V_S in m/s)	(V_S <100)	(100< V_S <300)	(200< V_S <500)	(500< V_S)
Offset (m)	1-5	5-10	10-20	20-40

Not only near offset effect should be considered but also the far offset effect should be prevented by selecting optimum acquisition parameters in the MASW survey. The far field effects are related to the offset range which is directly affected by the geophone spacing and channel numbers since high frequency, i.e., short wavelength components of fundamental mode of the surface waves attenuate rapidly with the distance away from the source. Therefore, if the offset range is too long, body waves and higher mode surface waves will dominate over the high frequency component of fundamental mode. This is called far offset effect and it results in rising the apparent velocity or decreasing linear coherency of the signal spectrum due to the interference between the low velocity fundamental mode Rayleigh wave and high velocity of the undesired high velocity higher order surface and body waves. Therefore, this effect limits the highest frequency which usually determines the upper most thickness of the layer corresponding to the measured phase velocity. (Park et al., 1999).

Park et al. (2002) also shows that the contamination of the fundamental mode increases with offset range. In the same study, it is also stated that the minimum offset range can not be determined by using single parameter such as wavelength like designating near offset. Indeed, it is recommended that offset range can be as large as 100 m in a normal MASW survey if a relatively heavier source (heavier than 10 pounds) is used to generate seismic waves. In addition, another study on the offset effects in MASW survey (Park et al., 2001) shows that higher number of channels can always result in the higher-resolution dispersion curve image only if it is associated with the longer receiver spread length (offset range), i.e., the increasing channel number without the lengthening the offset range does not effect the resolution of the dispersion curve which is used to separate the fundamental and higher mode of the Rayleigh wave if necessary. With the longer offset, the low frequency components of the surface wave are obtained (Park et al., 2002). However, due to attenuation of the high frequency components, it causes loss of information of the shallow layers. Moreover, if the channel number is fixed and the offset range is lengthened by the only increasing the geophone spacing, spatial aliasing problem can come out. To avoid the problem, geophone spacing should be less than half the shortest measured wavelength (Park et al, 1999).

Rather than the spatial aliasing and loss of information of the shallow layers problems, other problems related to the lateral inhomogeneity can be generated when using long offset range to take measurements in the MASW method. An assumption in the MASW method is that the near-surface material is layered and there is no lateral variation in the elastic properties. Therefore, to make this assumption valid, the entire spread should be as short as possible if there is any doubt about the presence of the lateral heterogeneity of the surface materials (Park et al., 1997, 1999, 2001 and 2002). The problem can be overcome by an additional measurement for the same array in the MASW survey. The presence of lateral heterogeneity can be clearly indicated by the comparison of experimental dispersion curves obtained by reverse and forward shots for the same receiver array without changing any other parameters and it also gives a chance to check the forward measurement results in the interpretation process (Foti, 2005). Therefore, by confirming whether or not lateral heterogeneity exists, the offset range can be kept longer by considering the far field effects.

There are several suggestions about the length of the survey and the geophone spacing. For example, the current rule of thumb is that offset range is at least twice the desired depth of the investigation (Foti, 2005). This is also supported by the recommendations of SeisImager software manual (2006). On the contrary, Park et al. (2006) suggests that recorded the minimum and maximum wavelengths are more or less equal to the geophone interval and offset range. Also, Park (2003) gives an equation to calculate geophone spacing (B) after the other parameters are determined, namely the maximum offset (C) and total number of traces (N). This is; $B = (C - A) / N$ (the used notations A, B and C are illustrated in Figure 4.6).

The acquisition parameters for a MASW survey are determined by Parkseismic LLC and given on the web page (MASW, 2009) and these are listed in Table 4.2. But, these values are valid for 24 or 48 channels and the recommended values given in the parenthesis can change in a range of ± 20% and this table is only given to explain the relationships between the parameters. As can be seen in Table 4.2, the desired investigated depth is the determinant, and the other parameters are changing

according to this as explained above. In general, it can be said that the receiver spacing is related to the minimum definable thickness and half of the receiver spread distance between the first receiver and the last receiver is equal to the maximum investigation depth (Xia et al, 2004).

Table 4.2. Table consisting of data acquisition parameters for MASW survey, namely, investigated depth, weight of source in pounds, natural frequency of the geophone, approximate spread length, near offset, geophone spacing, sampling interval, total recording time, number stacking data form calm, noisy and very noisy sites from left to right (MASW, 2009).

Depth (Z_{max}) (m)	**Source (lb)**	**Receiver type (Hz)**	**Receiver Spread (m)**				**Recording**				
			Length	Source Offset	Receiver Spacing		dt (ms)	T (sec)	Vertical Stack		
					24-ch	48-ch			C	V	VN
≤ 1.0	≤ 1 (1)	4.5 – 100 (40)	1-3 (2)	0.2-3 (0.4)	0.05-0.1 (0.1)	0.02-0.05 (0.05)	0.5-1.0 (0.5)	0.5-1.0 (0.5)	1-3 (3)	3-5 (5)	5-10 (10)
1-5	1-5 (5)	4.5 – 100 (10)	1-15 (10)	0.2-15 (2)	0.05-0.6 (0.5)	0.02-0.3 (0.25)	0.5-1.0 (0.5)	0.5-1.0 (0.5)	1-3 (3)	3-5 (5)	5-10 (10)
5-10	5-10 (10)	≤10 (4.5)	5-30 (20)	1-30 (4)	0.2-1.2 (1)	0.1-0.6 (0.5)	0.5-1.0 (0.5)	0.5-1.0 (1)	1-3 (3)	3-5 (5)	5-10 (10)
10-20	≥ 10 (20)	≤10 (4.5)	10-60 (30)	2-60 (10)	0.4-2.5 (1.5)	0.2-1.2 (1)	0.5-1.0 (0.5)	1.0-2.0 (1.0)	1-3 (3)	3-5 (5)	5-10 (10)
20-30	≥ 10 (20)	≤4.5 (4.5)	20-90 (50)	4-90 (10)	0.8-3.8 (2)	0.4-1.9 (1.5)	0.5-1.0 (1.0)	1.0-2.0 (1.0)	1-3 (3)	3-5 (5)	5-10 (10)
30-50	≥ 10 (20) or passive	≤4.5 (4.5)	30-150 (70)	6-150 (15)	1.2-6.0 (3)	0.6-3.0 (2)	0.5-1.0 (1.0)	1.0-3.0 (1.0)	1-3 (3)	3-5 (5)	5-10 (10)
> 50	≥ 10 (20) or passive	≤4.5 (4.5)	> 50 (150)	>10 (30)	>2.0 (6.0)	>1.0 (4.0)	0.5-1.0 (1.0)	> 1.0 (2.0)	1-3 (3)	3-5 (5)	5-10 (10)

4.1.3.1.1.2. Signal processing to construct the experimental dispersion curve in the MASW method

Accurate dispersion curve extraction is a very important element of the MASW method since any error in the dispersion curve would cause inversion to produce an inaccurate vertical Vs section (Park et al., 1999). Because of that, selection of the optimum acquisition parameters as discussed in detail above is an important stage before processing the other steps. After accurately recording the data in the field, a dispersion curve from the shot gather can be calculated. In this process, the

frequency range and phase velocity range of the ground roll need to be determined by analyzing data along the entire line. These two ranges are very important constraints to correctly extract the dispersion curve from the shot gather in order to eliminate the noise recordings and to help to define the thickness of the layer model (Park et al., 2001). Park et al. (2002) states that the fundamental mode surface wave generally can be recorded optimally in the frequency range between 5 Hz and 50 Hz and in the velocity range between 50 m/s and 1000 m/s with 100 m offset range and 10 m near offset.

After these, the dispersion curve, as seen in Figure 4.7, is calculated by using different transform based methods such as frequency-wavenumber (*f-k*) spectrum, slant-slack transform (McMechan and Yedlin, 1981) and phase shift methods (Park et al., 1999).

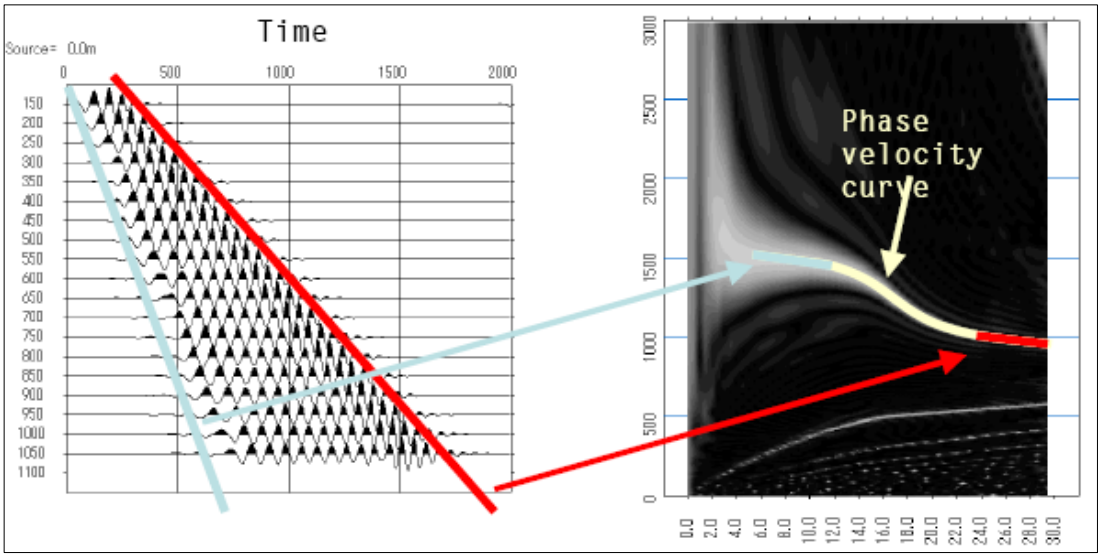

Figure 4.7. The experimental dispersion curve obtained from a MASW record (Hayashi, 2003).

As stated in Park et al., (1999), a clear dispersion curve is obtained by using the phase shift method, even if the shot gather consists of a relatively small number of geophones collected over a limited offset range. Thus, this transformation method is

selected as the transformation method in the construction process of the dispersion curves of the active surface wave measurement taken in this study.

In this method, firstly, a multichannel field record is decomposed via Fast Fourier Transformation (FFT) into individual frequency component, and then amplitude normalization is applied to each component. Then, the necessary amount of phase shifts is calculated to compensate for the time delay corresponding to a specific offset for a given testing phase velocity in a certain range, and it is applied to each individual component, and all of them are summed together to make a summed amplitude corresponding to a phase velocity at that frequency. The schematic illustration of the process is simply illustrated in Figure 4.8. This is repeated for different frequency components. Finally, phase-velocities are determined as the maximum amplitude in each frequency that represents the dispersion curve is displayed as phase velocity versus frequency domain (Hayashi, 2008 and MASW, 2009).

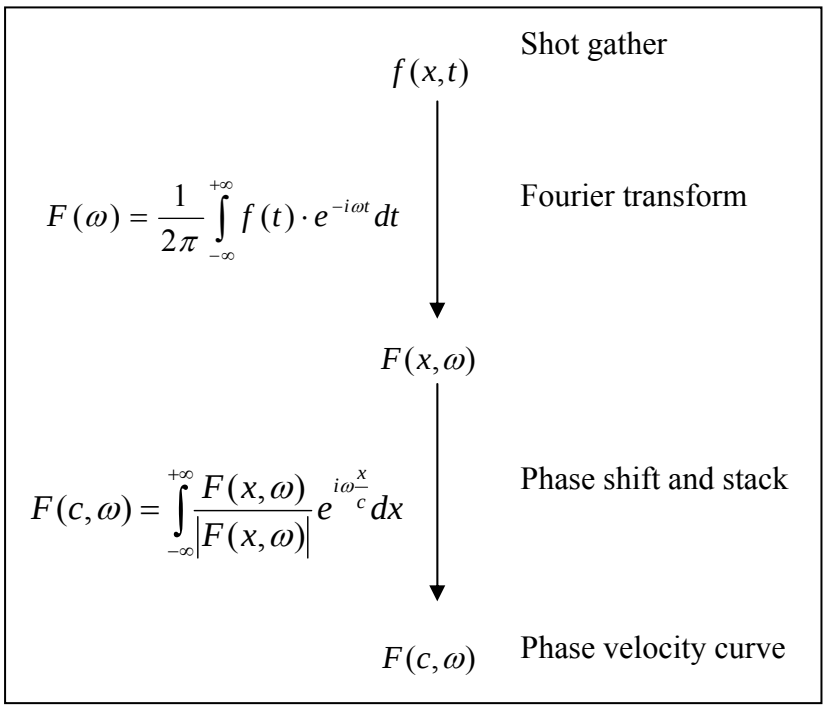

Figure 4.8. Outline of the phase shift transformation method (Park, 1999 as reported by Hayashi, 2008).

Where, x is the distance, t is time, ω is frequency, $f(x,t)$ is a shot gather in time-domain and $F(x,\omega)$ is the shot gather in the frequency-domain.

After the distribution of the peaks of the dispersion energy is determined over different frequency values in the *f-v* domain, an experimental dispersion curve is obtained. As mentioned before, finally, the third step is performed to invert the phase velocities to obtain the shear velocity profile.

4.1.3.1.1.3. Inversion process to obtain a 1D shear wave velocity profile

Typically, the model assumed is a stack of homogeneous linear elastic layers over a half space for interpretation of surface wave tests. Rayleigh-wave phase velocity of the layered-earth model is a function of frequency and four groups of earth properties such as *P*-wave velocity, *S*-wave velocity, density and thickness for each layer. For a model with n layers, including the halfspace, the number of unknowns is 4n-1 (except for half space of which thickness is not defined). As can be understood clearly, it is not possible to solve the surface wave inversion directly, it is necessary to adopt an optimization technique in order to reduce the number of unknowns and possibly to introduce constraints in order to obtain more reliable solutions (Foti, 2005).

The preferred way is that a priori value of density and Poisson ratio are assumed to reduce sensitivity of the dispersion curve with respect to these earth parameters, density and *P*-wave velocity (Foti, 2005). Xia et al (1999) defines the relatively effects of each earth properties on the dispersion curve by the analysis of the Jacobian matrix. According to the results and Xia et al (2004), the shear wave velocity is the most dominant parameter influencing changes in Rayleigh-wave phase velocity among other earth properties for the fundamental mode of high-frequency Rayleigh wave dispersion data (>2 Hz). Therefore, it is the fundamental basis for the inversion of shear wave velocity from Rayleigh-wave phase velocity. To reduce the effect of the other earth property, layer thickness on the dispersive curve should be

selected thinner; this means that the subsurface should be divided into 10 or 15 layers recommended by Hayashi (2008).

The initial model of the shear wave velocity structure is created before the inversion process takes the stage in the surface wave method. Initial model is an important factor to guarantee convergence of the inversion process. The construction of the initial model is based on a simple inversion formula defining the shear wave velocity the 1.09 times the phase velocity and it is assigned to a depth of 1/3-1/2th of the wavelength (Stokoe, 1994).

In the inversion stage, among many non-linear inversion methods such as the least square method, genetic algorithm, simulated annealing methods and so on, non-linear least square method (Xia et al., 1999) will be preferred in this study due to the its simplicity and high accuracy can generally provide reliable S-wave velocities with range of ±15% (Xia et al., 2002). This method iteratively modifies the initial model to minimize the difference from the observed data. After running through a number of iterations, which are generally 10, the modified initial model comes out with a root mean square error (RMSE). This is a measure of the relative error in a percentage for each layer of the initial model in comparison to theoretical criteria. It can be used as a measure of confidence in the calculation of the best match Vs curve from the observed data, RMSE should decrease after each iteration and the final error should be generally less than 5%. After running through a number of iterations, the theoretically calculated dispersion curve is the final S-wave model where the flow chart of this stage is given in Figure 4.9.

Dispersion curves reflect the average velocity model beneath the geophone spread and for 1D analysis, the resultant V_S profile is representative of the center of the geophone spread (SeisImagerSW Manual 2.2, 2006). Though, higher modes of Rayleigh wave can be used to obtain S- wave velocity profile with fundamental mode Rayleigh wave which is the motion having lowest velocity for any given frequency (Xia et al., 2004), this study only deals with the fundamental mode in MASW and MAM surveys to obtain one dimensional S-wave velocity profile.

Although it is possible to obtain a 1D shear wave velocity profile to nearly 30 m using the active dispersion curve, it should be noted that the shear wave velocities may be underestimated because of near-field effects. If passive tests are feasible, the combination of active and passive measurements may help to reduce near-field effects as well as provide a shear wave velocity profile to greater depth (Asten and Boore, 2005).

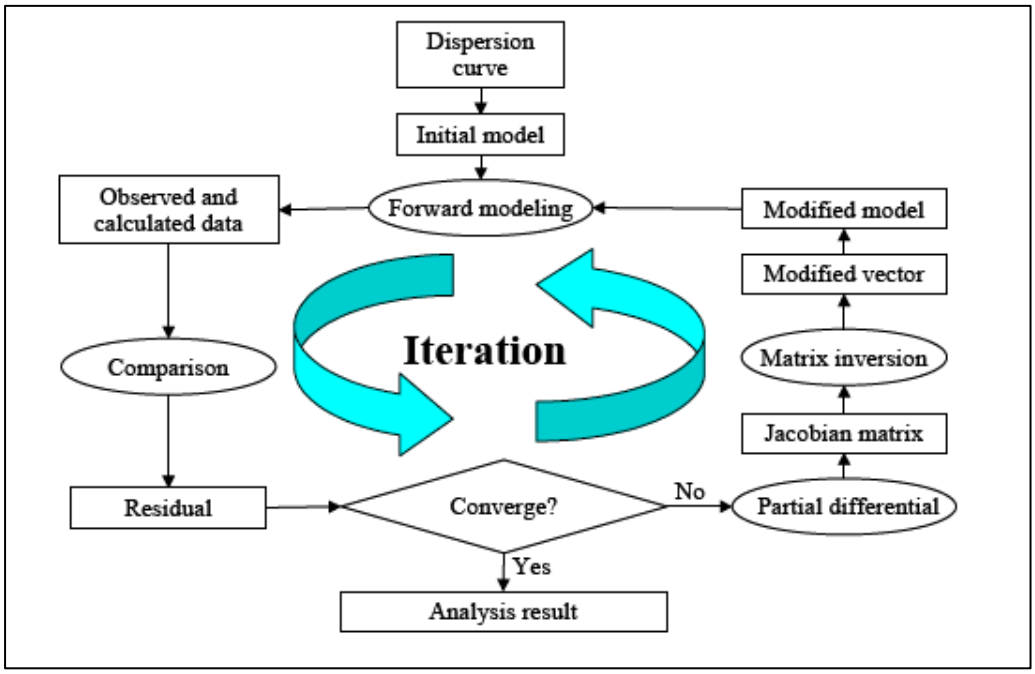

Figure 4.9. The flow chart of the inversion process (SeisImagerSW Manual 2.2, 2006).

4.1.3.1.2. Microtremor array method (MAM) method

As mentioned in the previous section, the MASW and SASW methods involve active sources, which are optimized for the purpose of the test as mentioned in the previous section, however, passive-source methods are based on recording ambient noise. When compared to the active methods, passive methods cover broader and deeper volumes. The microtremor array method (MAM) utilizes passive or ambient energy generated by cultural noise, traffic, factories, wind, wave motion, etc. The important

assumption related to passive surface wave methods is that the measured microtremors are mainly surface waves of primarily fundamental mode Rayleigh waves (Figure 4.2) (Aki, 1957; Asten and Boore, 2005; Park et al., 2007). As summarized by Figure 4.1, the analysis of measured microtremors is performed by spatial auto correlation (SPAC) transform based methods in microtremor array method (MAM) or p-f (slowness-frequency) in ReMi. Passive surface wave methods are named based on the used transform method. Passive surface wave methods are utilized to find the shear wave velocities characterizing deeper layer by different configurations (Asten and Boore, 2005). However, the passive methods can lack resolution in the near-surface and also are poorly suited for quiet locations due to insufficient passive energy (Tokimatsu 1997 and Rix, 2005) and local data quality variations depending on geology and the proximity and abundance of ambient noise.

Unlike the active surface wave methods, the passive method does not need any sources and needs two-dimensional arrays, such as triangle, circle or cross. Because the sources of the microtremors are distributed randomly in space, the microtremors do not have any specific propagation directions. Therefore, two dimensional arrays are required for calculating the phase-velocity of microtremors. Isotropic arrays, such as circle or triangle are theoretically best for passive analysis. However, sometimes it is difficult to use such isotropic arrays in an urban area. Irregular arrays such as L-shape array or linear array enable us to use the passive method in an urban area. These results lead to the conclusion that irregular arrays can be used for small-scale passive surface-wave method in which relatively high-frequency micro-tremors are used. Recently, several theoretical and experimental studies have been performed on the applicability of irregular arrays (eg; Louie, 2001; Louie et al., 2002; Pullammanappallil et al., 2003; Rucker, 2003; Jin et al., 2006;; Chavez Garcia et al., 2005, 2006 and 2007; Chavez Garcia, 2007; Panca, 2007; Yokoi and Margaryan, 2007; Hayashi, 2008) and they show that there is good agreement between the results of the linear Passive methods (ReMi and MAM) and also some of these results of the MAM and ReMi are compared with that of the active surface wave method and MAM with isotropic arrays give good correlations.

4.1.3.1.2.1. Data acquisition and field configuration in the MAM method

Passive surface wave methods help to determine shear wave velocities characterizing deeper layers by different configurations. Especially, in the ReMi method and anisotropic arrays of MAM, linear array or L shape array (only in MAM) configurations are used. However, the sources of the microtremors are distributed randomly in space. This means that the microtremors do not have any specific propagation directions. Therefore, isotropic arrays are the best alternatives for calculating the phase-velocity of microtremors in the passive methods. These give to get a broad frequency range between 0.2 Hz and 15 Hz (Aki, 1957; Hayashi 2003; Rix, 2005 and Hayashi, 2008). On the contrary, the isotropic arrays needs wide space and it is difficult to find such wide space in urban areas. The use of irregular arrays will enable us to apply the passive methods in an urban area. The main interest in the study is focused on the applicability of irregular array (i.e., linear array) in the SPAC method. Theoretically, isotropic arrays, such as a circle or an equilateral triangle, are preferable in the SPAC analysis. However, the isotropic arrays require wide space and it is difficult to obtain such wide space in urban areas. Recently, several theoretical studies have been conducted on the applicability of irregular arrays. The results of the SPAC analysis obtained from linear array compared with those of the isotropic array configurations (Yokoi and Margaryan, 2007 and Hayashi, 2008) and those of the ReMi results (Chavez Garcia et al., 2007). These studies show that the results obtained from linear array configuration in the SPAC analysis shows good agreement with the others. However, it still has drawbacks since microtremors do not always propagate parallel to the survey line. If microtremors propagate perpendicular to the survey line and reach all of the geophones at the same time, the phase velocity cannot be calculated. As the angle of propagation increases from parallel to perpendicular, the apparent phase velocity increases. In reality, sources of microtremors vary and energy radiates from many directions at unknown angles to the geophones. Since angles of propagation are unknown, with a linear array, the calculated phase velocity may be higher than the true Rayleigh-wave actual phase velocity unless a method independent of the source locations like SPAC is applied (Sesimager Manual, 2006).

In the MAM technique with linear array configuration like the MASW method equipment, common seismic refraction recording equipment is used to record effectively surface waves at frequencies as low as 2 Hz with 12 or more geophone sensor channels. Large array size and long period geophones are important for deep sounding (Asten and Boore, 2005). As explained before, 4.5-Hz natural frequency geophones are a more appropriate choice due to their relatively low cost and durability and also it must be noted that the dispersion curves obtained by the 4.5Hz geophones is almost identical down to the frequency of 2 Hz in the passive survey method (Hayashi, 2008).

As mentioned before, array size (receiver spread) is changing with respect to the investigation depth. Because a passive survey usually operates with much larger geophone spacing (generally 5 m or more) than normally used in an active survey, a processed dispersion image usually lacks information at shallower depths, or higher frequencies. To resolve shallow structures in more detail, shorter geophone spacing and a higher frequency geophone can be used. Also, lateral changes along the profile can be examined by selecting fewer terraces from the whole channels (12 or more) recorded. Although in theory this missing information can be filled through multiple surveys with progressively smaller dimensions, higher frequency components of passive surface waves may not be recorded effectively because of their relatively rapid attenuation properties (Park et al., 2007). Therefore, the best way would be to perform a separate active survey along the same profile.

Recent studies (Louie, 2001; Pullammanappallil et al., 2003; Panca et al., 2007; Hayashi, 2008) on passive surface wave methods show that a linear array can be used for the relatively small high frequency range for instance from 2 Hz to 15 Hz. Louie (2001) states that the passive method gives mechanical properties of the layer at 100 m depth by 200 m offset spread with an accuracy of 15%. As a rule of thumb the maximum depth resolution is about one third to one half the length of the array, but sometimes array size can be almost corresponding to an investigation depth in a SPAC analysis (SeisImager Manual, 2006 and Hayashi, 2008). The recommended one is 32 s for the recording length with 2 ms sampling interval (SeisImager Manual,

2006). However, more than one record length is required, since clearly, the longer the data, the better it is for statistical analysis in the spatial auto correlation (i.e. minimum RMSE value). However, long data acquisition decreases the convenience of the method. The suggested optimum number of data ranges between 5 and 20 in the literature (Pullammanappallil et al., 2003; Chavez Garcia et al., 2005; Hayashi, 2008).

4.1.3.1.2.2. Signal processing to construct the experimental dispersion curve in MAM method

Ambient noise recorded with linear array can be analyzed by both p-f (i.e. slowness-frequency) and SPAC (spatial auto correlation) in ReMi and MAM, respectively. In order to calculate the phase-velocity of microtremors by the multichannel analysis of surface waves, the propagating direction of microtremors has to be known. On the contrary, microtremors do not propagate into a specific direction, even though it is almost impossible to determine the propagating direction. Aki (1957) proposed a spatial auto correlation (SPAC) method in which microtremor data is statistically analyzed, for calculating the phase velocity of surface-waves. This method requires ambient noise records obtained in a circular array of stations with one station at the center. This geometry allows the frequency domain cross-correlation between stations at a given distance, averaged azimuthally and takes the form of a zero order Bessel function given in the following equation:

$$J_0\left(\frac{\omega}{c(\omega)}r\right)=\frac{1}{2\pi}\int_0^{2\pi}\cos\left(\frac{\omega\cdot r}{c(\omega)},\theta\right)d\theta \qquad (4.1)$$

where,

J_0 is the first kind of Bessel function;
$c(\omega)$ is phase-velocity at angular frequency ω;
r is the interstation distance between all station pairs; and,
θ is the direction of two sensors.

Microtremor array measurements based on the Spatial Auto Correlation has been developed by Okada (2003) and this study shows that it is possible to use the SPAC method without the limitations imposed by the circular array. If it is assumed that microtremors do not come from some specific direction and propagate in all directions homogeneously, the directional average in the equation (4.2) can be calculated even if arrays the are anisotropic (Hayashi, 2008).

$$SPAC(r,\omega)=\frac{1}{2\pi}\int_{0}^{2\pi} COH(r,\omega,\theta)d\theta \qquad (4.2)$$

where,

COH is the complex coherence of two sensors.
Eq (4.2) gives the definition of the other notations

After the distribution of the peaks of the dispersion energy is determined over different frequency values in the *f-v* domain, an experimental dispersion curve is obtained. The third step inversion process is same with the MASW method and defined in Section 4.1.3.1.1.3 and the schematic illustration of the inversion process can be seen in Figure 4.9.

In summary, by using optimum acquisition parameters mentioned in both methods, passive surface wave method (MAM) enables to get accurate information of deeper layers to construct shear wave velocity profile in 1D, whereas active surface wave method (MASW) has more capability to resolve successfully shallower layers for those purposes due to the nature of surface waves and their proximity to the geophone spread. Therefore, the passive surface-wave method, together with the active method, enables us to maximize the depth of investigation and yield a composite high-resolution result over all depths (30 m in this study) nondestructively from the surface.

4.2. Evaluation of the basic characteristics of ground motion by the H/V method

4.2.1. Introduction

Recent destructive earthquakes have clearly shown that near-surface local site conditions that can generate significant amplification that may lead to variations in the damage patterns of the earthquakes with respect to the local site conditions. Therefore, spatial variations of the ground motion show the significant importance of gathering information on soft soil response. Detailed assessment of the sediment characteristics (site effects and the predominant frequencies) over a wide area where significant amplification occurs can be obtained using many methods, but these explorations are still economically and technically difficult to make. On the other hand, measurement and analysis of microtremor recording by the H/V method, is a relatively easy and economically attractive method for especially in urbanized areas. The method involves using ambient seismic noise to evaluate the sediment-amplification potential and to establish the seismic microzonation map that is very useful in hazard assessments.

4.2.1.1. H/V (Nakamura) method

The H/V technique (Nakamura, 1989 and 1996) aims at estimating the site characteristics using microtremor measurements, and consists of deriving the ratio between the Fourier amplitude spectra of the horizontal and the vertical components of the microtremor recorded at the surface (Figure 3.4). This is, the technique based on recording ambient noise. Noise is the generic term used to denote ambient vibrations of the ground caused by sources such as tide, water waves striking the coast, turbulent wind, effects of wind on trees or buildings, industrial machinery, cars and trains, or human footsteps, etc (Claudet, et. al., 2006). All of the noise sources have two different origins namely natural (storm, sea waves, etc.) and cultural sources (plant, automobile, train, etc.) due to their frequency content. Therefore, this helps to differentiate microseisms and microtremors at relatively low and high frequency, respectively, with regard to their origins. (microseisms and microtremors

are corresponding to natural and cultural sources, respectively; Gutenberg, 1958; Asten, 1978; Asten and Henstridge,1984). It should be noted that cultural noise is of interest since it is predominant in an urban setting.

Short-period microtremors generated by cultural source are very low-amplitude oscillations of the ground surface to use records of ambient seismic noise. They are combination of various types of waves, from many natural sources such as traffic, industrial machinery, small magnitude earth tremors, and movement of objects triggered by wind (Kanai, 1966). The seismograph which has more than about a thousand times magnification, records the ground motions continuously in an ordinary place. Usually, the maximum amplitudes of the motions, from 0.1 to 1 micron, and the ranges of their periods are from 0.1 s to 1 up to 2 s (Kobayashi, 1991). The short-period microtremors are related to shallow subsurface structures several tens of meters thick (Kanai, 1983).

The application of short-period microtremors to estimate site effects has been investigated for many years by Kanai and Tanaka (1961); Kanai (1983) and Kobayashi et al. (1986). They assume that the microtremor horizontal motions at short-periods consist mainly of shear waves, and that the spectra of the horizontal motions reflect the transfer function of the ground at site. And also, they consider it possible to estimate dominant period and amplification level of soft sediments by measuring directly the dominant period of microtremors and its maximum amplitude in microns. This approach, with some variants, has been used to characterize site effects in a wide variety of seismic environments (e.g., Kanai and Tanaka, 1954; Kobayashi et al., 1986; Lermo et al., 1988; Field et al., 1990; Finn, 1991).

A microtremor observed at the ground surface is not always steady, but usually shows daily, weekly and seasonal changes. This is because the tremor is easily affected by the surrounding noise sources. As a result, frequency components of horizontal and vertical microtremors indicate effects not only on local site conditions but also on such noise sources. Thus, local site effects are hardly detected with a sufficient accuracy from the horizontal or vertical motion of the microtremor alone.

However, when a ratio of the frequency components between the horizontal and vertical motions is considered, it usually shows a steady spectrum, neglecting any contribution from deep sources. Due to its steady nature, the HVSR has become often used for analyses of microtremor data for site effect studies. It may be supposed that the vertical component of motion is not amplified by the soft soil layer according to HVSR (Campillo et al., 1988). One of the best techniques developed by Nakamura (1989) is based on an estimation of the transfer function using microtremors. Many theoretical (Lachet and Bard, 1994) and experimental (Lermo and Chavez-Garcia, 1994; Tevez-Costa et al., 1996) studies have shown that the spectral ratio obtained in this manner enables an adequate determination of the site fundamental frequency.

Despite the problems related to their interpretation will be mentioned below, microtremor measurements in the Nakamura method provide efficient applicability in terms of economy and quickness. In the microtremor measurements, the standard equipment generally used comprises a three-component velocity or acceleration seismometer (velocimeter or accelerometer) with an amplifier and PC as a data recorder. The study (Guillier et al., 2008) on the sensitivities of different brand velocimeters and accelerometers shows that all tested velocimeters is usable to record ambient noise in microtremor studies, but the accelerometers are not appropriate due to their insensitivity to noise measurements. Natural periods of sensors used are based on the period dependency (sensors are generally 1.0 s or longer than 1.0 s. especially for short period of range) of microtremors considering the purpose of the study. After recording the ambient noise, the ratio between the Fourier amplitude spectra of the horizontal and the vertical components of the microtremor recorded at the surface in the data processing stage of H/V ratio method.

Because of these advantages in the application and processing stage, Nakamura method has been widely used in microzonation studies for nearly two decades. Also, due to the simplicity of the theorem given below, most researchers have been trying to compare the results of this technique with that of well established experimental technique (SSR, details given in Chapter 3) and numerical methods (1D, 2D and 3D

analysis of soil columns). When the capability of H/V in the estimation of site effects is compared to the SSR method (Duval, 1995; Field and Jacob, 1995; Lachet et al., 1996; Tevez-Costa et al., 1996; Lebrun, 1997; Rodriquez and Midorikiwa, 2002; Haghshenas, et al., 2008) and to 1D numerical method (Bour et al., 1998; Cid et al., 2001; Satoh et al., 2001; Nguyen et al., 2004), the general agreement is that fundamental periods obtained by the Nakamura technique are similar to the results of the mentioned techniques. However, there is absence of correlation between the peak of the H/V and the actual site amplification. According to the amplification ratio of the site determined by mentioned techniques, the H/V peaks generally take place between the peak amplitude of 1D and SSR analyses.

There is still disagreement as to the type of seismic waves that form microtremors. Udwadia and Trifunac (1973) concluded that compressional, shear and surface waves all can be found in microtremor data. Others have determined that Rayleigh waves are the primary component (Akamatsu, 1984; Nakamura, 1989). However, surface waves have been known to act like body waves which internally reflect in a single layer above a half-space and thus may be modeled as such. Hence, a shear wave propagating vertically through a half space correctly predicted Rayleigh and Love wave amplification which was similar to a vertically propagating shear wave (Drake, 1980).

H/V spectral ratio basically depends on the ellipticity of Rayleigh waves because of the predominance of Rayleigh waves (in one sedimentary layer over a bedrock) in the vertical component (Figure 4.10). This ellipticity is frequency dependent and displays a sharp peak around the fundamental frequency for sites having a high enough impedance contrast between the surface and deep materials. The vertical component of ambient noise keeps the characteristics of source to sediments surface ground, is relatively influenced by Rayleigh wave on the sediments. Therefore, this method can be used to remove both of the source and the Rayleigh wave effects from the horizontal components (Nakamura, 2000).

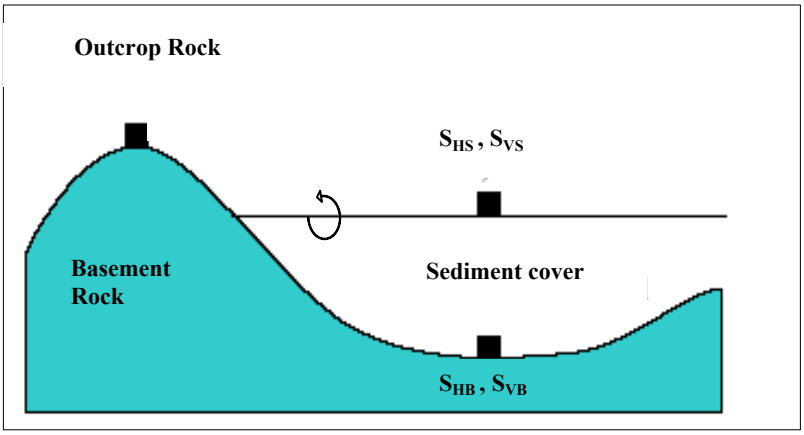

Figure 4.10. Simple model assumed by Nakamura (1989) to interpret microtremor measurements.

The HVSR technique assumes that microtremors are Rayleigh waves propagating through a single soil layer overlying a half-space of relatively higher velocity than the soil (Nakamura, 1989). Thus, there are two components of motion along the free surface and two components of motion along the low-to-high velocity interface. This method is based on the assumption that the horizontal component of Rayleigh waves is amplified by the soil at the surface, while amplification of the vertical component is negligible. It has already been recognized that this happens only at certain frequencies, but the general agreement is that it is the horizontal component of motion which is amplified mostly at the surface (Akamatsu, 1984; Nakamura, 1989; Lermo and Chavez-Garcia, 1994; Lachet and Bard, 1994). Another assumption is that the noise source is due to local cultural disturbances; therefore, deep sources can be neglected. This implies that local sources will not affect the microtremor motion at the base of the soil layer. Site effects due to surface geology are generally expressed as the transfer function of the surface layers is given by:

$$S_T = \frac{S_{HS}}{S_{HB}} \tag{4.3}$$

Where, the spectral ratio of transfer functions between the horizontal component of

microtremor spectrum at the surface (S_{HS}) and the horizontal component of microtremor spectrum on the substratum (S_{HB}).

Considering that the instrumental method consists of recording the ambient background noise (artificial noise) is not only propagated as body waves, but comprises an important part of Rayleigh waves, it is necessary to make a correction to remove the effect of surface waves. Nakamura assumes that the effect of Rayleigh waves (E_S) propagating in a soft surface layer overlying a stiff substratum is included in the vertical spectrum at the surface (S_{VS}) and not at the base ground (S_{VB}), and then it could be defined as:

$$E_S = \frac{S_{VS}}{S_{VB}} \tag{4.4}$$

Assuming also that the effect of Rayleigh waves on microtremor motion is equivalent for the vertical and horizontal components, Nakamura gives the new transfer function as:

$$S_{TT} = \left(\frac{S_{HS}}{S_{VS}}\right) / \left(\frac{S_{HB}}{S_{VB}}\right) \tag{4.5}$$

Three recordings gave results where the spectral ratio of the horizontal and vertical components of motion at the bottom of the layer (S_{HB} / S_{VB}) is nearly 1.0 for a relatively wide frequency range (0.2-20 Hz). Thus, the spectral ratio between the horizontal and vertical components of the background noise recorded at the surface of a soft layer enables to eliminate the effects of the Rayleigh waves (E_S), conserving only the effects resulting from the geological structure of the site. Therefore, this spectral ratio will be called the HVSR spectral ratio given as:

$$S_{H/V} = \frac{S_T}{E_S} = \frac{H_S}{V_S} \tag{4.6}$$

Many theoretical (Lachet and Bard, 1994) and experimental (Lermo and Chavez-Garcia, 1994; Tevez-Costa et al., 1996; Seekins et al., 1996) studies have shown that the spectral ratio obtained in this manner enables an adequate determination of the site fundamental frequency. Considering Eq. (4.6), the HVSR spectral ratio [$S_{H/V}$] was obtained by dividing the resultant spectra of the horizontal components of the sediment site [H_{NS} and H_{EW}] by the spectrum of the vertical component [V_S] of the sediment site:

$$S_{H/V} = \frac{\sqrt{\left(H_{NS}{}^2 + H_{EW}{}^2\right)}}{V_S} \tag{4.7}$$

As mentioned, many recent experimental studies seem to prove that it is possible to provide a good estimate of the characteristics of sedimentary sites using only one station. The spectral ratio of horizontal to vertical components proposed by Nakamura (1989) has been performed at several places seem to be able to provide all the information required for a reliable estimate of the site dominant period (e.g., Fäh et al., 1997; Duval et al., 1998; Guegen et al.,1998; Delgado et. al., 2000 and 2002; Bodin et al., 2001; Tevez-Costa, 2001; Koçkar, 2006; D'Amico et al., 2008). These observations are also supported by several theoretical investigations as well (e.g., Field and Jacob, 1993; Lachet and Bard, 1994; Lermo and Chavez-Garcia, 1994). However, the obtained amplification ratio from this technique is still questionable. Although some theoretical studies (e.g., Lachet and Bard, 1994 and Bard, 1999) and experimental studies (eg., Teves-Costa et. al., 1996; Bour, 1998 and Nguyen et. al., 2004) have shown that the spectral ratio obtained by Nakamura method does not seem to be able to provide all the information required for a reliable estimation of the amplification of surface ground motion, the other studies (Lermo and Chavez-Garcia, 1993; Nakamura, 1989, 1996 and 2000; Toshinawa et al., 1997; Konno and Ohmachi, 1998) show a good relationship between the amplitudes obtained by H/V ratio and the actual site amplification.

However, there is still some discussion about the applicability of short-period microtremors to determine fundamental frequency of soft soil sites, mainly because

of difficulties in discriminating source effects from pure site effects in noise recordings (Finn, 1991; Lermo and Chavez-Garcia, 1999) and discrepancies between noise and earthquake recordings (Udwadia and Trifunac, 1973; Aki, 1988). According to Tokimatsu (1997) it could be concluded that the natural period of the site could be equal to or slightly larger than (10-20%) the period of the HVSR peak; or approximately equal to twice the period of the HVSR minimum. The natural period estimated from above may not always correspond to the fundamental site period, but rather reflect the second one or the depth of the interface between layers with the high impedance ratio.

It is important to note the qualitative character of the maximum amplification values. Lachet and Bard (1994) conclude that the H/V spectral ratios on ambient noise records allow assessing the fundamental frequency but fail to reproduce the higher modes. The amplification factors obtained were too sensitive to a variety of parameters, such as the velocity contrast, Poisson's ratio and source-receiver distances. Therefore, the Nakamura method does not presently enable the level reached by the peak of the H/V spectral ratio to be related to the amplification of a signal at the surface relative to that in the bedrock during a strong tremor. Maximum level of H/V ratio could be an indication of relative signal amplification in case of strong motion (Bour et al. 1998; Duval et al., 2001). One should not forget that this technique is based on various assumptions, as yet not totally verified, concerning the nature of the incident background noise (Bour et al. 1998).

In summary, experimental approaches obtained by microtremor measurements should be used in conjunction with other site investigation or with available geological and geophysical information to obtain much more reliable and comprehensive information on soft soil response, and thus identifying and characterizing the site amplification and fundamental frequency in urban areas. By considering these, during the determination of the natural periods, this methodology has been used in conjunction with available geological information or with other geotechnical and geophysical data that were obtained from the project site.

CHAPTER 5

IN-SITU TESTING RESULTS AND ANALYSES

5.1. Data acquisition and analysis of in-situ tests

5.1.1 Data acquisition and analysis of surface wave methods

One simple way of determining site condition in seismic hazards estimations is to utilize the characteristic shear wave velocity in shallow depths to classify stiffness of the geomaterials and to produce a seismic hazard map. The average shear wave velocity for the uppermost 30 m of the soil profile is simply used in the seismic codes to classify sites into the categories that can be used for assessing the spatial variations of the ground motion in the area. Also, shear wave velocity is a valuable parameter to distinguish the lithologies quantitatively based on their deposition settings and age. Because of these purposes, 92 surface wave measurements were taken at 51 different locations to study the seismic response of different lithologies at the northern part of the Çubuk Plain. A total of the 41 in-situ measurements were taken through both passive (MAM) and active surface wave (MASW) methods, and at 10 site locations, only passive surface wave method was implemented. To characterize the geological sites according to their age and depositional settings, these measurements were carried out at sedimentary deposits which are Late Pliocene to Quaternary in age. A total of 38 and 13 data points fell on with in the units of the Quaternary alluvium and terrace, and the Upper Pliocene to Pleistocene sediments, respectively. The spatial distribution of the surface wave measurement points can be seen in Figure 5.1.

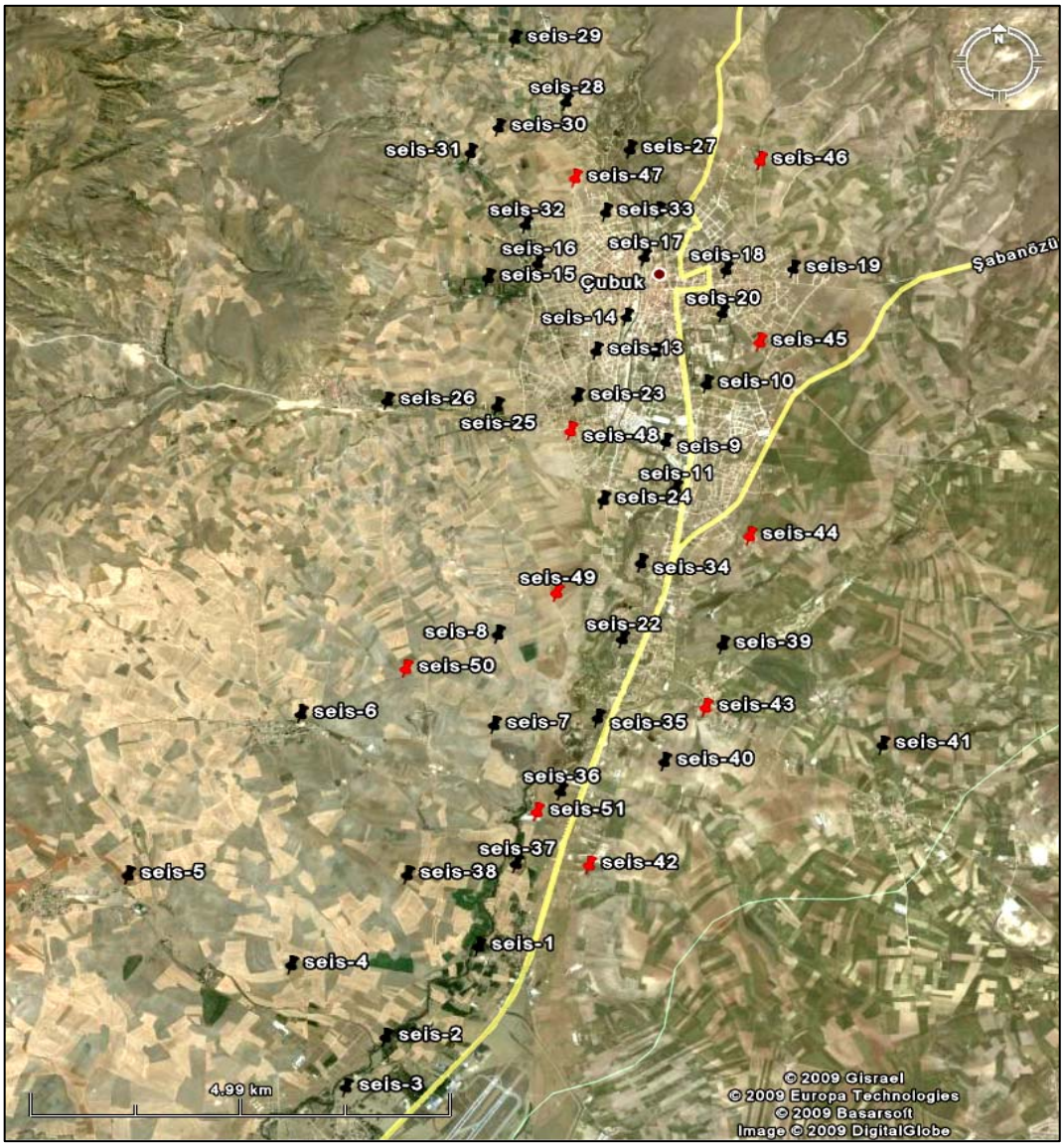

Figure 5.2. Spatial distribution of the measured surface wave points in the area. Red pins show the locations where both active and passive surface wave measurements were implemented. Black pins show the locations at which only passive surface wave measurements were taken.

In order to obtain more reliable information on the soil profile, the surface wave measurements were attempted to be taken at the same sites of the microtremor recordings utilizing a grid system. By using a grid system and a GIS query, site conditions with respect to a code-based site classification through incorporating shear wave velocity data were assigned.

All measurements were generally recorded in a linear array configuration with twelve 4.5 Hz natural frequency vertical geophones with 5 m spacing. As can be seen in Figures 5.2 and 5.3, geophones with spikes were connected to the seismograph through a spread cable and all the surface wave measurements were acquired by a ABEM-RAS 24 seismograph with 12 channels. The qualities of the recorded measurements were preliminarily checked by means of a laptop immediately after recording.

Figure 5.3. Photo A: A view of the Seis-2 site showing the general configuration of the surface wave method applied at the sites, photo B: a view of the 4.5 Hz geophones that were connected to the seismograph through a spread cable.

Figure 5.4. Photo A: A view of the surface wave measurement configuration from site Seis-19. Photo B: a view of the equipment used for data acquisition, monitoring and storage.

As mentioned in Chapter 4, the offset distance (i.e., the distance between the source and the nearest geophone) is fixed to 5 m in the MASW method. The source was generated by using a 6 kg (13.2 lb) sledge hammer hitting on a 35 x 35 cm striker plate. The source was placed with a trigger geophone at both ends of the survey line in order to ensure continuity of the lateral homogeneity (Figure 5.4). In order to eliminate the background noise of the environment, vertical stacking was implemented 3 or 5 times at each shot point of each array to increase the signal-to-noise ratio (i.e., to improve the quality of data). The recording length was selected as 2 s with a 1 ms sampling interval to record the generated surface waves. The phase shift transformation method was used to obtain the experimental dispersion curve as an input parameter for the inversion stage.

In the MAM survey, sampling time interval was selected as 2 ms. Ambient noise was recorded with 5 minute duration which corresponds to nine times 32 s records. The SPAC (Spatial Autocorrelation) analysis (Okada, 2003) was utilized to construct the

dispersion curve. A one-dimensional inversion using a non-linear least square technique has been applied to the phase velocity curves and a one dimensional S-wave velocity structure down to a depth of 30 m was obtained.

Figure 5.5. Photo A: A view showing the application of the MASW method. Photo B: ABEM RAS 24 seismograph. Photo C: The MASW equipment (sledge hammer, striker plate and trigger geophone).

According to the theory of the surface wave methods, the measured surface wave records are processed and analyzed by using SeisImager/SW™ V. 2.2 software in the analyses process of the active and passive surface wave measurements. SeisImager/SW is an easy-to-use yet powerful program that is capable of analyzing both multi-channel active and passive source of the surface wave data. The program contains four individual modules (i.e., Pickwin™ V. 3.3.0.3, Plotrefa™ V. 2.8.0.2, WaveEq™ V. 2.2.0.3 and GeoPlot™ V. 8.2.6.1.) It also contains surface wave analysis wizards which is not a separate module. The wizard consists of three modules related to the surface wave analysis namely Pickwin, WaveEq and GeoPlot (for only 2D analysis). It automatically activates the specific functions of these modules in order

of the processing steps. SeisImager/SW is mainly composed of two modules (Pickwin and WaveEq) for 1D surface wave analysis. In the analysis stages of the surface wave methods, these two main modules were used to obtain 1D shear wave velocity of the subsurface structure in this study.

During the analyses steps, firstly, the data acquisition parameters such as geophone spacing, near offset and number of the channels (i.e., offset range) were defined in the Pickwin module. Then, in order to transform the data to a phase velocity-frequency (*v-f*) domain, the start velocity (equal to zero) and the maximum expected end phase velocities of the site were determined according to the analyzed site conditions. This means that the end phase velocity should be adjusted differently for different sites in order to obtain more reliable results. To construct the dispersion curves in the *v-f* domain, the start and end frequencies were also defined according to the information given in the literature where, in general, 5-30 Hz for the MASW records and 2-15 Hz for the MAM records were deemed mostly appropriate for all sites (Park et al., 1999; Louei, 2001; Hayashi, 2008). Upon, assigning values to these terms, the transformation method was chosen as phase shift and SPAC 2D for the MASW and MAM records, respectively. Additionally, maximum and minimum wave length limitations were applied to both the MASW and MAM records in the transformation process as recommended by the SeisImager/SW Manual V. 2.2 and discussed in Chapter 4. Lastly, an experimental dispersion curve of the site was obtained (Figure 5.5). All of the procedure mentioned herein is performed in the Pickwin module of the Siesimager software.

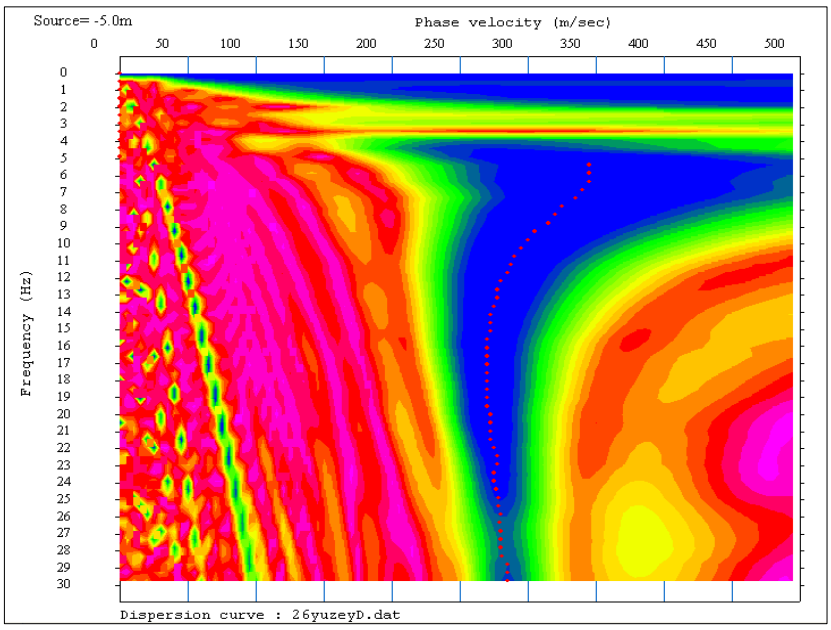

Figure 5.6. An example of the constructed experimental dispersion curve of a MASW record for the Sies-26 point.

After construction of the dispersion curve, the WaveEq module was activated to build an initial model of the 1D profile and to perform a non-linear least square method for the inversion process. In this step, firstly, the constructed phase velocity versus frequency graphs (dispersion curve) were checked based on their signal over noise ratio (S/N) curves which are a relative indicator of the quality of the data points. Due to the variation in the signal-to-noise ratio, the quality curve has peaks and valleys corresponding to the relatively higher and lower quality data points, respectively (Figure 5.6).

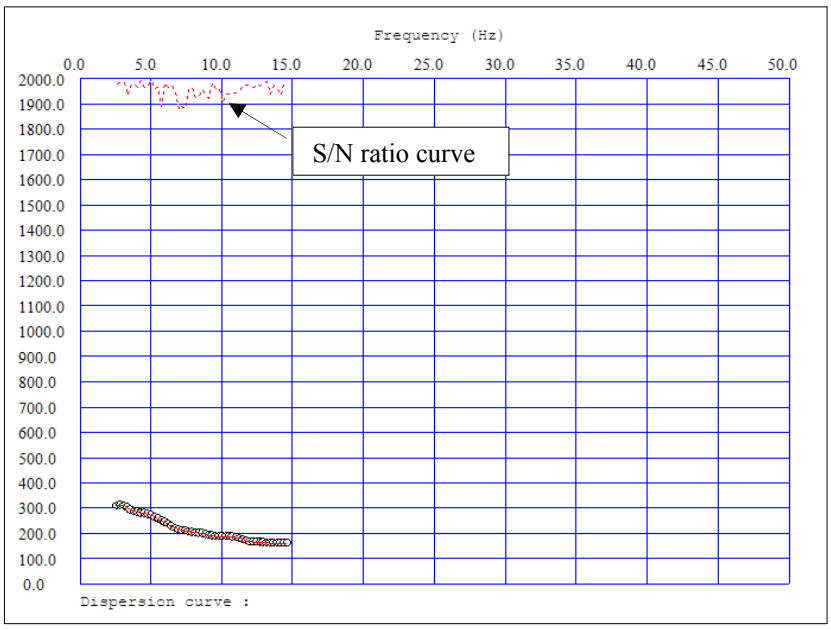

Figure 5.7. A view of the constructed dispersion curve in the WaveEq module of the MAM record for the Seis-17 point.

All necessary editing was applied at this stage to remove lower quality data and the higher modes of the Rayleigh wave. As can be seen in Figure 5.7, it is possible to detect higher modes of the Rayleigh wave which causes overestimation in calculation of the shear wave velocity. In addition to this, the variations in the S/N curve increases towards the higher mode of the Rayleigh wave. This situation also appears on the dispersion curve as shown by smaller circles in Figure 5.7. Generally, there were poor quality data (small circles) at low and high frequency ends of the curve. Therefore, this stage prior to the building the initial model of the soil profile was carefully performed for both active and passive surfaces. To obtain a reliable shear wave velocity model, data acquisition should be carried out properly and the dispersion curve should be constructed accurately in the analyses stage before the inversion process.

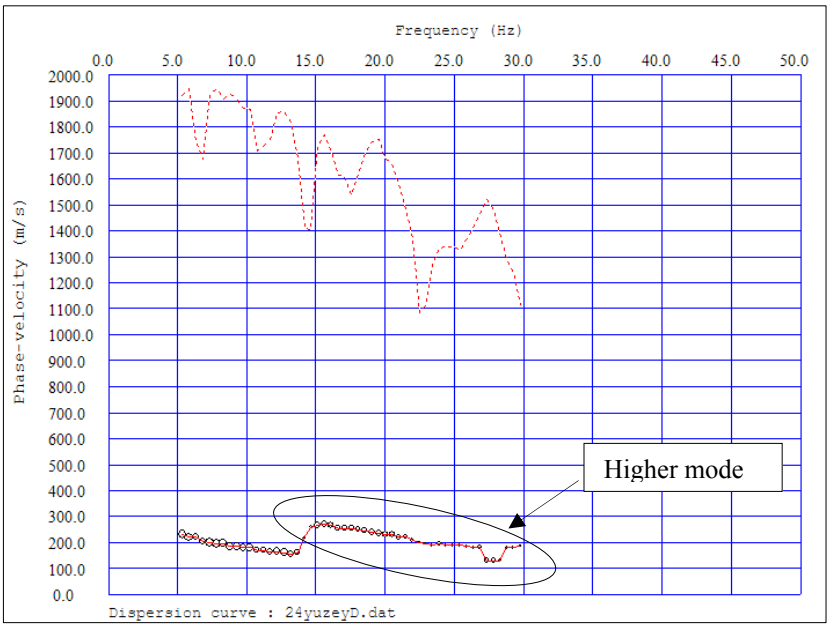

Figure 5.8. The experimental dispersion of the MASW record of the Sies-24 point.

Moreover, reverse and forward MASW records taken at each site were analyzed and it was confirmed that there was no lateral variations in the geologic units along the survey line (55 m). An example of this analysis can be seen in Figure 5.8. Also, it provides double check on the shear wave velocity profile at the same location.

The resolutions of the dispersion curves were very high due to utilization of a long offset range (Figure 5.6). Therefore, when the spectrum is contaminated by a higher mode, it is easily distinguished and separated from the fundamental mode Rayleigh wave. For some measurement points (Figures 5.7 and 5.8), it was not possible to catch high frequency components (greater than 15 Hz) of the fundamental mode Rayleigh wave because the nature of these components attenuated quite rapidly after being generated.

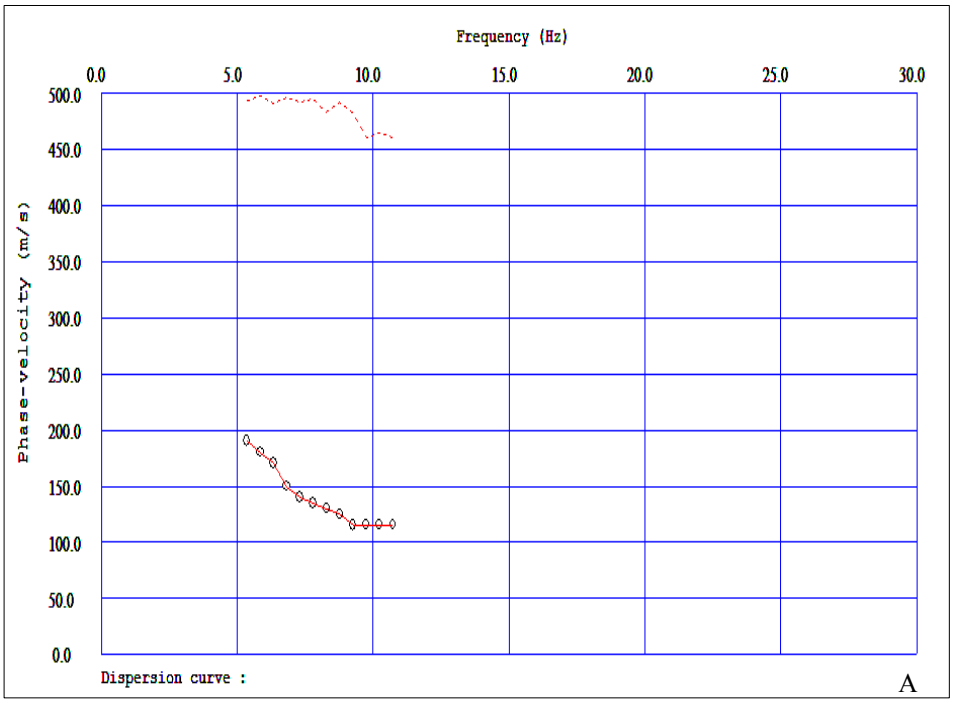

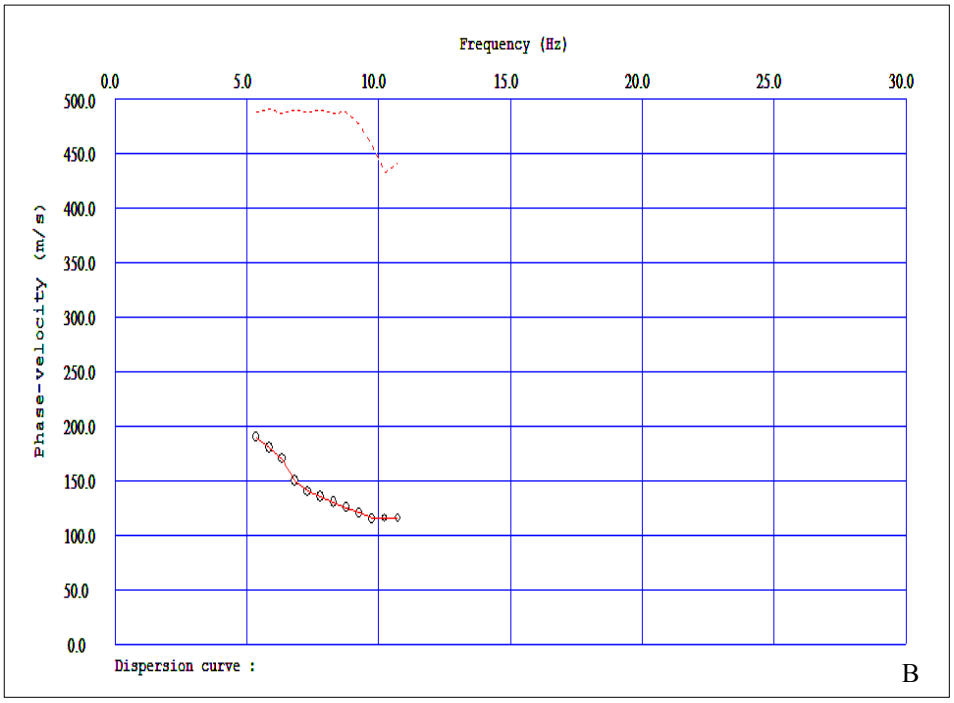

Figure 5. 9. The comparison of the dispersion curves obtained from the forward and reverse shot records of the MASW survey at Seis-22 point are illustrated on the Figures A and B, respectively.

After the construction of the dispersion curves of all surface wave measurements, initial models were generated by a simple wavelength-depth conversion. This method uses 1.1 times the phase velocity for an estimate of Vs and one-third-wavelength approximation for an estimate of depth. The minimum (phase) velocity and maximum (phase) velocity are automatically assigned corresponding directly to the low and high values observed on the dispersion curve. The maximum velocity is automatically assigned to the deepest layer. The number of layers was fixed at 15, and only the S-wave velocities were changed throughout the inversion process. After running 10 iterations, the modified initial model was built with a root mean square error (RMSE). In the inversion stage, extra attention was paid to check whether RMSE is decreased or not after each iteration and whether or not the final error was less than 5% between experimental and theoretical dispersion curves. After running through a number of iterations, the theoretically calculated dispersion curve was the final S-wave model (Figure 5.9). For one-dimensional inversion, a non-linear least square method was applied to the phase velocity curves and one dimensional S-wave velocity structures down to the depth of investigation were obtained for both methods.

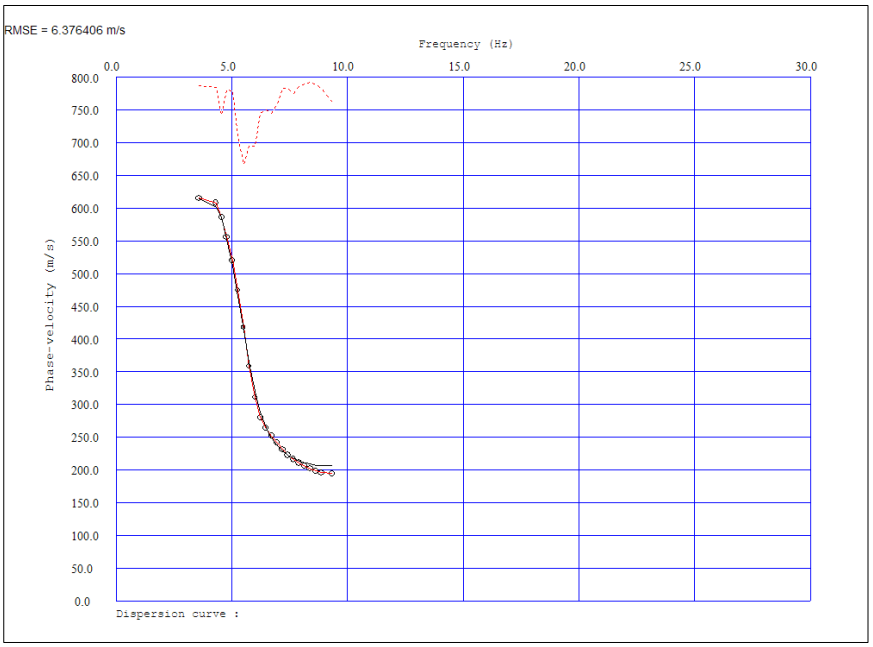

Figure 5.10. A comparison of the observed (red line) and theoretical (black line) phase-velocity curves from MAM measurement at Seis-3 point. It should be noted that the observed and theoretical dispersion curves nearly coincide.

The maximum depth of investigation obtained by the MASW method changes from 14 m to 25 m (Figure 5.10). Although, the field configuration (spread length, near offset and geophone spacing) and data acquisition parameters (record length, sampling interval, etc.) were adjusted according to the testing procedure, the maximum penetration depth which the MASW method was able to get information was equal to 25 m in this study. However, as mentioned previously, this varies from site to site depending on the weight of the active sources used and on the geological properties of the sites. On the contrary, the MAM method was also used at same locations where the MASW method was applied and geotechnical properties of the soil layers up to 55 m were determined (Figure 5.11). Therefore, passive source results were integrated with 1D MASW datasets to get more reliable information from deeper sites. By combining active and passive source dispersion curves obtained at the 41 sites, high-resolution V_S curves over the entire tested depth range were constructed successfully.

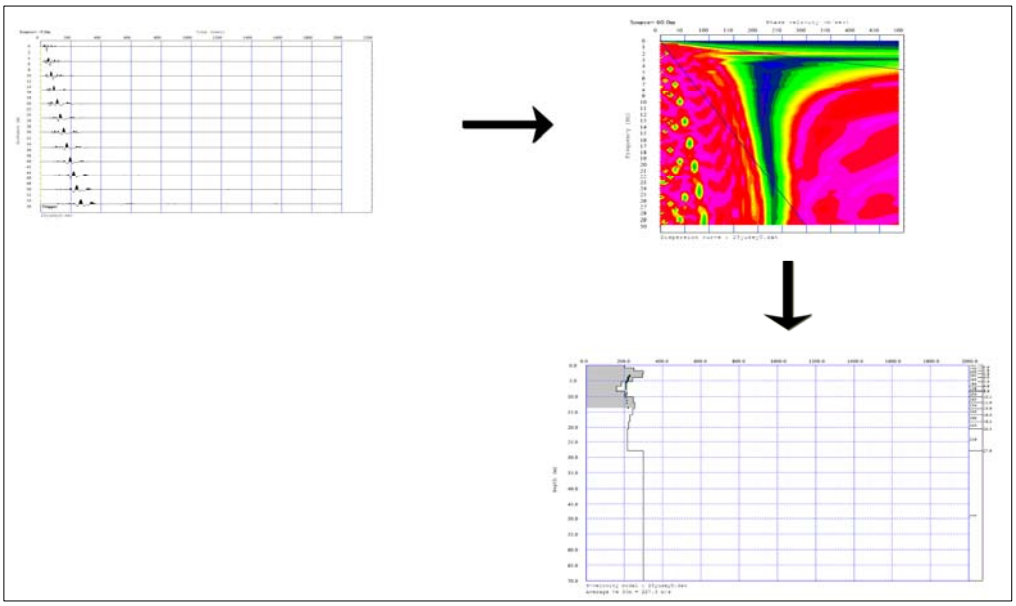

Figure 5. 11. A schematic diagram depicting the steps involved in obtaining the soil profile by the MASW method at Sies-25 measurement point.

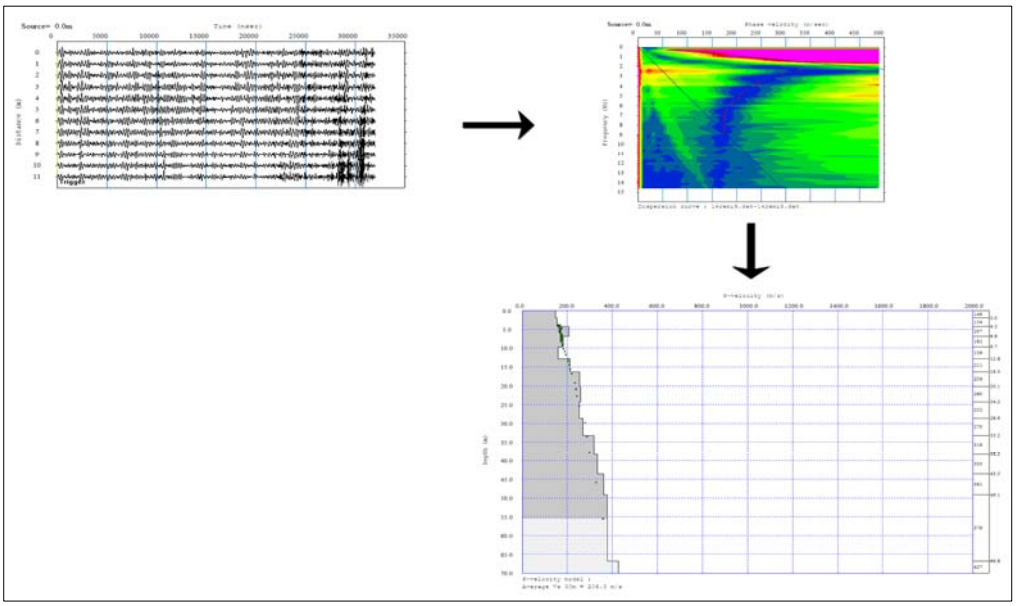

Figure 5. 12. A schematic diagram depicting the steps involved in obtaining the soil profile by the MAM method at Sies-14 measurement point.

The passive surface-wave method, together with the active method, enables us to maximize the depth of the investigation and to produce a composite high-resolution result over all depths (30 m in this study) nondestructively from the surface. As can be seen clearly in Figure 5.12, the combined dispersion curves obtained from the MAM and MASW methods characterize a larger frequency interval than the frequency range defined by only one method. Also, since the passive surface method aids in understanding subsurface structure up to a depth of 55 m, it has provided invaluable information for the Çubuk basin. The results obtained by the MAM measurements acquire more meaningful outputs in the interpretation stage because of the available information for layers present deeper than 30 m. Interpretation of the results of the MASW and MAM surface wave measurement methods and the generated V_{S30} map of the studies are given in the next section.

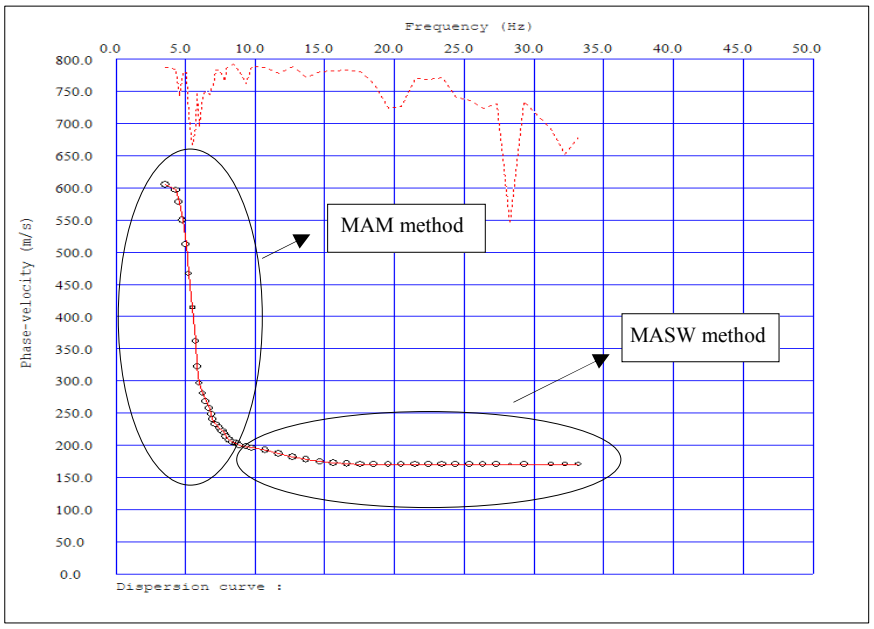

Figure 5.13. An example processed record from Seis-3 measurement point. Dispersion curves obtained by the MAM and MASW methods are plotted to the left and to the right sides of the figure, respectively.

5.1.2. Results of the shear wave velocity survey

In most geological studies, detailed geological descriptions are made and maps are produced for the major geological formation and their members by using their distinctive characteristics in lithology and their origin, however, the details of Quaternary geology having prominent importance on variation of ground motion and earthquake damage pattern are ignored. Most geological studies are compiled for goals other than investigating sediment characteristics and soil behavior (site effect) in an account for hazard assessments. On the other hand, the average shear wave velocity result in the upper 30 m of near-surface geologic unit and surface sediment thickness should be determined to characterize the geological units for estimating local site conditions. Using shear wave velocities by combining geological information for classifying site conditions give more reliable and more meaningful results instead of differentiating younger geological units based on only lithology and mode of origin.

In concordance with the aim of this study, the geological characteristics of the basin fill types of Neotectonic sedimentary units will be emphasized in detail. As can be seen in Figure 2.1, the basin fill types of the Upper Pliocene to Pleistocene and Quaternary sedimentary units are widely exposed and, cover a major part of the study area. To characterize these relatively younger deposits, shear wave velocity measurements at all 51 sites were carried out by using surface wave methods as mentioned above. In addition to this, the geological characteristics of these sedimentary units were compared with the engineering geological, geotechnical and seismic site characterization studies to classify and characterize the soil deposits. Therefore, the average shear wave velocity and variation of the shear wave velocity along the soil profile with supporting borehole information (given that it was available) were used in order to develop site categories which take site conditions into account according to the design codes of IBC 2003 and TSC 1998. Consequently, the regional site classification map of the north of the Çubuk Basin considering site classes was assessed based on the average shear wave velocity (V_{S30})

results in IBC 2003 and the shear wave velocity data and thickness of the surface layer based on the V_S in TSC 1998.

Determining the spatial distribution of V_{S30} and site classes have proved that their determination is a useful basis for future zonation studies since site effect studies were defined as a function of these parameters. Shear wave velocity measurements were taken within each of the mapped geologic unit. The relationships between the geologic units, vertical variations in sediment type, average shear wave velocity for the upper 30 m of the soil profile and site classes were investigated. The collected data and relationships were used to develop maps of V_{S30} and site classes that could be used in zonation studies.

Two site classification systems were applied to the study zone: the IBC 2003 and the Turkish Seismic Code 1998 (TSC) system, Prior to the determining site classes in regards to the design codes of IBC 2003 and TSC 98, shear wave velocities obtained by the MASW and MAM methods at 41 site locations were compared. It was found that the average shear wave velocity variations for the upper 30 m obtained by both methods were within 10% for the 33 measurement points. For the remaining 8 measurement points, the variation between the V_{S30} of two methods change between 11% and 20%. Considering the error margin of these methods (15 %), it can be suggested that these results are in good agreement with each other. Also, in determining the spatial distribution of V_{S30} and site class processes, V_{S30} parameters acquired by combination of the two methods were used in this study for all of the 41 data points. The degree of variation of the data obtained led to the utilization of the MAM method at the remaining 10 sites. The measured shear wave velocity ranges on the alluvial deposits (Quaternary sites) and fluvial deposits (Upper Pliocene to Pleistocene sites) are shown by the histogram presented by Figure 5.13.

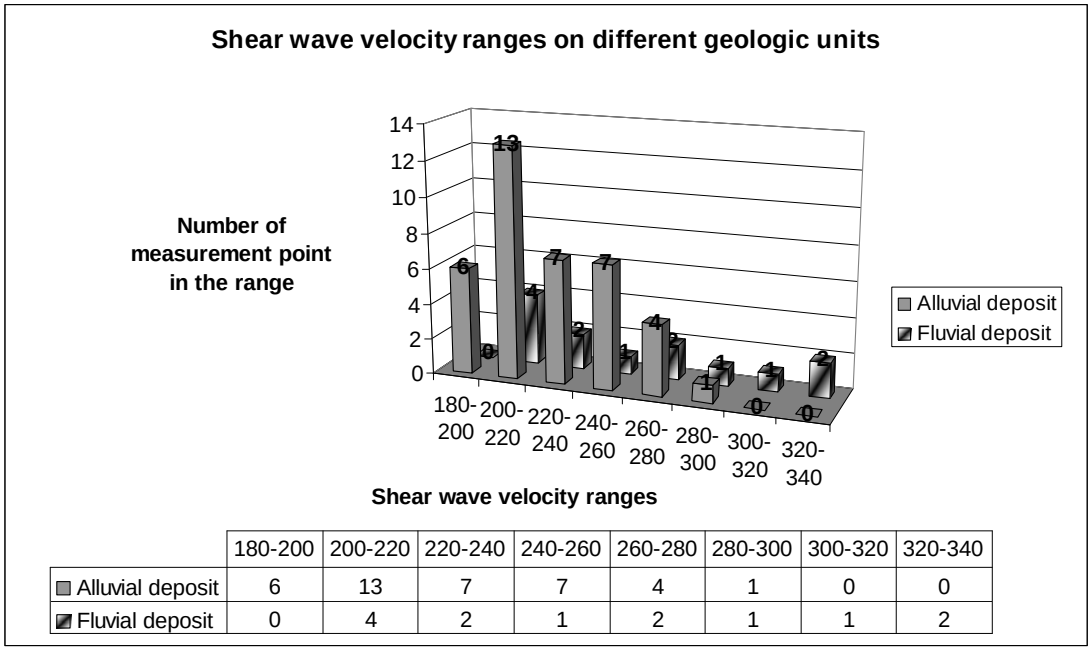

	180-200	200-220	220-240	240-260	260-280	280-300	300-320	320-340
Alluvial deposit	6	13	7	7	4	1	0	0
Fluvial deposit	0	4	2	1	2	1	1	2

Figure 5.14. The measured shear wave velocity range in different geologic deposits.

In the classification of the measurement results with respect to lithologies (Figures 5.14 and 5.15, and Table 5.1), two measurement points (Seis-4 and Seis-26) fell within the units of the Quaternary alluvium and terrace deposits but these points are close to the boundary between these deposits and the Upper Pliocene to Pleistocene sedimentary deposits. In addition to this, due to their characteristic shear wave velocity profiles, they were grouped in the Upper Pliocene to Pleistocene sedimentary deposits.

The mean shear wave velocity for upper 30 m of the soil profile (Eq 3.2) is utilized by the IBC 2003 (Table 3.1) to define site classes The general distribution of the site characterization data according to the geological setting and the average shear wave velocities and corresponding site classes according to the IBC -2003 can be seen in Figure 5.14. The shear wave velocity data in Figure 5.14 show that the alluvial deposits (Quaternary sites) and fluvial deposits (Upper Pliocene to Pleistocene sites) are classified as site class D in IBC 2003. Depending on the result of the implemented surface wave methods, the regional seismic zonation map of V_{S30} was prepared based on the design code of IBC 2003. According to the V_{S30} data (Figure

5.14), the depositional environment units could not be distinguished by the site classes in the design code of the IBC 2003. The results are within the range of site class D (between 180-360 m/s).

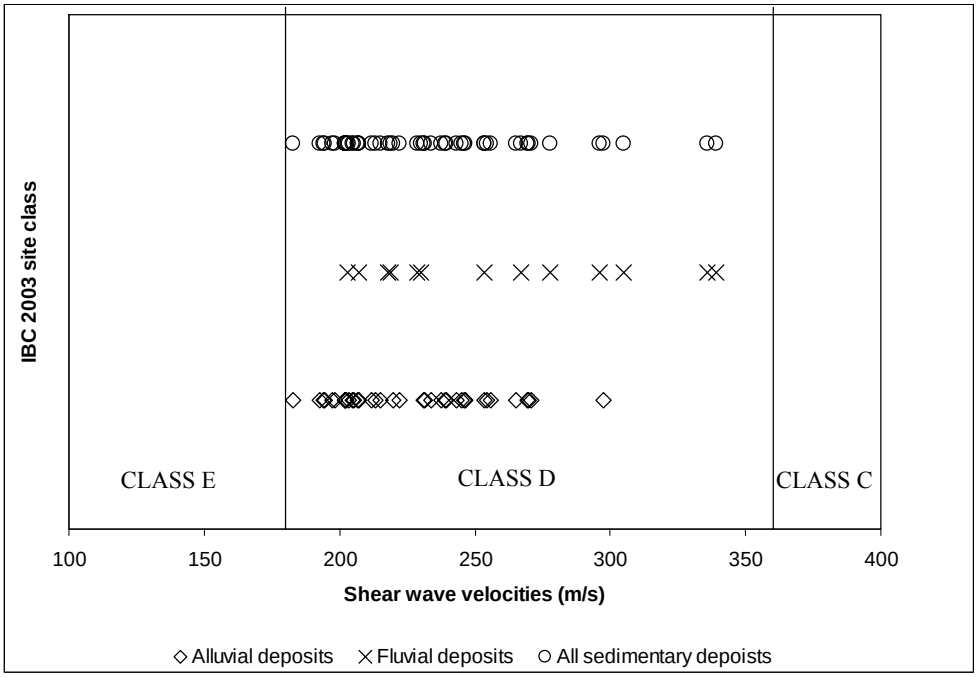

Figure 5. 15. The general distribution of the measured shear wave velocities in different geologic deposits and corresponding site classes based on IBC 2003.

All of the maps such as the regional seismic map and the other geologic and interpolation maps of the study area were prepared in a GIS environment by means of utilizing the TNT V. 6.9 software. In the generation of interpolation maps, the Kringing method was performed. Although, interpolation results of some areas that did not have any V_{S30} information were included as base map in the figure, the contour lines were passed through the areas where the shear wave velocity data were available.

A regional seismic map containing the V_{S30} values of the study area can be seen in Figure 5.15. As can be seen in Figure 5.15, the V_{S30} values around the Quaternary

deposit, i.e., towards the center of basin decrease as expected. Also, a similar trend is followed along the alluvium deposit. At the center of the basin, V_{S30} has a value of 183 m/s which is the boundary between stiff (D site) and soft soil (E site) profile according to IBC 2003. Moreover, V_{S30} has relatively greater values towards the Upper Pliocene to Pleistocene sedimentary deposits at the both sides of the plain. This means that the alluvium is gradually thinner towards the edges of the alluvial basin. Therefore, it is naturally observed that the V_{S30} results gradually increase when the thickness of the alluvium profile decreases within the first 30 m (Figure 5.19). Although the V_{S30} of Quaternary geologic units reflects the results of depositional environment settings at the area, some variations of V_{S30} in the unit were observed (Table 5.1). The variations may be related to grain size distribution, density, ground water levels and cementation in the deposits (Wills et al., 2000; Wills and Clahan, 2006).

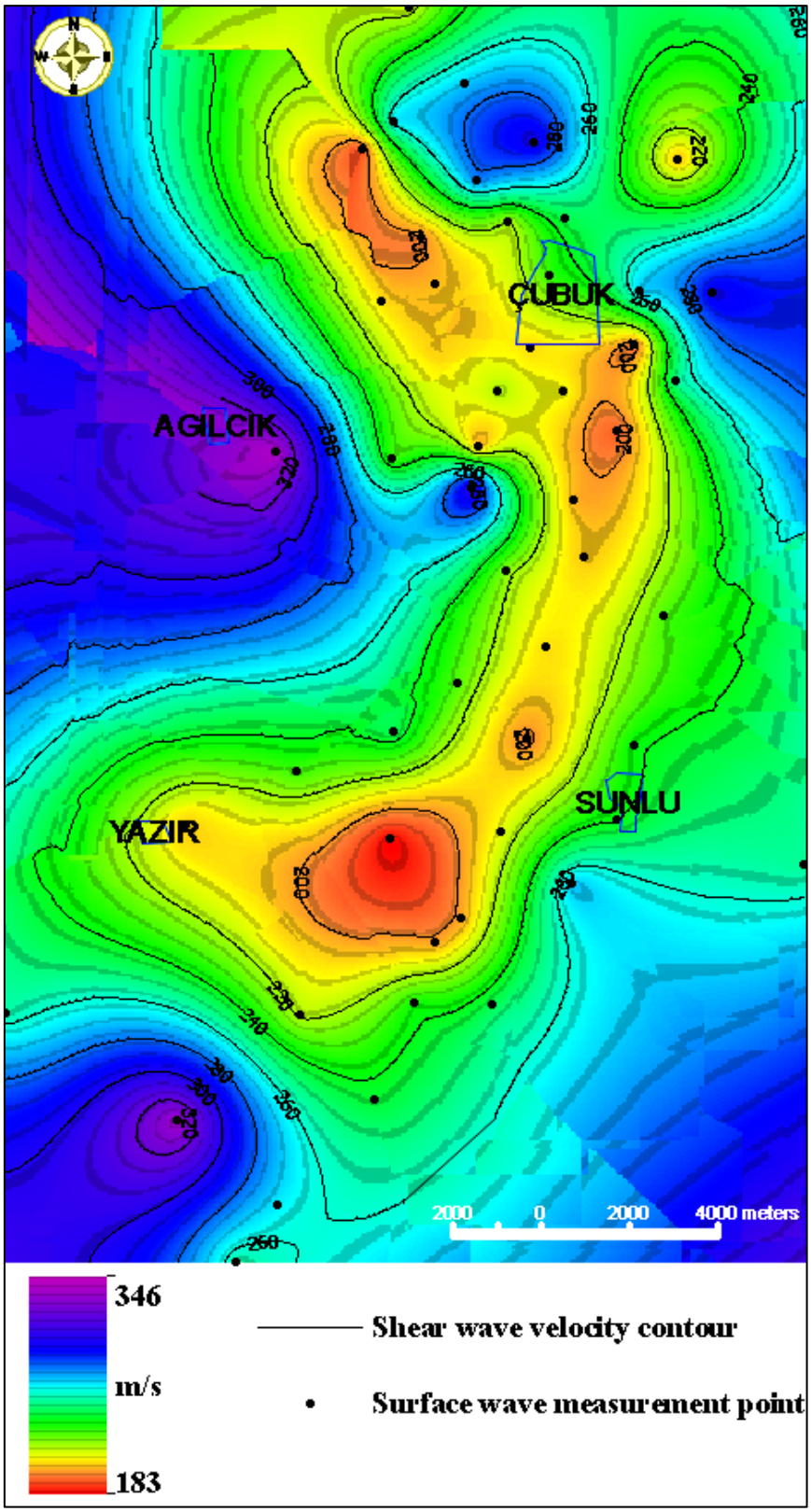

Figure 5.16. The regional seismic map based on measured mean V_{S30} measurements. The color gradient shows the spatial variations of the V_{S30} values in the area.

The statistics for Vs_{30} for the Quaternary and Upper Pliocene to Pleistocene sediments are given in Table 5.1. The mean values of Vs_{30} for the Quaternary and Upper Pliocene to Pleistocene deposits are 226.5 and 260 m/s, respectively. The coefficient of variation (COV = Standard deviation / mean) for the Quaternary deposits is 0.12, while the COV is 0.18 for the Upper Pliocene to Pleistocene fluvial deposits. The COV values represent small variability since this study focuses on geologic units that are geographically constrained to the Çubuk basin. However, as can be seen in Table 5.1, it should be noted that the number of shear wave velocity data for the fluvial deposit is relatively small when compared to the number of the measurements for the alluvial deposits. Therefore, the uncertainty in the data may be relatively high for the fluvial deposits from a statistical point of view. Also, it can be made mention of the uncertainty in the assignment of site classes in the IBC 2003 for this deposits due to the small amount of data.

Table 5.1. Summary of the V_{S30} measurements within the geologic unit and their IBC site classes.

Geologic Unit	Number of Data	Percentage (%)	V_{S30} (m/s)	±Std	COV	Site Class (IBC 2003)
Quaternary alluvial and terrace deposits	38	74,5	226,5	27,8	0,12	Class D
Upper Pliocene to Pleistocene fluvial deposits	13	25,5	260,0	47,6	0,18	

Regarding the V_{S30} results of the Upper Pliocene to Pleistocene fluvial deposits, although the V_{S30} values are around 300-340 m/s at Seis-4, -19, -26 and -48 testing points, the average shear wave velocity for the upper 30 m is very close to the mean V_{S30} value of Quaternary sediment deposits observed at Seis-15, -33, -38, -44, -46, and -49 measurement points. The V_{S30} measured on two different geologic units described by MTA, show the same characteristics at the interval between 202 and 267 m/s. Hence, in this case, it is very difficult to draw a sharp boundary between

these units based on these results. This difficulty can be due to two reasons. The first one is; the amount of data collected at the area is not sufficient to differentiate the possible boundary between the units. In fact, based on these results additional shear wave velocity measurements are necessary to catch the lateral variations of the geologic units. The second one is; the boundaries between the units do not properly separate the units by considering depositional environments included within each geological unit such as terrace sediments, alluvial fan deposits include levee, channel, and flood-basin facies. Because of this possibility, the various maps prepared for the region were examined. The geological (MTA, 1946), hydrogeological (Kupan, 1977 and DSI, 1979) and geomorphological (Erol, 1973) maps of the study area were compiled and compared with the reference map (Figure 2.1). There were noticed to be significant differences amongst each map and also the reference geologic map of the study area in described and mapped lithological units. Therefore, the updated one was preferred to be used as the geological map of the area, even though the reliability of the boundaries between the sediments of Neotectonic period is unfortunately suspicious. Briefly, Quaternary geology has to be studied in detail in the study area. As a result, another seismic code (TSC 1998) was utilized in order to classify the sites and compare the results with that of IBC 2003.

The shear wave velocity and variation of it with soil profile are utilized by the TSC 1998 to define site classes. The topmost soil thickness was determined by using a significant velocity contrast between the layers. It was checked by the borehole information at the sites where it was available. The shear wave velocity within the surface layer was used to define the soil group (Table 3.3), and the surface layer thickness was used to assign the site class based on the defined soil group (Table 3.4). A histogram, given in Figure 5.16, indicates the distribution of TSC site classes and soil groups for the alluvial sediments (Quaternary sites) and fluvial deposits (Upper Pliocene to Pleistocene sites). The figure indicates that all of the Quaternary sites contain soft soil at the surface (Soil Group D) were classified as either Z4 or Z3 in TSC 1998 based on the thickness of the soft alluvial deposits. However, the Upper Pliocene to Pleistocene sites give more variable and stiffer results in the site classes when compared to the Quaternary sites. These were classified as C-Z3, D-Z3 and D-

Z4 according to TSC 1998. The two sites (seis-46 and -49) which were classified as D-Z4 are close to the boundary of Quaternary and the Upper Pliocene to Pleistocene sediments, and also these are in close proximity to the faults in the region. As can be seen in Figure 5.17, a significant part of the study area is classified as D-Z4 and D-Z3 (the softest classes) based on TSC, 1998.

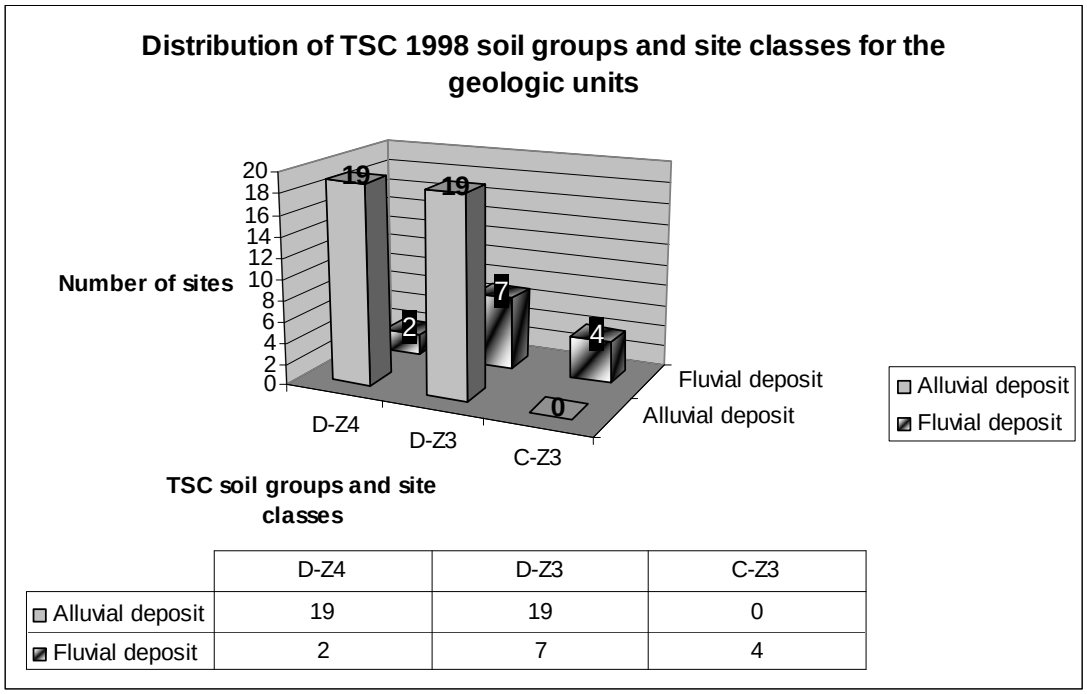

	D-Z4	D-Z3	C-Z3
Alluvial deposit	19	19	0
Fluvial deposit	2	7	4

Figure 5.17. The distribution of TSC site classes and soil groups for the geologic deposits in the area.

A regional site classification zonation map of the study area based on TSC 1998 can be seen in Figure 5.17. As can be seen in the figure, Site class D-Z4 is confined to the center of the basin where the thick alluvial deposit is present. Towards the edge of the basin, site class D-Z3 encompasses both the Quaternary and Upper Pliocene to Pleistocene sediments. The site class C-Z3 appears to be situated away from basin towards the basement rocks at the study area for the latter sediments.

When the assigned site classes based on the IBC 2003 and TSC 1998 are compared, TSC 1998 distinguishes the depositional sediments more successfully. All of the sites

fell within the boundaries of site class D in the IBC 2003 based on the average shear wave velocity data. On the other hand, the Quaternary and Upper Pliocene to Pleistocene sites were divided into two and three site classes in the TSC 1998 based on the surface layer thickness besides of the S-wave. Moreover, although the centeral part of the basin was classified as class D according to the IBC 2003, based on the TSC 1998, this part of the basin was categorized as D-Z4 (the softest class) which is softer class when compared to the class D of the IBC 2003.

Based on the shear wave velocity data, it was assumed that the boundaries of the shear wave velocity between the alluvium deposit and older units were determined as 250 m/s. Hence, the thickness of alluvium deposits is changing between 15 and 30 m at the center of the alluvium basin according to results at the testing sites [i,e., Seis-10 (28.6 m), Seis-11 (24.2 m), Seis-22 (15.4 m) and Seis-36 (16.3 m)]. Note that the numbers in parentheses show the thickness of alluvium measured at the site by using surface wave method. Towards the north where the alluvium deposit basin starts to narrow, thickness of this deposit also decreases down to 6.8 m at the testing point (i.e., Seis-28).

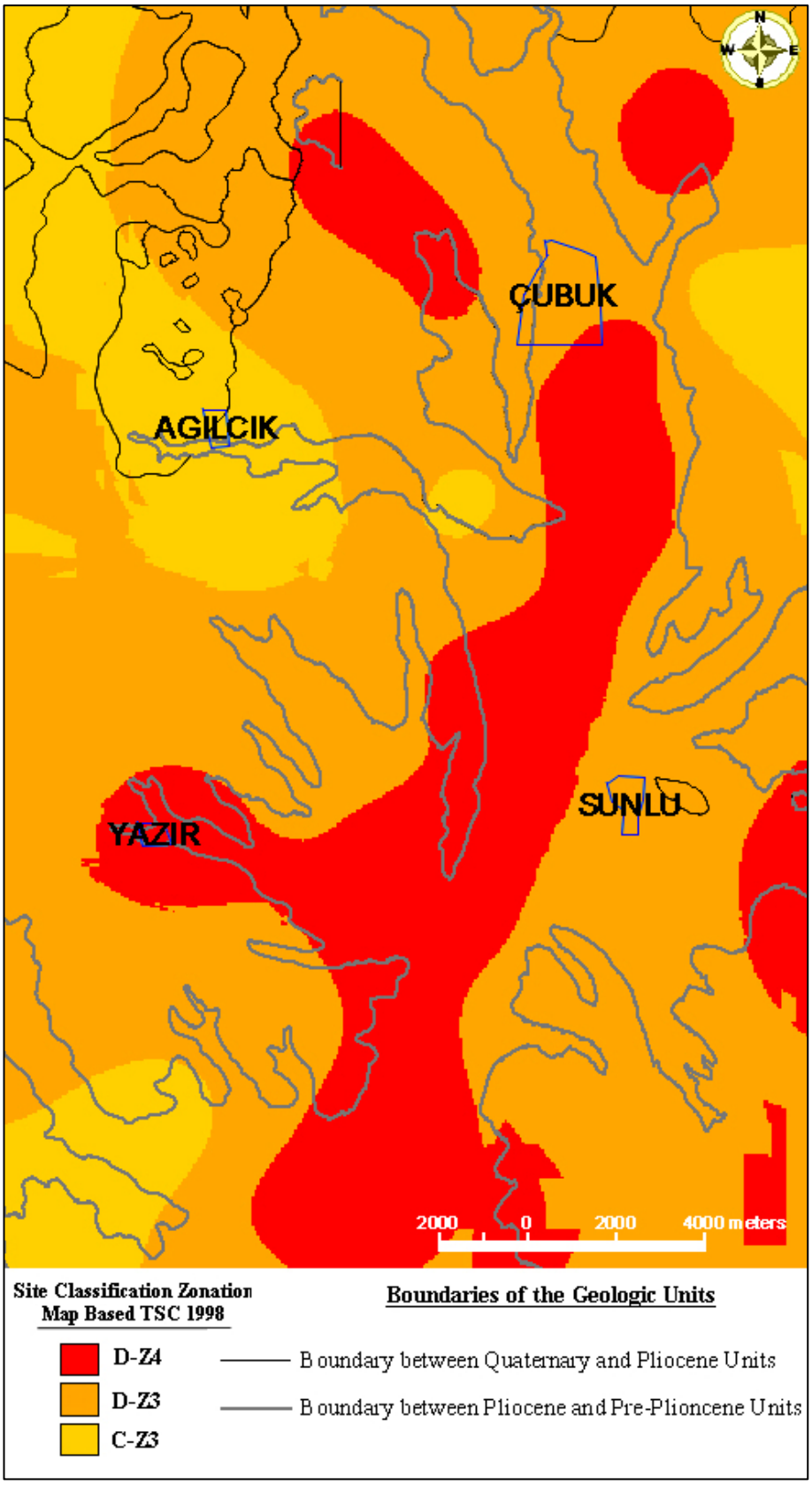

Figure 5.18. Regional site classification zonation map of the study area based on TSC 1998.

During the analyses of the results, it was observed that the shear wave velocity of the surficial layers of the alluvium deposits varied in the range of 100 and 175 m/s within the first 6 m depth. Naturally, most of the measurement points with younger (Holocene) alluvium at the surface include older alluvium or terrace deposits which are at a relatively higher elevation than the surrounding environment of the younger alluvium. The transition from Holocene to Pleistocene or terrace deposits may not be reliably differentiated by using only surface wave methods without any other supportive site characterization methods such as borehole data. Therefore, geotechnical, geological and hydrogeological boring studies were utilized to combine these seismic data with the borehole information (geotechnical parameters, stratigraphic positions of the layers, groundwater level, etc.). The borehole data compiled included previous studies which were conducted by MTA for thermal spring survey, by DSİ for hydrogeological investigations, by private companies for ground survey and also in this study, geotechnical studies conducted at seven sites at the project site. However, since the project site area is a recently developing area, the compiled geotechnical data from previous studies were deemed not to be sufficient to characterize the different geological units. Therefore, these compiled data were used as complementary data to characterize the depositional sediments and to support the site classification study. According to the geotechnical boring studies implemented at the study area, the Quaternary alluvium sediments are classified predominantly as low plastic clay (CL), with some high plastic clay (CH), clayey sand (SC) and sandy gravel (GM) according to the Unified Soil Classification System (USCS). Furthermore, the Pliocene sediments are generally classified as high plastic clay (CH). Complementary studies coupled with the seismic data pursued in this study revealed that the thickness of alluvium deposit ranges between 16-30 m. Groundwater levels vary within the alluvium, depending upon the soil characteristics of depositional environment and upon the proximity to the major course of the recent stream beds. The ground water level ranges between 4.20 m and 5.80 m, with a mean of 4.67 m. Regarding the conducted boring study, it can be observed that it is difficult to obtain reliable N_{SPT} results at the study area due to the presence of gravel lenses or layers generally at depths between 5 and 13 m and clay deposits beneath this unit (Figure 5.18). Since refuse results were obtained within these layers, the

standard penetration test is deemed not to be a suitable method to characterize these types of units. Furthermore, liquefaction analysis was also implemented at the sites. According to the geotechnical information revealed from the 15 geotechnical boring studies, three susceptible sites for liquefaction (FS<1) were pinpointed but, since the liquefiable thickness of these layers were less than 2 m, it was determined that these layers were not susceptible to liquefy and hence, liquefaction analysis was not included in this study.

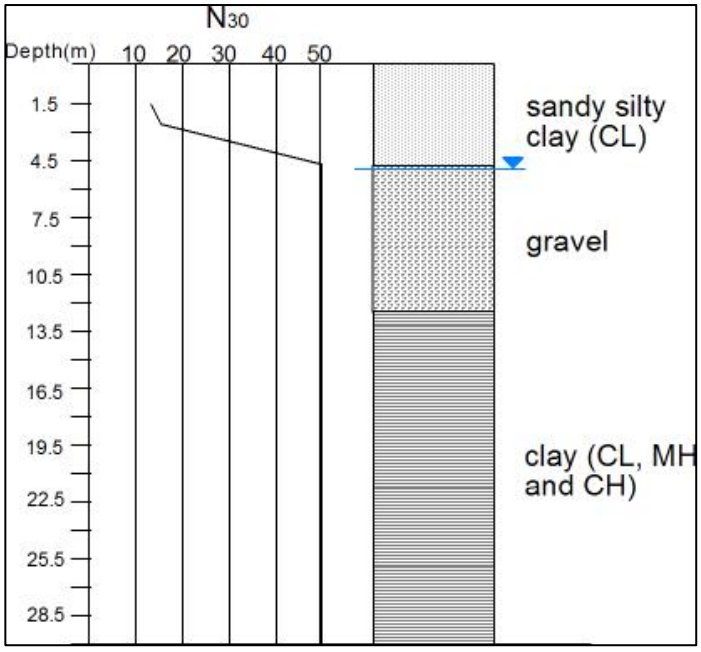

Figure 5.19. The log of the BH-1 drilled in the content of this study.

The two soil profiles acquired from Quaternary and Pliocene sediments at Seis-7 and -19 by combining surface wave method are given as an example in Figure 5.19. As can be seen in this figure, the shear wave velocities of the layers are different between the sites. Also, the V_{S30} values of these reflect the same condition. However, towards the deeper parts of the soil profiles (greater than 30 m) the V_S values of the layers are smaller than 750 m/s at a depth of 55 m. This means that the engineering bedrock or the base rock is deeper than 55 m. Although the light grey color areas of the soil profiles show the unreliable estimations for the V_S parameters, it may give an

idea about the variation trend of the shear wave velocity towards the deeper parts. Additionally, these parts have lower shear wave velocities that do not satisfy the condition for the engineering bedrock.

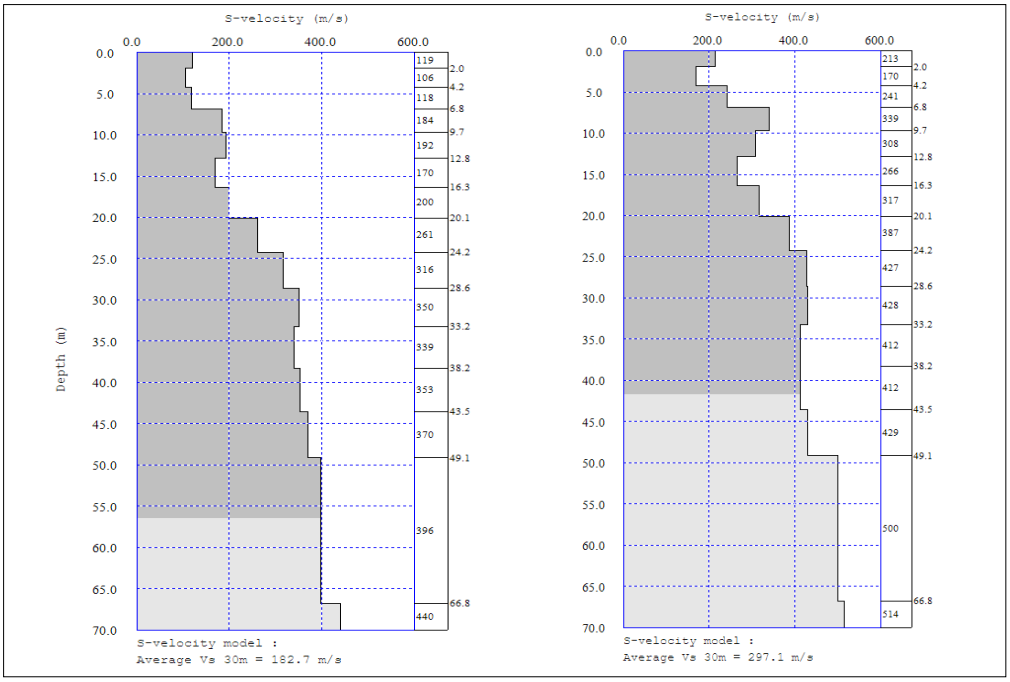

Figure 5.20. Examples from shear surface velocity profile from two sites, namely, Seis-7 and Seis-19 located towards the left and towards the right side of the figure, respectively. The dark grey parts show the reliable parts of the shear wave velocity profiles.

Because of these reasons, using the V_{S30} parameter only to characterize a region may not sufficiently estimate the local amplification potential at the area. Rather than this, it is necessary to use actual engineering rock depth for site amplification study. However, the applied surface wave method with the equipment utilized was only capable of characterizing the sites up to a depth of 55 m in places. In addition to these, if Figure 5.15 is examined carefully, it is clearly seen that the lower V_{S30} contours are concentrated towards the east side of the plain. A possible reason for this is that Çubuk River has moved its course from the east to where the present river bed is located. Therefore, the alluvial deposits at the ancient river beds and their

flood-basins might have generated this situation. Moreover, as described above, the fluvial sediments have a lower V_{S30} value than expected. In Figure 5.15, if the 240 m/s contour is to be examined carefully, it can be clearly seen that the contour line passes through both sides of the basin and divides the area into three parts approximately at the south-north direction. When the shear wave velocity profiles of the measurement points (Seis-1, -7, -8 and -25 at the west; Seis-42, -44 and -49 at the east) that are located at the route of the contour line are considered, it may be noticed that shear wave velocity has lower values than expected. This is probably due to the thickness of the soft materials. The tectonic activity (as discussed in Chapter 2) within the region might be the answer to the question why the thickness of the soft material is greater than anticipated.

The lower velocity layers at a depth of more than 30 m are also observed on the fluvial deposits. Most of the testing points having considerably low V_{S30} values are located at the fluvial sites where the probable deformation zones of the faults are present (Figure 2.1). Therefore, other than classification of the geologic unit based on age, depositional environment and lithology, presence of structural element is also believed to have a significant effect on the stiffness character distribution of the geologic units in the study area.

5.2.1. Data acquisition and analysis of microtremor measurement

Site response analyses for estimating the earthquake characteristics on the ground surface and the interpretation of the results for microzonation of a site is a key component of any local seismic hazard analysis. Therefore, preliminary site effect characterization has become significant for newly developing cities in the proximity of moderate seismically active areas. In this context, a future event could possibly prove to be destructive due to local site effects in and around these developing cities. In order to determine the fundamental periods and maximum values of the amplification of the specified sites, microtremor measurements were recorded and analyzed by the Nakamura (1989) technique.

A total of the 106 sites were measured by taking ambient noise recordings to anticipate the seismic response of different lithologies at the northern part of the Çubuk Plain. These measurements were carried out at sedimentary deposits which are Quaternary and Late Pliocene to Pleistocene in age along with the bedrocks. A total of 53 and 35 measured data fell within the units of the Quaternary alluvium and terrace, and the Upper Pliocene to Pleistocene sediments, respectively. The 15 of these measurements are on the boundaries of the Quaternary and Pliocene deposit according to geological map given in Figure 2.1. The remaining 3 measurements were taken from rock sites at the northwest part of the Çubuk district.

The field measurements were conducted by adopting a grid system and the microtremor recordings were attempted to be spaced approximately 750 m to eliminate the effects of different distances among measurement points during the preparation of the seismic zonation map for the hazard assessment. But, this grid system had to be modified due to the environmental noise, heavy vegetation and accessibility problems. Spatial distribution of the microtremor measurement points in the study area is given by Figure 5.20.

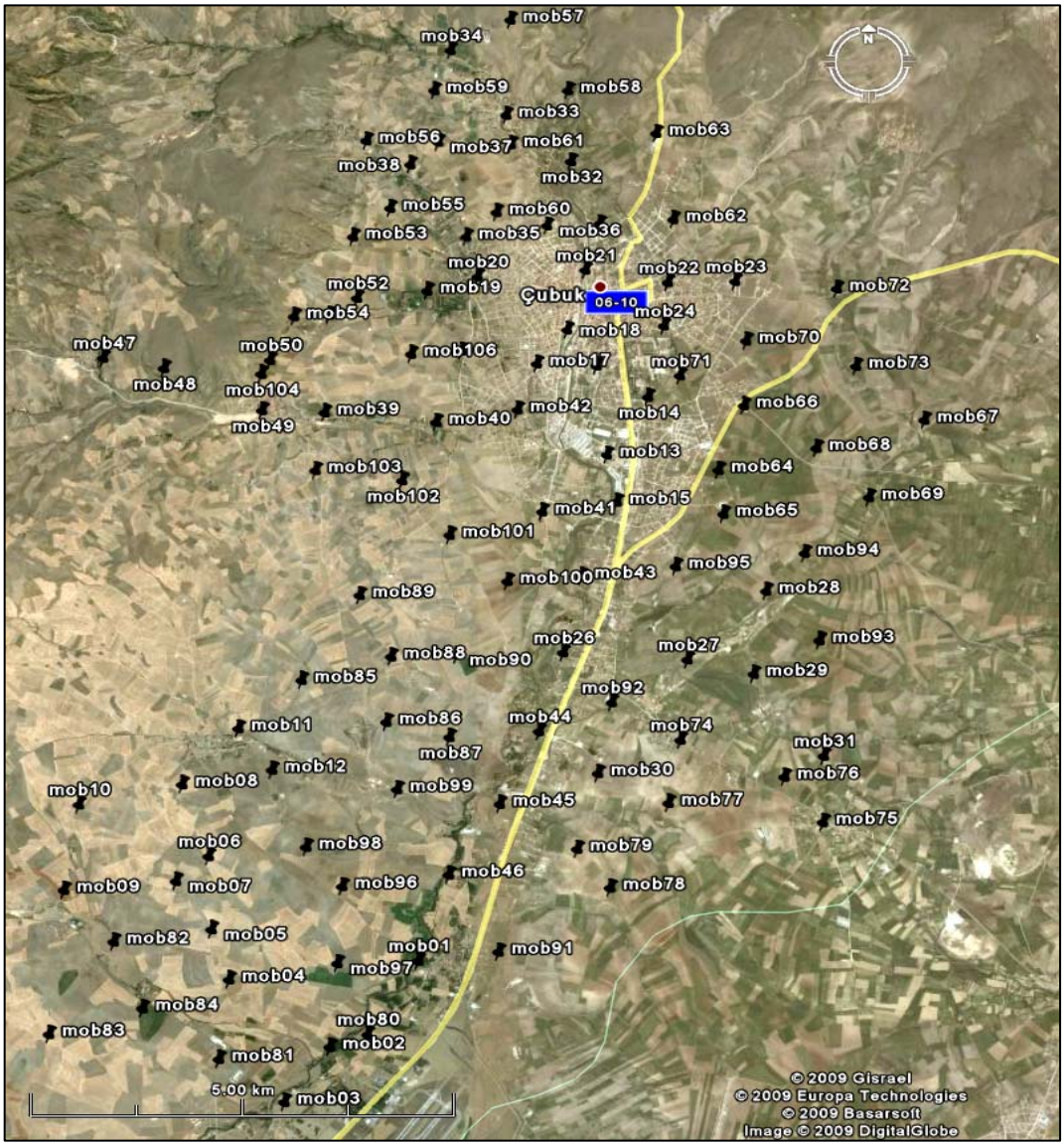

Figure 5. 21. Distribution of the measured microtremor points in the study area.

Microtremor measurements were recorded by a NS/A model PC connected to a three directional UP-255s seismometer with a natural period of 1 s (Figure 5.21). All the measurements have been taken by using an amplifier. The microtremors were recorded during 5 minutes at each site with a frequency sampling range of 100 Hz. The qualities of the taken measurements were simultaneously checked by means of a laptop during the recording (Figure 5.22).

Figure 5.22. Photo A: A view from the microtremor measurement at the Mob-89 site. Photo B: a close view of the UP-255s seismometer, Photo C: a view of the inside of the seismometer.

Figure 5.23. Photo A: A view from the microtremor measurement at the Mob-49 site. Photo B: the amplifier (black box) and the laptop used during recording ambient noise.

During the data processing, to take only a quiet section of the recorded ambient noise (i.e., less disturbed parts of the ambient noise by cultural activities than the remaining part, noise filter in a level range of 3.5 and 4.5) was applied to the recorded raw microtremor data (Figure 5.23). Each record was divided into windows of 2048 samples (20 s) with more than 3 windows per measurement (Figure 5.24). A Fast Fourier Transform (FTT) procedure was applied on selected window (2048 points; 20 s) after period analysis. Then, the Fourier spectrum of the window was smoothed by selecting bandwidth as 0.3 Hz to catch all possible peaks in the acceleration spectrum. The spectrum was also smoothed by applying a 0.1 Hz low and 10 Hz high Butterworth band-pass filter to eliminate the spectral contribution of the low period spikes which were present in the time series.

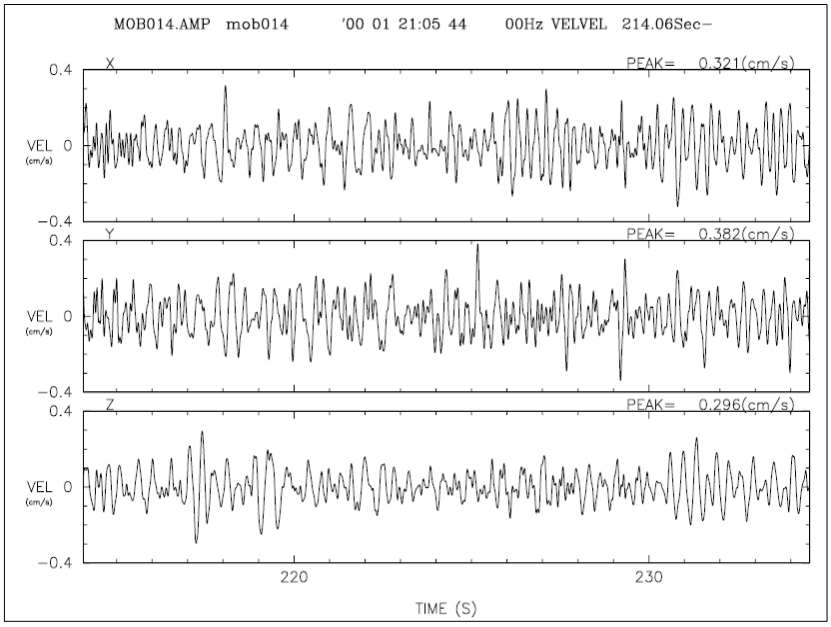

Figure 5.24. An example of the most quiet 20 s part of the 5 min data record from the Mob-14 measurement point.

This procedure was repeated with the remaining windows and the average spectral ratio of the horizontal to vertical noise components ($S_{H/V}$) was obtained by dividing the resultant spectra of the horizontal components of the sediment site (H_{NS} and H_{EW}) by the spectrum of the vertical component (V_S) of the sediment site (Eq 4.7)

After, the spectral ratios of all the windows for the same measurement were calculated, their arithmetic average was calculated to obtain the H/V spectrum of the site. During the analyses of the measured ambient noise, the recorded files have been processed and analyzed by Micplot Version 1.1 for UNIX (Motoki, 2002 and Mirzaoğlu, 2005).

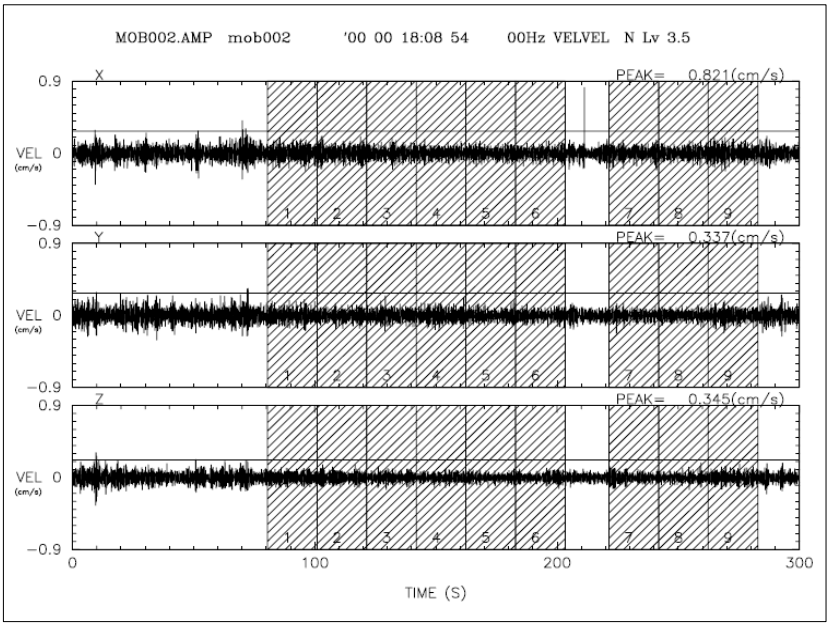

Figure 5.25. An example of the waveform from the unprocessed 5 min microtremor data from microtremor measurements in the field operations of this study (measurement point Mob-2) and also the hatched nine rectangular areas are the selected 20 s windows.

An example of H/V spectrum is given in Figure 5.25. As can be seen in the figure, the vertical axis of the spectrum gives the amplification ratio and the horizontal axis is corresponding to the fundamental period. The applied noise level and bandwidth parameters are presented on the top the spectrum.

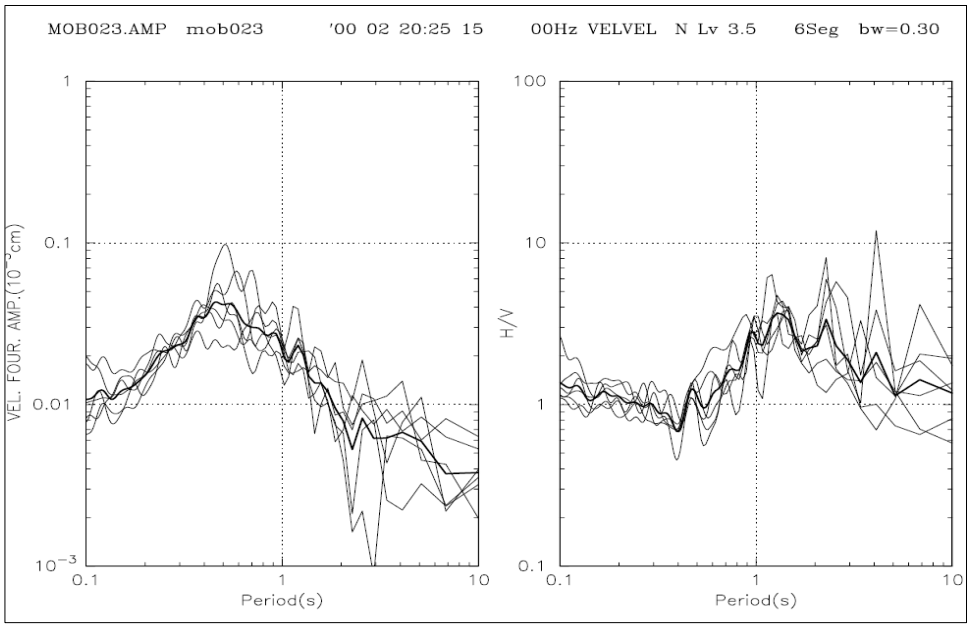

Figure 5.26. An example of the H/V spectrum from measurement point Mob-23. The FFT and H/V spectra of the selected 20 s windows can be seen on left and right sides of the figure, respectively. The thin lines represent the spectra of selected windows and the thick lines show the mean values of them

5.2.2. Results of the microtremor survey

A significant part of damage during strong or moderate ground shaking is associated with local site effects. Detailed assessment of site effects and the predominant periods in which significant amplification occurs can be obtained using several techniques. Among these techniques, the H/V spectral ratio, which is one of the experimental technique for the ambient vibrations (microtremors), has been widely used in microzonation studies as it is cost-effective and an easy procedure for application (Claudet, 2004). In the Nakamura technique (Nakamura, 1989), the vertical component of ambient seismic noise is relatively uninfluenced by the sediments. Thus, this technique can be used to remove the source effects from the horizontal components. The horizontal to vertical-component noise ratios can be used to identify the fundamental resonant frequency of the sediments (Lermo et al 1994) (for detailed information please see Section 4.2.1.1).

In the study of the Çubuk basin, different lithologies associated with typical amplification factors have been identified and surveyed using the field approach of the short-period noise recordings. Regarding the results obtained from the microtremor study, a fundamental period and a maximum value for the amplification were estimated from each measurement point at the site studied. According to the fundamental period results given as a histogram in Figure 5.26, generally, high fundamental periods were measured at the sites. The results show large variability in the H/V spectrum. As can be seen in the figure, the H/V peaks are observed at the periods ranging between 0.22 and 1.34 s with their amplitude changing from 2.1 to 9. The relatively higher thickness of the soft soil deposits is a possible explanation for this situation.

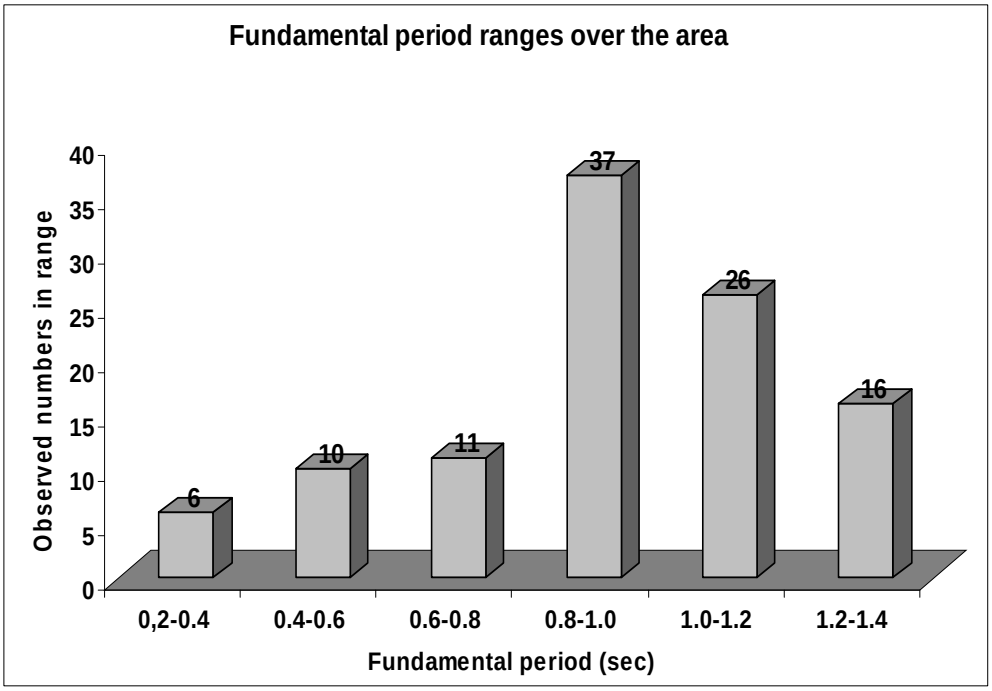

Figure 5.27. The number of fundamental periods observed in the ranges for all sedimentary deposits.

As mentioned previously, the center of the plain was affected excessively as a result of tectonic movements and subsided along the NE-SW trending normal faults. The

faults present at the west and east of the basin caused to form a graben structure at that time. Because of this reason, thick sedimentary units have deposited at the basin bounded by the faults. Also, the shear wave velocity measurements at the study area prove the presence of a thick soft sediment layer in the region in the soil profiles generally up to a depth of 55 m.

Through performing spatial interpolation between these points in a GIS environment, the maps of resonance periods and their amplification factors over the study area were prepared and are given in Figures 5.27 and 5.28, respectively. As can be seen in Figure 5.27, distribution of the fundamental periods of the site is clearly associated with thickness of the soft material. The area has high predominant period towards the basin center, most probably due to the tectonic activities as mentioned previously. The bedrock depth especially at around the center of the basin is below over 100 m. Towards the northern part of the region, as expected, site predominant period results for the Quaternary deposits are decreasing with thinning of soil thickness. By analyzing the period peaks, H/V technique with subsurface geology is capable of revealing the presence of soft sediments along the Çubuk basin. This capability shows itself more clearly when the impedance contrast ratio between the relatively stiff and soft sediments is high. In Figure 5.27, the fundamental periods of the sites are decreasing towards the both sides (east and west) going away from the Çubuk plain. However, when the distribution of the fundamental period on the west and east sides of plain is examined, it is explicitly seen that the resonance periods of deposit at the west part of the plain are generally greater than those of the east part. There may be several reasons for this observation. However, the most logical one is probably the presence of the old alluvium deposits (terrace deposits) over the wide area at this part due to the migration of the Çubuk plain towards the west. This is also supported by the results of shear wave velocity survey. Also, subsidence of the area due to the tectonic activities and deformation zones of the faults may be the other reasons for obtaining a high fundamental period in even the Upper Pliocene to Pleistocene sediments. This is also observed in the shear wave velocity measurements.

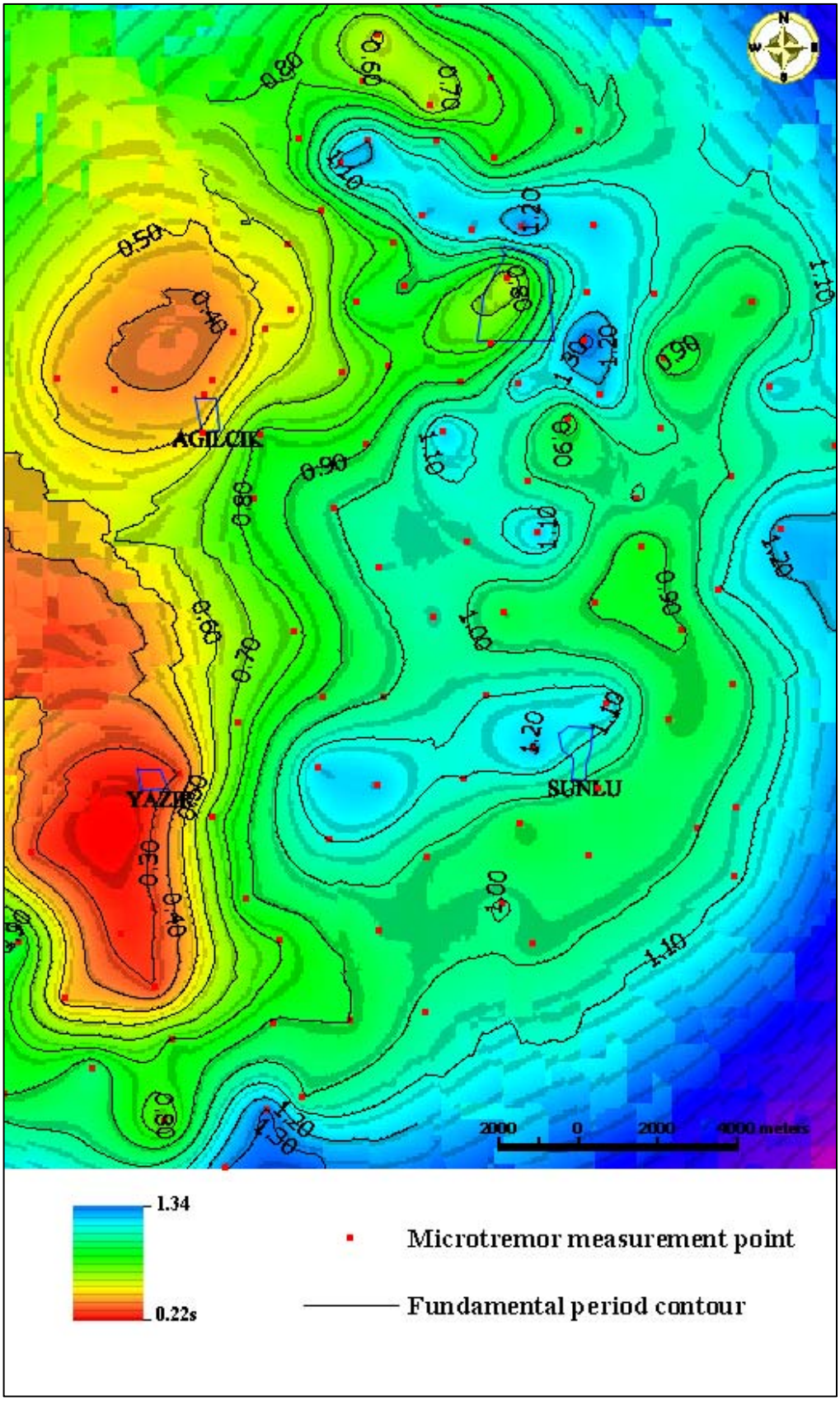

Figure 5.28. Fundamental period map of the region.

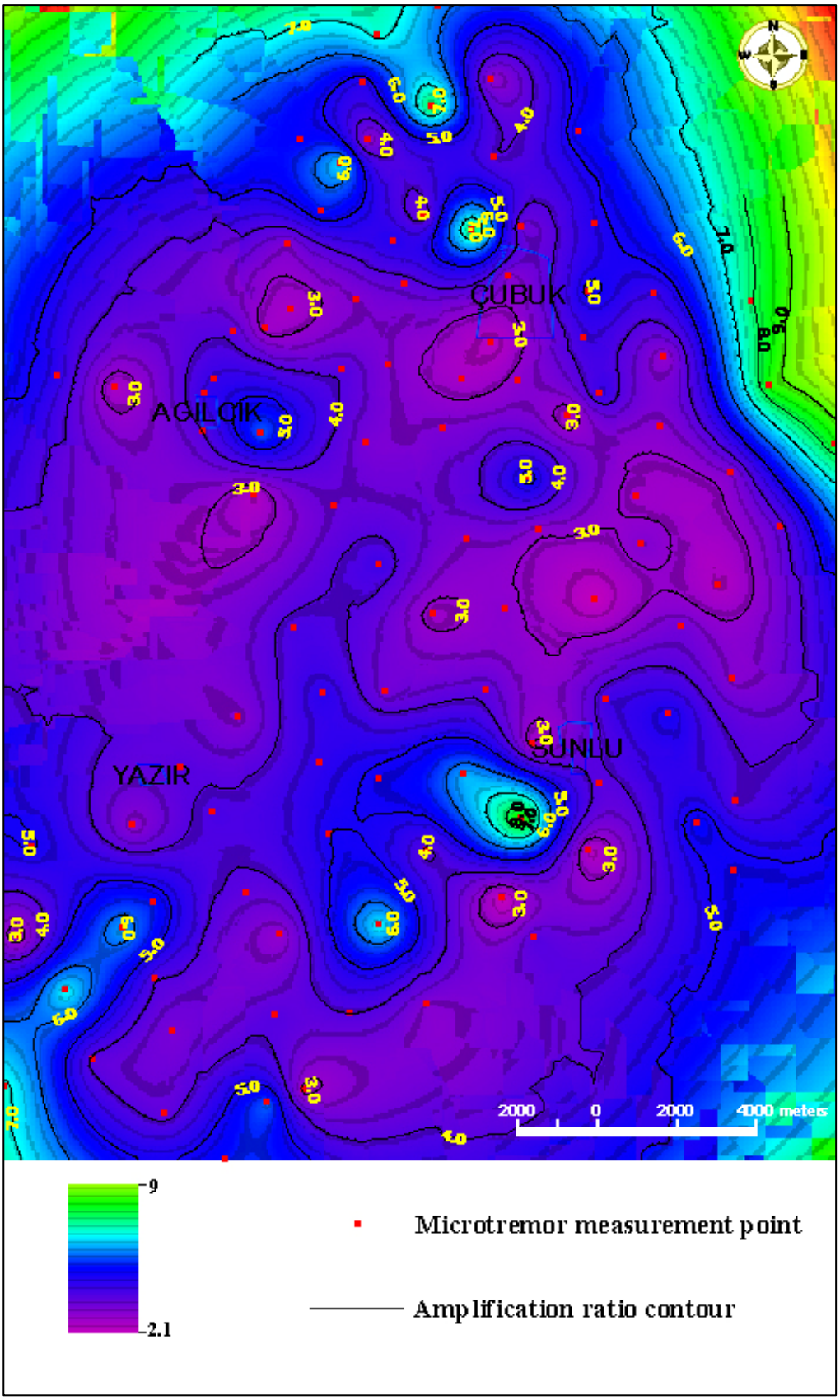

Figure 5.29. Amplification ratio map of the region.

According to Figure 5.28, H/V peaks vary irregularly among even closely spaced sites. The peak is one of the indicators of the presence of the impedance contrast between soft and stiff material at the corresponding resonance frequency. As can be seen in Figure 5.28, the amplification ratio increases towards the edge of the basin, since the more stiff units overlain by the soft sediments are relatively more close to the surface going away from the center of the basin. Also, a high amplification ratio can be observed in the alluvium within the plain due to the presence of very soft materials at the surface. When Figures 5.18 and 5.28 are compared, the average shear wave velocity map of the region shows that there are very soft sediment deposits where very high amplification ratio is present. The variation of the H/V peak period may reflect the geologic profile in such way that the larger the H/V peak period, the thicker the alluvial deposits (Figure 5.27). These outcomes were also confirmed by the results of shear wave measurements that were conducted at these particular sites. Comparisons of the results obtained at the two testing points are given in Figures 5.29 and 5.30.

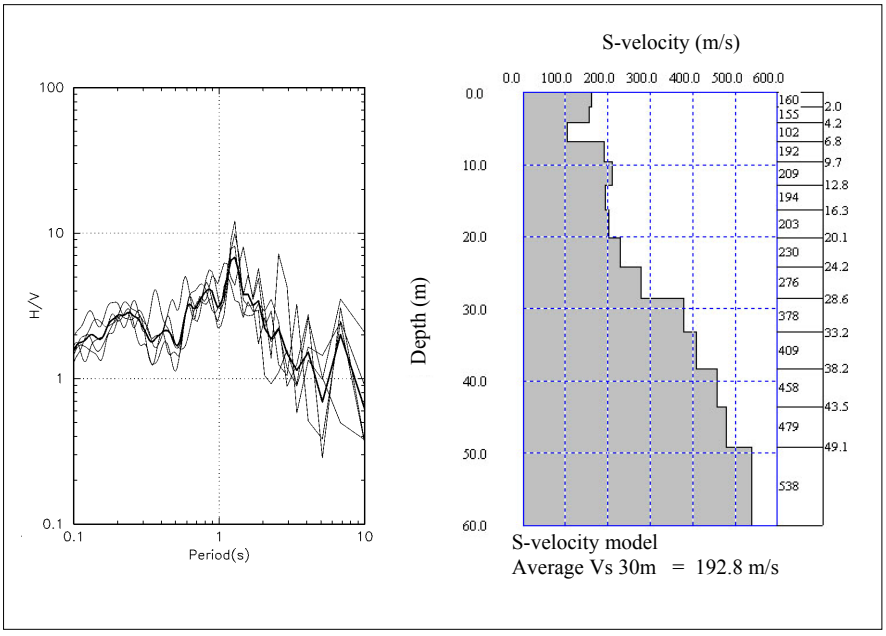

Figure 5.30. Comparison of the results obtained by the H/V method (left) and surface wave methods (right) at the Sies-31 testing point.

As can be seen on the left side of Figure 5.29, the expected horizontal to vertical-component noise ratios were found to exhibit a sharp peak at the fundamental S-wave resonant frequency amplification ratio of the site. When the shear wave velocity of the soil profile is examined through the figure on the right side of Figure 5.29, there is significant velocity change towards a depth of 30 m and engineering bedrock (>750 m/s) is not present along the soil profile. Because of these, the amplification ratio and fundamental period of the site are very high. On the contrary, for the sies-34 given in Figure 5.30, there is no discrete velocity change between the layers in the upper 30 m of the soil profile. Therefore, amplification value of the site is relatively smaller. However, fundamental period is high due to the presence of thick soft sedimentary deposits as explained above.

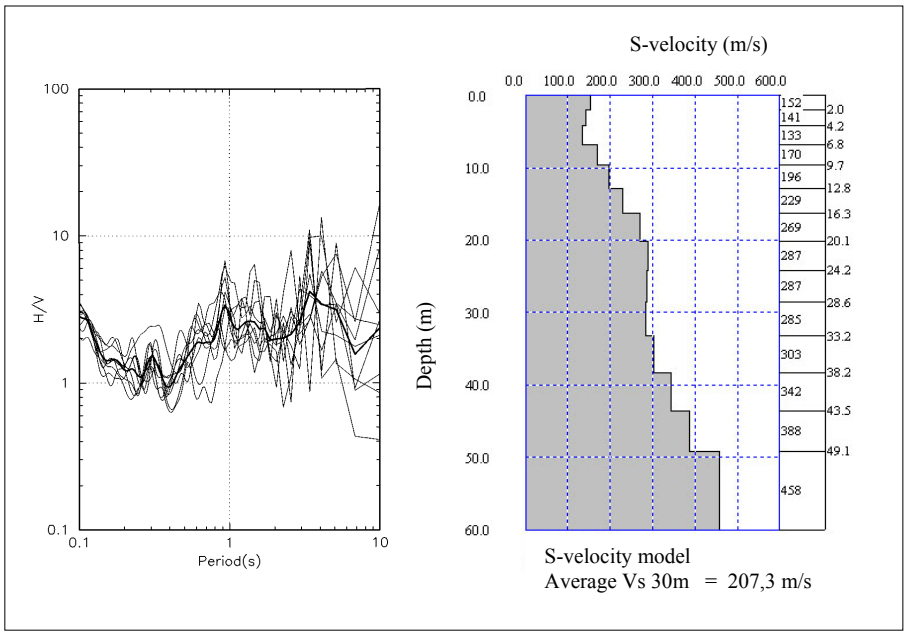

Figure 5.31. Comparison of the results obtained by the H/V method (left) and surface wave methods (right) at the Sies-34 testing point.

Moreover, the same conditions are valid for the results of the Seis-34 site. However, since the impedance contrast between the layers is not so significant, the amplification ratio is relatively small. But, fundamental period is high due to the

thick sediment deposit. In addition to this, towards the center of the alluvial plain, amplification ratio of 3 contour line dominantly represents the region (Figure 5.28). This can be related to the topographic effect since the Çubuk plain sediments has deposited in the graben form structure due to the tectonic activities since at the end of Miocene. In addition, due to the low impedance ratio at the site, amplification ratios of the deposits at the center of the valley are relatively low. Although the measured fundamental periods are directly proportional to the sediment thickness, the distribution of the amplification ratio obtained by the H/V method should not be used in geologic characterization of a geological unit. Rather than this, only the relative amplifications between the two measurement points are assumed to be significant (Bour, 1998; Duval, 2001 and Koçkar, 2006).

CHAPTER 6

SUMMARY, CONCLUSIONS AND RECOMMENDATIONS FOR FUTURE RESEARCH

The geological, engineering geological, geophysical and geotechnical properties of the Neotectonic units, namely, Upper Pliocene to Pleistocene fluvial and Quaternary alluvial and terrace sedimentary deposits in the Çubuk basin were investigated for seismic hazard assessment. These sediments are deposited in and along the fault controlled depression. This study covers a 120 km^2 area between the northern part of the Çubuk basin and the Çubuk district which is situated approximately 38 km north of Ankara.

This thesis mainly focused on the development of a methodology to integrate the various components necessary for a regional multi-hazard seismic risk analysis that includes dynamic soil characterization and determination of site effect which have not been carried out for this area up to date. Based on the results, site classification systems were assigned and dynamic soil properties of the basin were determined for seismic hazard assessment studies.

Depending on the results of the implemented surface wave methods, the regional seismic zonation map of V_{S30} was prepared based on the design code of IBC 2003. The mean shear wave velocity data of the Quaternary sites range between 182.7 – 297.6 m/s with a COV of 0.12, while those of the Upper Pliocene to Pleistocene sites change with a range of 202.9 – 339.3 m/s with a COV of 0.18 in the study area. According to these V_{S30} results, the sediments could not be differentiated by the site classes. The results are within the range of site class D (between 180-360 m/s) based

on the IBC 2003. Therefore, the design code could not distinguish the depositional environment units properly in the characterization study. Since the area used to be a graben, the sedimentary unit forms thick deposits. Also, it was confirmed that these soft deposits continue over a depth of 55 m in the area. In other words, the engineering bedrock was not encountered down to this depth. Therefore, another seismic code (TSC 1998) was utilized in order to classify the sites apart from the IBC 2003. Since the TSC 1998 assigns the site class based on topmost layer thickness (different from IBC 2003), other than the defined soil group (similar in the IBC 2003), the sediments were classified more reliable by using the TSC 1998 for the study area.

According to the TSC 1998, the Quaternary sites are classified as D-Z4 or D-Z3 based on the thickness of the soft alluvial deposits and the Upper Pliocene to Pleistocene sites are classified as C-Z3, D-Z3 and D-Z4. Although the all mean S-wave results of these sites fell within the boundaries of the class D in the IBC code, two different classes were assigned for the Quaternary sites and the Upper Pliocene to Pleistocene sites were divided into three different zones based on the TSC code due to the taking the surface sediment thickness into account.

Since most geological studies are compiled for goals other than investigating sediment characteristics and soil behavior (site effect) in relation to hazard assessments, the properties of the Neotectonic sediments, especially the Quaternary sediments and their members are ignored. Because of this, the Upper Pliocene to Pleistocene fluvial and Quaternary alluvial and terrace sedimentary deposits were mapped as Pliocene and Quaternary with respect to their age in the referenced geological map of this study. Nearly the entire region covered by Pliocene sediments was mainly formed by Upper Pliocene deposits. Also, the boundaries between the Neotectonic units unfortunately are not realistic. According to the result of this investigation, additional shear wave velocity measurements are necessary in order to delineate quantitatively more reliable boundaries between the geologic units.

In the estimation of the site effect studies, according to the ambient noise measurement processed by the H/V technique, higher fundamental periods were observed than expected which varied from 0.22 and 1.34 s. This is also thought to be related to thick unconsolidated sediment deposits in and near the fault controlled basin as proved by the shear wave velocity profiles. Thicker sediment deposits have higher fundamental periods at the site. This especially can be seen more clearly when the measurements on the center of the plain are compared with those at the edge of plain. Towards the edge, fundamental periods become lower, nevertheless, they were greater than anticipated. This is also thought to be due to the presence of terrace deposits particularly towards the east of the plain and the presence of the faults and their deformation zones in the area.

Instead of ascribing a meaning to the distribution of the amplification ratio obtained by the H/V method, the relative amplification values between two points were analyzed. Since, H/V peaks vary irregularly among even closely spaced sites between 2.1 to 9. The high amplitude might be an indicator of the presence of the impedance contrast between soft and stiff material at the corresponding resonance frequency. Amplification ratio increases towards the edge of the basin, since the more stiff units overlain by the soft sediment are relatively more close to the surface going away from the center of the basin. Also, high amplification ratios were observed at the center of the basin. However, at the center of the basin, relatively lower amplification ratios are dominantly encountered due to mainly the topographic (valley) effect. The amplification ratio results are generally very high at the sites located near the center of the basin with relatively low shear wave velocity values and whereas the sites locate at the edge of the basin with high impedance contrast.

The depositional setting of the area which took its final form due to the tectonic activities in the area was quantitatively analyzed and the results revealed that the distribution of the unconsolidated, thick sediments spread out in an extensive area in the region. The effects of the presence of the geological structural elements (normal faults), their deformation zones, and excessive deposition of the terrace sediments and as well as widespread Upper Pliocene and Pleistocene sedimentary units in the

area were analyzed and detected by utilizing in-situ tests. Especially, the shear wave velocity (V_S) profiles of the Quaternary sediments follow a low trend to a depth of 55 m. However the same case was also observed for the terrace sediments and the Upper Pliocene and Pleistocene fluvial deposits, due to the presence of the faults and their deformation zones (Figure 2.1). Another reason of the presence of the thick soft sediments is that the depositional settings are dominant in the area. Due to the cut and fill process, the sediments are deposited in the area under the control of the depositional (not erosional) setting. Although the collected data is not enough to estimate the boundaries between the considered units, they can be utilized as background information in Quaternary geological studies.

Moreover, the application of these evaluation results by using the integrated seismic zonation methodology is very crucial for the Çubuk Region in regards to findings potential areas for new urbanization. Additional care should be given to the sites where the average shear wave velocity is around 180 m/s (or D-Z4 sites) and the predominant period and the amplification ratio are high. Generally, these critical sites in regards to the average shear wave velocity and the predominant period are thought to be located towards the center of the basin. Especially, the D-Z4 sites should be taken into consideration carefully because of the presence of the thick soft alluvial deposits. For preliminary evaluations, emergency response, general land-use planning and defining the regions where need specific investigation in the area, a final seismic zonation map was created and given in Figure 6.1.

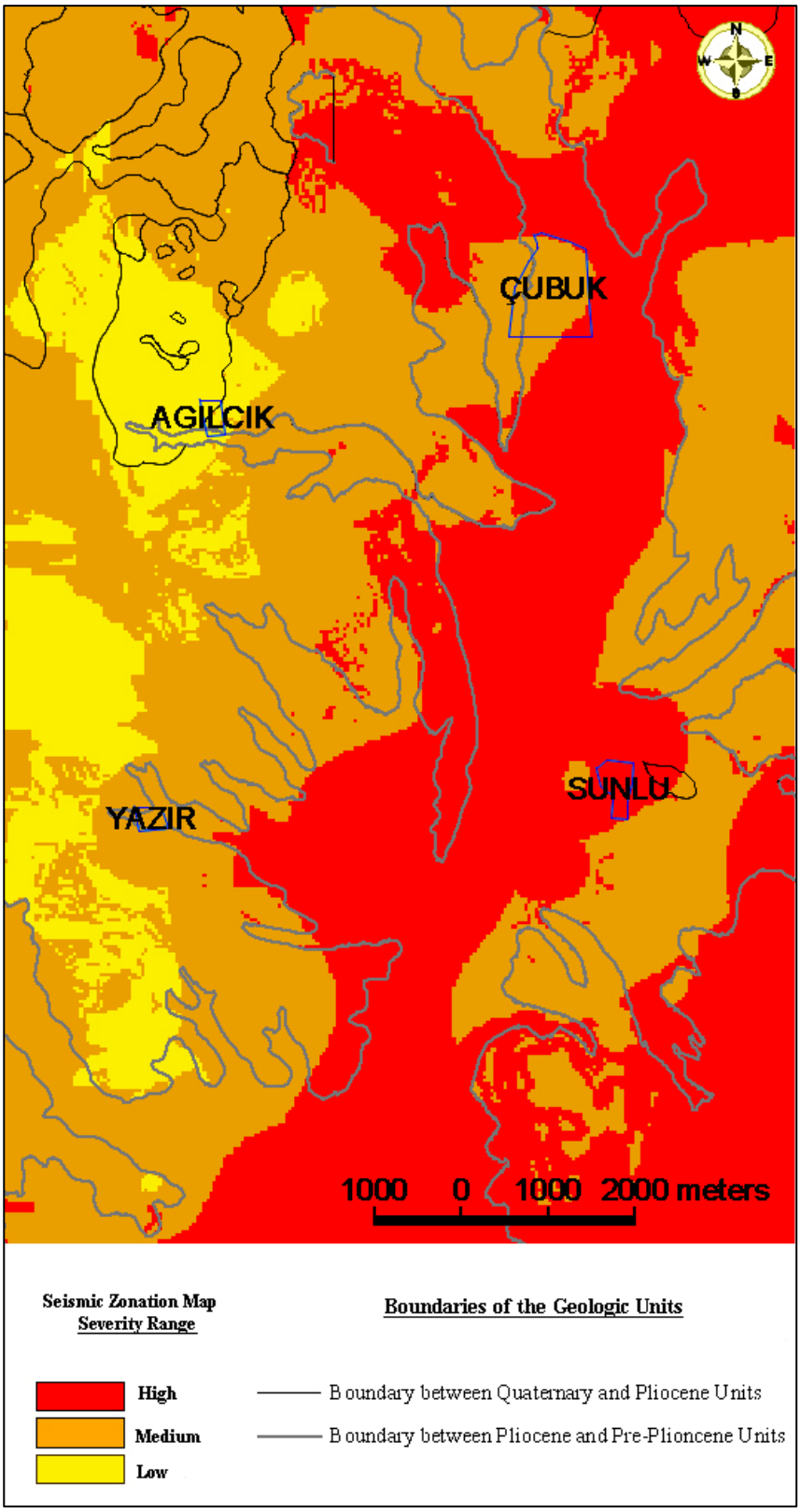

Figure 6.1. A final seismic zonation map in the account of seismic hazard assessment for the Quaternary and Upper Pliocene to Pleistocene sediments in the Çubuk Basin

The previously prepared five map layers [regional site classification zonation map of the Çubuk Basin based on Turkish Seismic Code (Figure 5.17), fundamental period (Figure 5.27), amplification ratio (Figure 5.28), geological (Figure 2.1) and slope maps of the study area], each of which defines a criterion necessary to be considered in seismic hazard assessment studies were prepared and explained in detail in previous chapter. To construct the final map, the Multi-Criteria Decision Analysis (MCDA) technique was utilized in order to define seismic zones in the Geographic Information System (GIS) environment. As can be seen in Figure 6.1, the study area was divided into three seismic zones which are A, B and C according to the degree of seismic severity. A significant part of the Quaternary sediments has a high hazard potential in the face of a probable destructive future earthquake. Therefore, a systematic urbanization will be implemented in regards to taking this study into account. A study like the one presented herein is a chance for assessing landuse planning especially for developing cities that are under the threat of a potential earthquake. However, it should be noted that additional site-specific studies should be implemented before major development is approved for the high potential study zone.

For the future studies, H/V spectral ratios will be compared with the transfer functions obtained from a one-dimensional numerical simulation in order to integrate the various components necessary for a regional multi-hazard seismic risk analysis that includes consideration of hazards due to local site effects. By comparing the results obtained by experimental and numerical techniques in the seismic hazard assessment studies, the amplification ratio and fundamental period of the some specific sites where the available borehole study present will be checked by considering the topographic effect and soft soil thickness. In the future additional seismic studies are planned to be conducted at different sites in an attempt to expand the database in the region in order to characterize the units more accurately by using the seismic codes and also by using the appropriate classification systems in the literature. Furthermore, seismic reflection studies are thought to be implemented to detect the throw and trend of the faults more accurately in the area. Continuation

between the Çubuk and Dodurga Fault Zone by the aid of the deep seismic study above mentioned.

REFERENCES

Abrahamson, N., Silva, W., 2008, "Summary of the Abrahamson & Silva NGA Ground-Motion Relations", Earthquake Spectra, Vol.24, No.1, pp.67-97.

Akamatsu, J., 1984, "Seismic Amplification by Soil Deposits Inferred From Vibrational Characteristics of Microseism", Bulletin of Disaster Prevention Research Institute, Kyoto University, 34, 105-127.

Aki, K., 1957, "Space and Time Spectra of Stationary Stochastic Wave With Special Reference to Microtremors", Bull. Earthq. Res. Inst., Tokyo University, 35, 415-17.

Aki, K., 1988, "Local Site Effects on Strong Ground Motion", Earthquake Engineering and Soil Dynamics II - Recent Advances in Ground Motion Evaluation (J.L. Von Thun, ed.), ASCE GSP 20, 103-155.

Aksay, A. ve Duru, M., 2002. "1/100.000 Ölçekli Türkiye Jeoloji Haritaları, Adapazarı H24 paftası. MTA Yayınları, Pafta No: 37.

Akyürek, B., Bilginer, E., Çatal, E., Dağer, Z., Soysal, Y. ve Sunu, O., 1980, "Eldivan-Şabanözü (Çankırı) Hasayaz-Çandır (Kalecik-Ankara) Dolayının Jeolojisi", MTA Rap. 6741 (yayımlanmamış).

Akyürek, B., Duru, M., Sütçü, Y.F., Papak, İ., Şaroğlu, F., Pehlivan, N., Gönenç, O., Granit, S. ve Yaşar, T., 1996, "Ankara İlinin Çevre Jeolojisi ve Doğal Kaynaklar Projesi (1994 yılı Jeoloji grubu çalışmaları) ", MTA Derleme No. 9961 (yayınlanmamış).

Akyürek, B., Bilginer, E., Akbaş, B., Hepsen, N., Pehlivan, S., Sunu, D., Soysal, Y., Dager, Z., Catal, E., Süzen, B., Yıldırım, H., and Hakyemez, Y., 1984. "Ankara-Elmadağ-Kalecik Dolayının Temel Jeoloji Özellikleri", Jeoloji Müh. Dergisi, v. 20, p. 21-46.

Anderson, J.G., Lee, Y., Zeng, Y. and Day, S., 1996, "Control of Strong Motion by the A 30 Meters", Bull. Seis. Soc. Am., 86, 6, 1749-1759.

Ansal, A., Biro, Y., Erken, A., Gülerce, Ü., "Seismic Microzonation: A Case Study", Recent Advances in Earthquake Geotechnical Engineering and Microzonation, ed. by A. Ansal, (2004), Kluwer Academic Publishers, p.253..

Ansal, A., Tönük, G., 2007, "Source and Site Factors in Microzonation" Earthquake Geotechnical Engineering, Springer, 73-92.

Asten, M.W., 1978, “Geological Control on the Three-Component Spectra of Rayleigh Wave Microseisms”, Bull., Seism. Soc. Am., v. 68, p. 1623-1636.

Asten, M.W., and Henstridge, J.D., 1984, “Array Estimators and the Use of Microseisms for Reconnais-sance of Sedimentary Basins”, Geophysics, v. 49, p. 1828-1837.

Asten, M.W., and Boore, D.M., eds., 2005, “Blind Comparisons of Shear-Wave Velocities at Closely Spaced Sites in San Jose, California”, U.S. Geological Survey Open-File Report -1169.

Bailey, E.B. and McCallien, W.J., 1950, “Ankara Melanjı ve Anadolu Şariyajı”, MTA Bulletin, 15, 40, 12-22.

Bard, P-Y., 1999, Microtremor Measurements: A Tool for Site Effect Estimation?, In: “The Effects of Surface Geology on Seismic Motion”, Irikura, Kudo, Okada & Sasatani (Eds.), Rotterdam, 1251-1279.

Bodin P, Smith K, Horton S, Hwang H, 2001, “Microtremor Observations of Deep Sediment Resonance in Metropolitan Memphis, Tennessee”, Eng. Geol. 62, 159– 168.

Bonnefoy-Claudet, S., Cotton, F., Bard, P.Y., 2006, “The Nature of Noise Wavefield and Its Applications for Site Effects Studies A Literature Review”, Earth-Science Reviews 79, 205–227.

Boore, D. M., Joyner W. B., and Fumal T. E., 1993, “Estimation of Response Spectra and Peak Accelerations from Western North American Earthquakes”, An Interim Report, U.S. Geol. Surv. Open-File Rept. 93-509, 72 p.

Boore, DM, 2006, “Determining Subsurface Shear-Wave Velocities: A Review”, Third International Symposium on the Effects of Surface Geology on Seismic Motion Grenoble, France, p: 103.

Borcherdt, R.D. 1970, “Effects of Local Geology on Ground Motion Near San Francisco Bay”, Bull. Seism. Soc. Am. 60, 29-61.

Borcherdt, R. D., 1994, “Estimates of Site-Dependent Response Spectra for Design (Methodology and Justification)”, Earthquake Spectra, 10, 617–653.

Bour, M., Fouissac, D., Dominique, P. and Martin, C., 1998, “On the Use of Microtremor Recordings in Seismic Microzonation, Soil Dynamics and Earthquake Engineering”, 17, 465-474.

Bozkurt, E., 2001, “Neotectonics of Turkey - A Synthesis”, Geodinamica acta, 14(1), 3-30.

Brennan, A.J., Thusyanthan, N.I., and Madabhushi, S.P.G., 2005, "Evaluation of Shear Modulus and Damping in Dynamic Centrifuge Tests", Journal of Geotechnical and Geoenvironmental Engineering, 131(12): 1488–1497.

Cara, F., Cultrera, G., Azzara, R., Rubeis, V., Guilio, G., Giammarinaro, M., Tosi, P., Vallone, P. and Rovelli, A., 2008, "Microtremor Measurements in the City of Palermo, Italy", Analysis of the Correlation between Local Geology and Damage. Bull. Seism. Soc. Am. 98-3, 1354-1372.

Cid, J., Susagna, T., Goula, X., Chavarria, L., Figueras, S., Fleta J., Casas A., Roca A., 2001, "Seismic Zonation of Barcelona Based on Numerical Simulation of Site Effects", Pure Appl Geophys V. 158, pp. 2559–2577.

Chaput, E., 1931, "Ankara Mıntıkasının 1/135000 Mikyasında Jeolojik Haritasına Dair İzahat", İstanbul Darülf., Jeol. Enst. Neşriyatı, 7, 46p.

Chaput, E., 1947, "Türkiye'de Jeolojik ve Jeomorfojenik Tetkik Seyahatleri", İstanbul Publication, 324, 326p.

Chavez-Garcia, F.J., Sanchez L.R. and Hatzfeld D., 1996, "Topographic Site Effects and HVSR. A Comparison Between Observations and Theory", Bull. Seism. Soc. Am., 86-5, 1559-1573.

Chavez-Garcia, F.J., Rodriguez, M., Stephenson, W.R., 2005, "An Alternative Approach to the SPAC Analysis of Microtremors: Exploiting Stationarity of Noise", Bulletin of the Seismological Society of America 95 (1), 277–293.

Chavez-Garcia, F.J., Rodriguez M., Stephenson W.R., 2006, "Subsoil Structure Using SPAC Measurements Along a Line", Bull. Seism. Soc. Am. 96: 729–736

Chavez-Garcia, F.J., Dominguez, T., Rodriguez, M., Perez, F., 2007, "Site Effects in a Volcanic Environment: a Comparison between HVSR and Array Techniques at Colima", Mexico. Bull. Seism. Soc. Am. V. 97, pp. 591-604.

Chavez-Garcia, F.J., 2007, "Site Effects: From Observation and Modeling to Accounting for Them in Building Codes", Earthquake Geotechnical Engineering, pp. 53-72.

D'Amico, V., Picozzi, M., Baliva, F., Albarello, D., 2008, "Ambient Noise Measurements for Preliminary Site-Effects Characterization in the Urban Area of Florence, Italy", Bull. Seism. Soc. Am.. V. 98(3), pp. 1373-1388.

Delgado, J., Lopez Casados, C., Giner, J., Estevez, A., Cuenca, A., Molina, S., 2000, "Microtremors as a Geophysical Exploration Tool: Applications and Limitations", Pure and Applied Geophysics 157 (9), 1445–1462.

Delgado, J., Alfaro, P., Galindo-Zaldivar, J., Jabaloy, S., Lopez Garrido, A.C., Sanz De Galdeano, C., 2002, "Structure of the Padul- Nigüelas Basin (S Spain) from H/V Ratios of Ambient Noise: Application of the Method to Study Peat and Coarse Sediments" Pure and Applied Geophysics 159 (11–12), 2733–2749.

Dobry, R., Borcherdt, R. D., Crouse, C.B., Idriss, I.M., Joyner,W.B., Martin, G.R., Power, M.S., Rinne, E.E., and Seed, R.B., 2000, "New Site Coefficients and Site Classification System Used in Recent Building Seismic Code Provisions", Earthquake Spectra, 16, 41–68.

Drake, L.A., 1980, "Love Waves and Rayleigh Waves in an Irregular Soil Layer", Bull. Seism. Soc. Am., 70, 571-582.

DSİ., 1979 , "Hydrogeological Report of Çubuk Plain". General Directorate of the State Hydraulic Works, Geotechnical Service and Groundwater Chief Office Publication.

Duval, A.M., Bard, P.Y., Mèneroud J.P. and Vidal, S., 1995, "Mapping Site Effects with Microtremors". In: Proceedings of Fifth International Conference on Seismic Zonation, vol 2, 17–19 October, 1995, Nice, France. 1994, pp 1522–1529

Duval, A.M., Méneroud J.P., Vidal, S., and Singer, A., 1998, "Relation Between Curves Obtained from Microtremor and Site Effects Observed After Caracas 1967 Earthquake", Proceedings of the 11th European Conference on Earthquake Engineering. Paris, France.

Duval, A.M, Méneroud, J.P, Vidal, S., Singer, A, De Santis, F., Ramos, C., Romero, G., Rodriguez, R., Pernia, A., Reyes, A. and Griman, C., 2001, "Caracas, Venezuela, Site Effect Determination with Microtremors", Pure appl. geophy., V.158, pp.2513-2523

Duru, M., Aksay A., 2002, "1/100.000 Türkiye Jeoloji Haritaları H29 Paftası", MTA. Erentöz, C., 1975, 1/500 000 Ölçekli Türkiye Jeoloji Haritası Derlemesi, Ankara Paftası, MTA Enstitüsü Yayını, 111p.

Erol, O., 1954, "Ankara ve Civarinin Jeolojisi Hakkinda Rapor", M.T.A. Enstitüsü Rapor No.2456. Ankara (Unpublished-Turkish).

Erol, O., 1955, "Ankara-Haymana-Aydos Dağı Arasındaki Bölgenin Jeomorfolojisi", Ankara University, D.T.C.F. Doçentlik Tezi (Unpublished-Turkish).

Erol, O., 1956, "A Study of the Geology and Geomorphology of the Region SE of Ankara in Elmadağ and Its Surroundings (Summary)", Ph.D. Thesis, M.T.A. Institute Report, No:9, Ankara.

Erol, O., 1961. “Ankara Bölgesinin Tektonik Gelişmesi ”, Türkiye Jeoloji Kur. Bült., 712, 57-74.

Erol, O., 1966, “The Geomorphological Importance of the Remains of Fossils Mammals Found between Üçbaş and Akdoğan Villages in the Northwest of Ankara (Summary) ”, Ankara University Geographic Research Bulletin, No.1, pp. 109-120, Ankara.

Erol, O., 1973. “Ankara Şehri Çevresinin Jeomorfolojik Ana Birimleri”, A.Ü. Dil Tarih ve Tarih Coğrafya Fakültesi Yayınları no. 240, 29 s.

Erol, O., 1980, “The Neogene and Quaternary Erosion Cycles of Turkey in Relation to the Erosional Surfaces and Their Correlated Sediments”, Geomorphology, V.8, pp. 1-40 (in Turkish-English Abstract).

Erol, O., Yurdakul, M.E., Algan, Ü., Gürel, N., Herece, E., Tekirli, E., Ünsal, Y., Yüksel, M., 1980 “Geomorphological Map of Ankara, General Directorate of Mineral Research and Exploration (M.T.A.) ”, Report No: 6875, 300p. (in Turkish) Bailey, E. B., McCallian, W. C., 1953. The Ankara Melange and the Anatolian Thrust: Royal Society of London, Philosophical Transactions, 62, 403-442.

Erol, O., 1993, “Ankara Yöresinin Jeomorfolojik Gelişimi”, A. Suat Erk Jeoloji Sempozyumu (2-5 Eylül 1991) Bildirileri, Ankara s. 25.35.

Faccioli, E. 1991, “Seismic Amplification in the Presence of Geological and Topographic Irregularities”, In: Proceedings of the Second International Conference on Recent Advances in Geotechnical Earthquake Engineering and Soil Dynamics, March 11-15, St.

Fah, D., Ruttener, E., Noack, T. and Kruspan, P., 1997, “Microzonation of the City of Basel”, Journal of Seismology, 1, 87-102.

Field, E.H., Hough, S.E. and Jacob K.H., 1990, “Using Microtremors to Assess Potential Earthquake Site Response, A Case Study in Flushing Meadows, New York City”, Bull. Seism. Soc. Am., 80, 1456-1480.

Field E.H., and. Jacob K.H., 1993, “The Theoretical Response of Sedimentary Layers to Ambient Seismic Noise”, Geophysical Res. Lett. 20-24, 2925-2928.

Field, E.H. and Jacob K.H., 1995, “A Comparison and Test of Various Site Response Estimation Techniques, Including Three That are not Reference Site Dependent”, Bull. Seism. Soc. Am., 85, 1127-1143.

Finn, W.D., 1991, “Geotechnical Engineering Aspects of Seismic Microzonation”, In: Proceedings of the Fourth International Conference on Seismic

Zonation, August 25-29, Stanford, California, E.E.R.I. (ed), Oakland CA, I, 199-250.

Foti, S., 2005, "Surface Wave Testing for Geotechnical Characterization, Surface Waves in Geomechanics – Direct and Inverse Modeling for Soil and Rocks", Lai and Wilmanski Ed., CISM Lecture Notes, Springer-Verlag, Wien-Newyork.

Fumal, T.E., 1978, "Correlations between Seismic Wave Velocities and Physical Properties of Near-Surface Geologic Materials in the Southern San Francisco Bay region", California, U.S. Geol. Surv. Open-File Rept. 78-1067.

Fumal, T.E., and. Tinsley J.C., 1985, "Mapping Shear-Wave Velocities in Near-Surface Geological Materials, in Evaluating Earthquake Hazards in the Los Angeles Region-An Earth Science Perspective", J. I. Ziony (Editor), U.S. Geol. Surv.Profess. Paper, 1360, 127-150.

Geli, L., Bard, P.Y. and Jullien, B, 1988, "The Effect of Topography on Earthquake Ground Motion: A Review and New Results'', Bulletin of the Seismological Society of America, Vol.78, No.1, pp.42-63.

Geometrics Inc., 2006, "SeisImager/SW^{TM} V. 2.2 Manual", San Jose, California, USA., 281 pp.

Geometrics Inc., 2007, "SeisImager/SW, Surface Wave Analysis Software". San Jose, California, USA.

Geovision, 2009, "Retrieved April 12, 2009 from", Web site: http://www.geovision.com/seismic.html

Global Mapper Software Inc., 2006, "V 8.00", Parker CO., USA.

Google Inc., 2007, "Google Earth V. 4.2 ".

Gosar, A., Stopar, R., and Roser, J., 2008, "Comparative Test of Active and Passive Multichannel Analysis of Surface Waves (MASW) Methods and Microtremor HVSR method", RMZ - Materials and Geoenvironment, Vol. 55, No. 1, pp. 41-66.

Guillier B., Atakan K., Chatelain J.L., Havskov J., Ohrnberger M., Cara F., Duval A.M., Zacharopoulos S., Teves-Costa P., Accera C., Alguacil G., Azzara R., Bard P.Y., Blarel F., Borges A., Grandison M., Rao S., Theodulidis N., Tvedt, E., Utheim, T., Vidal, S. and Vollmer D., 2008, "Influence of Instruments on the H/Vspectral Ratios of Ambient Vibrations", Bull Earthq Eng., V. 6, pp 3-31.

Gutenberg, B., 1958. "Microseisms", Advances in Geophysics 5, 53–92.

Haghshenas, E., Bard, P.Y. and Theodulidis, N., 2008, "Empirical Evaluation of Microtremor H/V Spectral Ratio", Bull Earthq. Eng., V. 6 pp 75-108.

Havenith, H.B., Fäh, D., Polonu, U. and Roullé, A., 2007. "S-wave Velocity Measurements Applied to the Seismic Microzonation of Basel, Upper Rhine Graben", Geophys. J. Int. , 170 , 346–358

Hatipoğlu, M., 1996, "Mineralogical and Gemological Investigation of Bared and Banded Agates of Çubuk (Ankara) Area", PhD Thesis, Dokuz Eylül University, 128 p.

Hayashi, K., 2003, "Data Acquisition and Analysis of Active and Passive Surfac Waves", Symposium on the Application of Geophysics to Environmental and Engineering Problems Short Course Notes, 106 pgs.

Hayashi, K., 2008, "Development of Surface-Wave Methods and Its Application to Site Investigations Phd, thesis", Kyoto University.

ICC 2003, International Code Council, 2003, "International Building Code, Structural and Fire-And Life-Safety Provisions Covering Seismic, Wind, Accessibility, Egress, Occupancy and Roofs Codes", 672 p.

Idriss, I. M. (1991) "Earthquake Ground Motions at Soft Soil Sites", Proceedings of the Second International Conference on Recent Advances in Geotechnical Earthquake Engineering and Soil Dynamics, March 11-15, 1991, St. Louis, MO, Ed., S. Prakesh, University of Missouri-Rolla, 3.

İlyüz, N., 1940, "Ankara Sekileri", Y.E.Z. Çalışmaları, No.104, Ankara.

Jibson, R., 1987, "Summary of Research on the Effects Topographic Amplification of Earthquake Shaking of Slope Stabilitiy.'' U.S. Geological Survey, Open-File Report 87-268, Manlo Park, California, USA.

Jin, X., Luke, B., and Louie, J., 2006, "Comparison of Rayleigh Wave Dispersion Relations from Three Surface Wave Measurements in a Complex-Layered System", Proc., ASCE Geocongress 2006 (Atlanta), ASCE Press, Neew York

Joyner, W.B., and Fumal, T.E., 1985, "Predictive Mapping of Earthquake Ground Motion", in Evaluating Earthquake Hazards in the Los Angeles Region-An Earth Science Perspective, J. I. Ziony (Editor), U.S. Geol. Surv. Profess. Pap. 1360, 203-220.

Kanai, K. and Tanaka T., 1961, "On Microtremor VIII'', Bull. Earthq. Res. Inst., Tokyo University, 39, 97-114.

Kanai, K., and Tanaka, T., 1961, "Measurement of the Microtremor 1", Bulletin of the Earthquake Research Institute, University of Tokyo, 32; 200-208.

Kanai, K., 1966, “Observations of Microtremors XI”, Bull, Earthq. Res.Inst., University of Tokyo, 44, 1297-1333.

Kanai, K., 1983, “Engineering Seismology”, University of Tokyo Press, Tokyo, 251p.

Kaplan, T., 2004, “Neotectonics and Seismicity of The Ankara Region: A Case Study of The Uruş Area”, Master Thesis, Middle East Technical University, Ankara. p.98.

Kasapoğlu, K.E., 1980, “Ankara Kenti Zeminlerinin Jeomühendislik Özellikleri”, Doçentlik Tezi, Hacettepe University, Geological Engineering Department, Beytepe, Ankara.

Kasapoğlu, K.E., 2000, “Ankara Kenti Zeminlerinin Jeoteknik Özellikleri ve Depremselliği”, Jeoloji Müh. Odası Yayını. Yayın No.:54, 180 s.

Ketin, I, 1959, “Türkiye’nin Orojenik Gelişmesi”, MTA Bulletin, 53, Ankara.

Kılıç, H., Özener, P.T., Ansal, A., Yıldırım, M., Özaydın, K., Adatepe, S., 2006, “Microzonation of Zeytinburnu Region with respect to Soil Amplification: A Case Study”, Journal of Engineering Geology, 86: 238-255.

Kobayashi, H., Seo, K., Midorikawa, S., 1986, “Part 1, Estimated Strong Ground Motions in the Mexico City due to the Michoacan, Mexico Earthquake of September 19, 1985 based on Characteristics of Microtremor”, “Part 2, Report on Seismic Microzoning Studies of the Mexico Earthquake of September 19”, 1985, The Graduate School of Nagatsuta, Tokyo Institute of Technology, 34-68.

Kobayashi, H., 1991, “Utility of Microtremors to the Effects of Surface Geology on Seismic Motions, Proceedings”, Fourth International Conference on Seismic Zonation: August 25th-29th, 1991, Stanford University, Stanford, California, USA, 361-368.

Koçkar, M., 2006, “Engineering Geological and Geotechnical Site Characterization and Determination of the Seismic Hazards of Upper Pliocene and Quaternary Deposits Situated Towards The West of Ankara”, Ph.D. Thesis, 401 p.

Koçkar MK., Akgün H., 2008, “Development of a Geotechnical and Geophysical Database for Seismic Zonation of the Ankara Basin, Turkey”, Enviromental Geology, 55, 165–176.

Koçyiğit, A., 1987, “Hasanoğlan (Ankara) Yöresinin Tektono-Stratigrafisi: Karakaya Orojenik Kuşağının Evrimi”, Hacettepe Üniversitesi Yerbilimleri, 14, 269-293.

Koçyiğit, A., 1989, “Suşehri Basin: An Active Fault-Wedge Basin on the North Anatolian Fault Zone”, Turkey, Tectonophysics, 167, 13-29.

Koçyiğit, A., 1991, “Changing Stress Orientation in Progressive Intercontinental Deformation as Indicated by the Neotectonics of Ankara Region”, NW Central Anatolia, TAPG Bulletin, 31, 43-55, Ankara.

Koçyiğit A., Türkmenoğlu, A., 1991, “Geology and Mineralogy of the So-Called ”Ankara Clay Formation”: A Geologic Approach to the “Ankara Clay” Problem. In: Zor, M. (ed.), 5th National Clay Symposium, 16-20 September 1991, Eskişehir, Proceedings, pp. 112-126.

Koçyiğit, A., Rojay, B., Cihan, M. and Özacar, A., 2001, “The June 6, 2000 Orta(Çankırı, Turkey) Earthquake: Sourced from a New Antithetic Sinistral Strike-Slip Structure of the North Anatolian Fault System”, the Dodurga Fault Zone. Turkish Journal of Earth Sciences, 10, 69-82.

Koçyiğit, A., 2003, “General neotectonic characteristics and seismicity of Central Anatolia”, TPJD, Special Publication 5:1–26 (in Turkish with English Abstract)

Koçyiğit, A., 2008, “Ankara ve Çevresinin Deprem Kaynakları”, Ankara’nın Deprem Tehlikesi ve Riski Çalıştayı, Bildiriler Kitabı, s 34-53, Gazi Üniversitesi, 19 Mart, Ankara.

Koçyiğit, A., 2009, “Ankara’nın Depremselliği ve 2005-2007 Afşar (Bala-Ankara) Depremlerinin Kaynağı”, Harita Dergisi, S.14;1-12;01.

Konno, K. and Ohmachi T., 1998, “Ground-Motion Characteristics Estimated from Spectral Ratio between Horizontal and Vertical Components of Microtremor”, Bull. Seism. Soc. Am. 88-1, 228-241.

Kramer, S.L., 1996, “Geotechinal Earthquake Engineering, ed. William J. H., Prentice-Hall International Series in Civil Engineering and Engineering Mechanics”, New Jersey, USA.

Kupan, İ., H., 1977, “Ankara’nın Kuzeyindeki Çubuk Ovası’nın Yeraltısuyu Etüdü”, Ph.D. Thesis, İstanbul University, İstanbul, p.130.

Lacave, C., Bard, P., Koller, M., 2002, “Microzonation: Techniques and Examples”.

Lachet C. and Bard P. Y., 1994, “Numerical and Theoretical Investigations on the Possibilities and Limitations of Nakamura’s Technique”, J.Phys.Earth., 42, 377-397.

Lachet, C., Hatzfeld, D., Bard, P.-Y., Theodulidis, N., Papaioannou, C. and Savvaidis, A., 1996, “Site Effects and Microzonation in the City of

Thessaloniki (Greece): Comparison of Different Approaches", Bull. Seism. Soc. Am., 86, 1692-1703.

Lahn, E., 1949, "On the Geology of Central Anatolia", TJK Bulletin, 2, 1, Ankara

Lebrun, B. 1997, "Les effets de site: étude expérimentale et simulation de trois configurations", De l'Université Joseph Fourier - Grenoble I, November 27, Ph. D. Thesis, 208 p. (in French).

Lebrun, B., Hatzfeld, D., Bard, P.Y., 1999, ''Experimental Study of Ground Motion on a Large Scale Topography'', J. of Seismology, 3(1): 1-15.

Lebrun, B., Hatzfeld, D., Bard, P.Y., 2001, "Site Effect Study in Urban Area: Experimental Results in Grenoble (France)", Pure and Applied Geophysics, 158 (12), 2543–2557.

Lermo, J., Rodriguez, M. and Singh, S.K., 1988, "Natural Periods of Sites in the Valley of Mexico from Microtremor Measurements and Strong Motion Data", Earthquake Spectra, 4, 4, 805-814.

Lermo J. and Chavez-Garcia. F.J., 1993. "Site Effect Evaluation Using Spectral Ratios with Only One Station", Bull. Seism. Soc. Am. 83, 1574-1594.

Lermo, J. and Chavez-Garcia., 1994, "Are Microtremors Useful in Site Response Evaluation?", Bull. Seism. Soc. Am. 84, 1350-1364.

Lin, C.P., Chang, T.S., and Cheng, M.H., 2004, "The Use of MASW Method in the Assessment of Soil Liquefaction Potential", Soil Dynamics and Earthquake Engineering V. 24 p. 689–698

Lin, Y.C., 2007, "Characterizing Shear Wave Velocity Profiles by the SASW Method and Comparison with Other Seismic Methods Ph.D. Thesis", The University of Texas at Austin, 2007, 308 pages

Liu, Y., Luke, B., Pullammanappallil, S., Louie, J., and Bay, J., 2004, "Combining Active- and Passivesource Measurements to Profile Shear-Wave Velocities for Seismic Microzonation", Submitted to Geofrontier.

Louie, J.N., 2001, "Faster, Better: Shear-Wave Velocity to 100 meters Depth from Refraction Microtremor Arrays", Bull. Seism. Soc. Am., v. 91, n. 2, p. 347-364.

Louie, J.N., Abbott, R.E. and Pullammanappallil, S., 2002, "Refraction Microtremor and Optimization Methods as Alternatives to Boreholes for Site Strength and Earthquake Hazard Assessments", Proceedings 15th Annual Symposium on the Application of Geophysics to Environmental and Engineering Problems (SAGEEP '02), February 11-13, Las Vegas, Nevada.

McMechan, G., and Yedlin, M.J., 1981, "Analysis of Dispersive Waves by Wave Field Transformation", Geophysics, v. 46, n. 6, p. 869-874.

Microimages Inc., 2004, "TNTmips V. 6.9", Lincoln, USA.

Midorikawa, S., 1987, "Prediction of Isoseismal Map in Kanto Plain due to Hypothetical Earthquake" Journal of Structural Dynamics, 33B, 43-48.

Miller, R.D., Xia, J., Park, C.B., and Ivanov, J.M., 1999, "Multichannel Analysis of Surface Waves to Map Bedrock", Kansas Geological Survey, the Leading Edge, December, p. 1392-1396.

Ministry of Public Works and Settlement Government of Republic of Turkey, 1998, "Turkish Seismic Code, Specification for Structures to Be Built in Disaster Areas", Ankara, Turkey.

Multichannel Analysis of Surface waves (MASW) 2009, Retrieved May 1, 2009 from http://www.masw.com".

Nakamura, Y., 1989, "A Method for Dynamic Characteristics Estimation of Subsurface sing Microtremor on the Ground Surface", Quarterly Report of Railway Technical Research Institute (RTRI), 30, 1.

Nakamura, Y., 1996, "Real Time Information Systems for Seismic Hazards Mitigation UrEDAS, HERAS and PIC", Quarterly Report of RTRI, 37, 3, 112-127.

Nakamura Y., 2000, "Clear Identification of Fundamental Idea of Nakamura's Technique and its Applications", Proc. 12th World Conf. on Earthq. Engng. (CD-ROM), Paper ID 2656, 8p.

Nath, S.K., 2007, "Seismic Microzonation Framework – Principles & Applications, Proceedings of Workshop on Microzonation", Indian Institute of Science, Bangalore, pp 9-35

Nazarian, S., Stokoe II, K.H., and Hudson, W.R., 1983, "Use of Spectral Analysis of Surface Waves Method for Determination of Moduli and Thicknesses of Pavement Systems", Transp. Res. Rec. v. 930, Washington DC, p. 38-45.

Nazarian, S., 1984, "In Situ Determination of Elastic Moduli of Soil Deposits and Pavement Systems by Spectral-Analysis-of-Surface-Waves Method: Ph.D. Dissertation", Univ. of Texas, Austin.

Nguyen, F., Van Rompaey, G., Teerlynck, H., Van Camp, M., Jongmans, D. and Camelbeeck, T., 2004, "Use of Microtremor Measurement for Assessing Site Effects in Northern Belgium-Interpretation of the Observed Intensity During the Ms=5.0 June 11 1938 Eearthquake", Journal of Seismology 8 (1), 41–56.

Nogoshi, M. and Igarashi, T., 1971, “On the Amplitude Characteristics of Microtremor (Part 2)”, Jour. Seis. Soc. Japan, 24, 26-40.

Okada, H., 2003, “The Microtremor Survey Method; Geophysical Monograph Series”, no. 12, Published by Society of Exploration Geophysicists (SEG), Tulsa.

Oliveira, CS., 2004, “The Influence of Scale on Microzonation and Impact Studies” Recent Advances in Earthquake Geotechnical Engineering and Microzonation, Kluwer Academic Publishers, 3-26.

Panca, A., Anderson, J.G., and Louie, J.N., 2007, “Characterization of Near-Surface Geology at Strong-Motion Stations in the Vicinity of Reno”, Nevada, Bull. Seism. Soc. Am. V. 97, pp. 2096-2117.

Park, C.B., Miller, R.D., and Xia, J., 1997, “Multi-Channel Analysis of Surface Waves (MASW) "A Summary Report of Technical Aspects, Experimental Results, and Perspective"”, Kansas Geological Survey Open File Report No: 97-10.

Park, C.B., Miller R.D. and Xia J., 1999, “Multi-Channel Analysis of Surface Waves”, *Geophysics*, v. 64, n. 3, p. 800-808.

Park, C.B., Miller, R.D., Xia, J. and Ivanov, J., 2000, “Multichannel Seismic Surface Wave Methods for Geotechnical Applications”.

Park, C.B., Miller, R.D., and Xia, J., 2001, “Offset and Resolution of Dispersion Curve in Multichannel Analysis of Surface Waves (MASW)”, Proceedings of the SAGEEP 2001, Denver, Colorado, SSM-4.

Park, C.B., Miller, R.D., and Miura, H., 2002, “Optimum Field Parameters of an MASW Survey” [Exp. Abs.]: SEG-J”, Tokyo, May 22-23.

Park, C.B., 2003, “SurfSeis V. 1.5 User Manual”, Kansas Geological Survey.

Park, C.B., Ivanov, J., and Brohammer, M., 2006, “SurfSeis V. 2.0 User Manual”, Kansas Geological Survey, 38 pp.

Park, C.B., Miller, R.D., Xia, J., and Ivanov, J., 2007, “Multichannel Analysis of Surface Waves Active and Passive Methods”, the Leading Edge, January - (MASW).

Park Seismic, 2009, Retrieved May 4, 2009, “From, Web site: http://www.parkseismic.com SurfaceWaveSurvey.html”.

Parolai, S., Richwalski., S.M. and Milkereit, C., 2006, “S-wave Velocity Profiles for Earthquake Engineering Purposes for the Cologne Area (Germany)”, Bulletin of Earthquake Engineering ,V.4, p. 65–94.

Pfannenstiel, M., 1940, "Ankara'nın Diluvial Moloz Şekilleri ve Avrupanın Kuvaterner Kronolojisine Göre Tasnifleri", Translation: Tiraje Tansu, Y.Z.E. Enstitusü Çalışmaları, Sayı 120. Ankara 1941 (in Turkish).

Pitilakis, K., 2004, "Site Effects, Recent Advances in Earthquake Geotechnical Engineering and Microzonation", Ansal (Ed), Kluwer Academic Publishers, Dordrecht, the Nederland, 354p.

Pullammanappallil, S., Honjas,W., and Louie, J.N., 2003, "Determination of 1-D Shear Wave Velocities Using the Refraction Microtremor Method", Proceedings of the Third International Conference on the Application of Geophysical Methodologies and NDT to Transportation and Infrastructure, Orlando, Florida, USA.

Richart, F.E., Hall, J.R., Woods, R.D., 1970, "Vibrations of Soils and Foundations", Prentice-Hall International Series in Theoretical and Applied Mechanics, Englewood Cilffs, New Jersey, 414 p.

Rix, G.J., 2005, "Near-Surface Site Characterization Using Surface Waves, Surface Waves in Geomechanics – Direct and Inverse Modeling for Soil and Rocks", Lai and Wilmanski (Ed), CISM Lecture Notes, Springer-Verlag, Wien-Newyork.

Rodriquez-Marek, A., Bray, J.D., and Abrahamson, N.A., 2001, "An Empirical Geotechnical Seismic Site Response Procedure", Earthquake Spectra, 17, 1, 65 87.

Rodriguez-Marek, A., Eeri, M., Bray, J., Abrahamson, N., 2001, "An Empirical Geotechnical Seismic Site Response Procedure", Earthquake Spectra, Vol. 17, No.1.

Rodriguez, V.H.S. and Midorikawa, S., 2002, "Applicability of the H/V Spectral Ratio of Microtremors in Assessing Site Effects on Seismic Motion", Earthq Eng Struct Dyn V. 31 pp.261–279.

Rucker, M.L., 2003, "Applying the Refraction Microtremor (ReMi) Shear Wave Technique to Geotechnical Characterization, Proceedings of the Third International Conference on the Application of Geophysical Methodologies and NDT to Transportation Infrastructure", Dec. 8-12, 2003, Orlando, Florida, USA.

Salamon-Calvi, W., 1936, "Ankara'nın Su Vaziyeti", Y.Z.E. Çalış. No.20, Türkiye Cumhuriyeti Jeol. Gör., No. 1.

Salomon-Calvi, W., 1940, "Ankara Civarında Jeolojik Geziler", M.T.A. Dergisi, 20, 380-40; 21, 601-619, Ankara.

Satoh, T., Kawase, H., Shin'Ichi, M., 2001, "Estimation of S-Wave Velocity Structures in and Around the Sendai Basin, Japan, Using Arrays Records of Microtremors", Bull. Seism. Soc. Am., 91 (2), 206–218.

Sayısalgrafik, 2009, "Turkey Deprem Haritası, Retrieved July 2", 2009 from http://www.sayisalgrafik.com.tr/deprem/tr_frames.htm

Schwarz, S.D. and Musser, J.M., 1972, "Various Techniques for Making In situ Shear Wave Velocity Measurements- A Description and Evaluation", Proceedings of the International Conference on Microzonation for Safer Construction, Research and Application.

Seekings, L.C., Wennerberg, L., Margheriti, L. and Liu, H.-P., 1996, "Site Amplification at Five Locations in San Francisco, California: A Comparison of S Waves, Codas and Microtremors", Bull. Seism. Soc. Am., 86, 2, 627-635.

Sitharam, T.G. and Anbazhagan, P., 2008, "Seismic Microzonation: Principles, Practices and Experiments", EJGE Bouget08

Stokoe II, K.H., Wright, S.G., Bay, J.A., and Roesset, J.M., 1994, "Characterization of Geotechnical Sites by SASW method, in Geophysical Characterization of Sites", ISSMFE Technical Committee #10, edited by R.D. Woods, Oxford Publishers, New Delhi.

Sürgel, A., 1976, "A Survey of The Geotechnical Properties of Ankara Soils", M.Sc. Thesis, METU Civil Engineering Department, 96p.

Şengör A.M.C., 1979, "The North Anatolian Transform Fault: Its Age, Offset and Tectonic Significance", Journal of Geological Society of London, C.136, 269-282.

Tabban, A., 1976, "Ankara'nın Deprem Bölgesinde Bulunmasının Nedenleri", Deprem Araştırma Enstitüsü Bülteni, 14, 1-34 (in Turkish).

TC4-ISSMGE, 1999, "Manual for Zonation on Seismic Geotechnical Hazard", Revised edition, Technical Committee for Earthquake Geotechnical Engineering (TC4) of the International Society of Soil Mechanics and Geotechnical Engineering (ISSMGE) 209 p.

Telford, W.M., Geldart, L.P., and Sheriff, R.E. and Keys, D.A., 1976, "Applied Geophysics", 1st Edition, Cambridge University Press, New York, 860p.

Tevez-Costa, P., Matias L., Bard P.Y., 1996, "Seismic Behaviour Estimation of Thin Alluvium Layers Using Microtremor Recordings", Soil Dynamics and Earthquake Engineering 15 (3), 201–209.

Teves-Costa P., IM Almeida, PL Silva., 2001, "Microzonation of the Lisbon Town: 1D Theoretical Approach", Pageoph, 158, 2579-2596.

Tokay, M., ve Lünel, A.T., and Koçyiğit, A., 1988, "Geology and Petrology of the Gökdere Stock of the Orhaniye Syenite", Journal of Pure and Applied Sciences, S.A., Geosciences I., V.21, No. 1-3, pp.1-38

Tokimatsu, K., 1997, "Geotechnical Site Characterization Using Surface Waves", Isihara Ed, Earthquake Geotechnical Engineering, pp 133-1368, Balkema Rotertdam

Toshinawa, T., Taber J.J., and Berrill J.J., 1997, "Distribution of Ground Motion Intensity Inferred from Questionnaire Survey, Earthquake Recordings, and Microtremor Measurements – A Case Study in Christchurch", New Zealand, During the 1994 Arthurs Pass Earthquake. Bull. Seism. Soc. Am. 87-2, pp. 356-369.

Udwadia, F.E. and Trifunac M.D., 1973, "Comparison of Earthquake and Microtremor Ground Motions in El Centro", California, Bull. Seism. Soc. Am., 63, pp. 1227-1253.

Üzüm, S., 1984, "Çubuk (Ankara) Civarının Jeolojisi", M.Sc. thesis, İstanbul University.

Xia, J., Miller, R.D. and Park, C.B., 1999, "Estimation of Near-Surface Shear-Wave Velocity by Inversion of Rayleigh Wave," Geophysics, 64(3), pp. 691-700.

Xia, J., Miller, R.D., Park, C.B., Hunter JA., Harris JB., and Ivanov J., 2002, "Comparing Shear-Wave Velocity Profiles Inverted from Multichannel Surface Wave with Borehole Measurements", Soil Dynamics and Earthquake Engineering, 22 (3), pp. 181-190.

Xia, J., Miller, R.D. and Park, C.B., 2004, "Utilization of High Frequency Rayleigh Waves in Near Surface Geophysics", the Leading Edge (August).

Xu, Y., Xia, J., and Miller, R.D, 2006, "Quantitative Estimation of Minimum Offset for Multichannel Surface-Wave Survey with Actively Exciting Source", Journal of Applied Geophysics, pp. 117-125.

Wills, C.J., Petersen, M., Bryant, W.A., Reichle, M., Saucedo, G.J., Tan, S., Taylor, G. and Treiman, J., 2000, "A Site-Conditions Map for California based on Geology and Shear Wave Velocity", Bull. Seism. Soc. Am., 90, 6B, pp.187-208.

Wills C.J. and Clahan K.B., 2006, "Developing a Map of Geologically Defined Site ConditionCategories for California", Bull Seism Soc Am 96(4A):1483-1501.

Yokoi, T. and Margaryan S., 2007, “Interpretation of SPAC Method based on Seismic Interferometry - Theory and Observation”, 50th Anniversary Earthquake Conference Commemorating the 1957 Gobi-Altay Earthquake.

Yoon, S. and Rix, G., 2004, “Combined Active-Passive Surface Wave Measurements for Near-Surface Site Characterization”, Proceedings of the SAGEEP 2004, Colorado Springs, CO, SUR03, Proceedings on CD ROM.

Zhang, S., X., Chan, L., S., and Xia, J., 2004, “The Selection of Field Acquisition Parameters for Dispersion Images from Multichannel Surface Wave Data”, Pure and Applied Geophysics, p 185-201.